

Natural and Anthropogenic Impacts on Mercury Cycling and
Distribution in the Sub-Arctic Hudson Bay Marine Environment

by

Alexander Abram Hare

A Thesis submitted to the Faculty of Graduate Studies of
The University of Manitoba
in partial fulfilment of the requirements of the degree of

DOCTOR OF PHILOSOPHY

Department of Environment and Geography
University of Manitoba
Winnipeg

Copyright © 2009 by Alexander Abram Hare

THE UNIVERSITY OF MANITOBA
FACULTY OF GRADUATE STUDIES

COPYRIGHT PERMISSION

Natural and Anthropogenic Impacts on Mercury Cycling and
Distribution in the Sub-Arctic Hudson Bay Marine Environment

By

Alexander Abram Hare

A Thesis/Practicum submitted to the Faculty of Graduate Studies of The University of
Manitoba in partial fulfillment of the requirement of the degree
Of

DOCTOR OF PHILOSOPHY

Copyright © 2009 Alexander Abram Hare

Permission has been granted to the University of Manitoba Libraries to lend a copy of this thesis/practicum, to Library and Archives Canada (LAC) to lend a copy of this thesis/practicum, and to LAC's agent (UMI/ProQuest) to microfilm, sell copies and to publish an abstract of this thesis/practicum.

This reproduction or copy of this thesis has been made available by authority of the copyright owner solely for the purpose of private study and research, and may only be reproduced and copied as permitted by copyright laws or with express written authorization from the copyright owner.

Abstract

This thesis provides information on how mercury moves to and from Hudson Bay, and how it is distributed within the system. The first comprehensive survey of total mercury concentrations in river and marine waters and in marine sediments permits a compilation of mercury mass budgets that are used to model the modern and preindustrial mercury cycles in Hudson Bay. This model demonstrates that an internal process of sediment recycling provides the largest amount of mercury to the burial flux offshore. It further reveals that most modern mercury fluxes to Hudson Bay have increased by large amounts over the preindustrial era. Histories of sediment mercury deposition determined at 12 locations reveal that mercury originating from anthropogenic activities contributes to the increased sediment fluxes in most areas. However, underlying natural processes have also increased mercury concentrations in some areas, and natural variability of mercury within the sediments is similar in magnitude to the enrichments observed during the industrialized era. Consistent with the large role of recycled sediment in Hudson Bay, the distribution of mercury appears to be largely governed by oxidized, reworked marine carbon, rather than labile or residual carbon fractions. In areas demonstrating naturally increasing sediment mercury enrichments, greater proportions of marine carbon appear to drive the higher mercury concentrations.

Acknowledgements

The opportunity to work in remote Arctic and sub-Arctic environments was a very rewarding experience which I greatly appreciate. I thank Dr. Tim Papakyriakou and Dr. David Barber for introducing me to the ArcticNet community and encouraging me to pursue environmental studies of the Arctic. I thank my supervisors, Dr. Gary Stern and Dr. Feiyue Wang, for providing encouragement, patience and instruction during my studies. I am also grateful for the encouragement and direction I received from my committee members, Dr. Gordon Goldsborough, Dr. Tim Papakyriakou, and Dr. Robie Macdonald. I am particularly indebted to Dr. Robie Macdonald who provided additional mentorship that greatly improved my understanding of marine systems. I am also indebted to Dr. Zou Zou Kuzyk for countless valuable scientific discussions that improved my understanding of marine biogeochemistry and provided valuable insights into the Hudson Bay marine ecosystem. Thanks also to Dr. Hamed Sanei who provided analytical resources and mentorship for the organic matter study in this thesis. My fieldwork could not have taken place without help from Team ZAM, Monica Pazerniuk, Dan Leitch, Mary O'Brien, Debbie Armstrong, Joanne Delaronde, Chyongong "Z" Zhang, Harmoni Hoffman, fellow scientists from ArcticNet, the crew of the CCGS *Amundsen*, and many people in the communities of Churchill, Baker Lake, Povirnituaq, Umiujaq, and Kuujjuarapik. Financial support from ArcticNet, The Northern Scientific Training Program, and Manitoba Hydro is gratefully acknowledged. Finally, I would like to thank my friends and my family for their constant positive encouragement during this time.

Table of Contents

Abstract	ii
Acknowledgements.....	iii
List of Tables	vi
List of Figures	vii
List of Common Abbreviations	ix
Manuscript Claims	x
Outline of Thesis Chapters.....	xi
Chapter 1	1
General Introduction	1
1.0 Thesis Objectives	1
1.1 Overview of the Mercury Issue.....	1
1.2 Hg Exposure to Humans	2
1.3 Relevance of Environmental Inorganic Hg Studies.....	5
1.4 Extent of Human Impact on the Global Circulation of Hg.....	7
1.5 Human Impact on Hg in Aquatic Sediments of North America.....	9
1.6 Vertical Particle Flux of Hg.....	10
1.7 Relevance of Recent Scientific Investigations to this Study	13
1.8 Rationale for Hg studies in the Hudson Bay marine system	14
1.9 References.....	16
Chapter 2.....	27
Contemporary and Preindustrial Mass Budgets of Mercury in the Hudson Bay Marine System: The Role of Sediment Recycling	27
2.0 Introduction.....	28
2.1 Experimental Methods	30
2.1.1 Study Area	30
2.2.2 Water Sampling and Analysis of Hg	33
2.2.3 Sediment Sampling and Analysis of Hg	36
2.2.4 Atmospheric Monitoring of Hg	38
2.2.5 Evasion of Dissolved Gaseous Mercury	38
2.2.6 Ancillary Data.....	39
2.3 Results.....	40
2.3.1 Hg in the Marine Waters of the HBS.....	40
2.3.2 Oceanic Hg Fluxes to the HBS	42
2.3.3 Air-sea Exchange of Hg.....	43
2.3.4 Riverine Hg Flux to the HBS.....	46
2.3.5 Coastal Erosional Hg Flux to the HBS	49
2.3.6 Mercury Removal by Sedimentation	50

2.3.7 Mercury Recycling via Sediment Resuspension.....	51
2.4 Discussion.....	54
2.4.1 Contemporary Mercury Mass Budgets in the HBS	54
2.4.2 Preindustrial Mercury Mass Budget in the HBS.....	56
2.4.3 Sedimentary Capture and Control of Hg in the HBS.....	57
2.4.4 Sensitivity to Climate Change	59
2.5 Conclusion	63
2.6 References.....	64
Chapter 3.....	71
Natural and Anthropogenic Mercury Distribution in Marine Sediments from Hudson Bay, Canada	71
3.0 Introduction.....	72
3.1 Experimental Methods.....	74
3.1.1 Study Site	74
3.1.2 Sample Collection.....	74
3.1.3 Sample Analyses.....	76
3.1.4 Hg Inventories.....	77
3.1.5 Modeling of Hg Flux Histories.....	78
3.2 Lateral and Vertical Variations of Hg in HB Sediments	78
3.3 Atmospheric Contribution to Sedimentary Hg	83
3.4 Non-atmospheric Contributions to Sedimentary Hg	84
3.5 Anthropogenic Hg loadings, Sediment Hg Fluxes and Surface Enrichment Factors.....	87
3.6 Impact of Anthropogenic Hg on marine sediment Hg distribution	95
3.7 References.....	97
Chapter 4.....	102
Biogeochemistry of Organic Matter and Mercury in Recent Marine Sediments from Hudson Bay, Canada.....	102
4.0 Introduction.....	103
4.1 Experimental Methods.....	104
4.1.1 Study Area	104
4.1.2 Sample Collection.....	106
4.1.3 Grain size analysis	108
4.1.4 Organic Matter measurements	108
4.1.5 Elemental and Isotopic Analyses.....	109
4.2 Results and Discussion	110
4.2.1 Contributions of terrestrial and marine OM.....	110
4.2.2 Contributions of fresh and degraded OM	114
4.2.3 Comparison of RE and Elemental analyses.....	117
4.2.4 Labile and humic classes of compounds.....	122
4.2.5 Impact of reworked OM on the transport and fate of Hg in HB.....	123

4.3 References.....	128
Chapter 5.....	133
Synthesis of Results.....	133
5.0 Overview of Research.....	133
5.1 The Role of Sediment Recycling and Lateral Transport of Hg in HB	134
5.2 The Impact of Anthropogenic Hg to HB	137

List of Tables

Table 2-1. The Hudson Bay Marine System as defined in this study.....	31
Table 2-2. Water and sediment fluxes of the Hudson Bay System	35
Table 2-3. Riverine Hg fluxes to the Hudson Bay System.....	48
Table 2-4. Calculations of Biotic Hg Inventory in the HBS.....	53
Table 2-5. Estimates of contemporary and historic mercury fluxes to the HBS	55
Table 3-1. Basic physical parameters of Hudson Bay sediment cores.	76
Table 3-2. Input functions for modeled Hg flux histories.	79
Table 3-3. Observed and modeled onset of major changes in Hg flux in sediments from North America and Greenland.	81
Table 3-4. Hg concentrations, fluxes and surface enrichments in Hudson Bay sediment cores.	83
Table 4-1. OICO, OI and $\delta^{13}\text{C}$ measurements in cores 6 and 9.....	121
Table 4-2. Correlation Coefficients and Prevalence of Significant Relationships between Carbon Fractions, Hg distribution, and Grain Size.....	125
Table A-1. Vertical Distribution of Hg in Dissolved and Particulate Phases in the Churchill River Estuary	147
Table A-2. Horizontal and Vertical Distribution of Hg in Dissolved and Particulate Phases in the Nelson and Hayes River Estuaries, July 2005	148
Table A-3. Horizontal Hg Distribution in Dissolved and Particulate Phases in Estuary Surface Waters of the Hudson Bay System	149

List of Figures

- Figure 2-1. Hydrographical components and bathymetry of the Hudson Bay system, showing the sampling locations for rivers (circles), marine waters (diamonds), marine sediment cores (squares), and air (triangle). The map was created using Ocean Data View (<http://odv.awi.de>)..... 29
- Figure 2-2. Collection of a box core and preparation for sectioning. Top Left: After the box core has been lowered quickly to the sediments at ~ 1 m/s and penetrates the sediments up to 50 cm deep, a swing arm closes the bottom of the box core and it is retrieved slowly by a winch onto the ship deck. Bottom Left: Careful removal of the box core from the frame preserves the vertical structure of the sediments. Right: One face of the box core is removed and all sediment in contact with the box core walls is discarded before sectioning of the core begins. 37
- Figure 2-3. Regional depth profiles of HgT concentrations in the HBS. Each region is composed of 3 to 5 stations ($n = 2$ to 8 per depth). Error bars are standard deviations of the mean; dashed line represents the approximate depth of the region. 41
- Figure 2-2. Relationships between the HgT concentration in river water and A) the water discharge, and B) the latitude of the river mouth. The rivers identified by the filled circles were excluded from the analysis..... 47
- Figure 2-5. Relationship between the HgT concentration in surface sediment (top 1 cm) and the water depth. 52
- Figure 2-6. Mass balance model for Hg in the HBS for A) preindustrial and B) contemporary times..... 62
- Figure 3-1. Sediment core locations, Hg concentrations and inventories. Graphs: circles and lines are measured and modeled Hg concentrations, respectively; horizontal error bars are the range or standard deviation ($n = 2$ to 5); dashed lines represent the depth of the surface mixed layer. Map: circles represent core locations, bars represent Hg inventories (see legends)..... 75
- Figure 3-2. Vertical profiles of Hg concentrations in marine sediment cores taken from Hudson Bay. Open boxes represent background Hg layers..... 82
- Figure 3-3. Co-variation of Hg and $\delta^{13}\text{C}$ Hg in two offshore cores (cores 10 and 13). Vertical error bars represent the intrinsic time resolution of each core. 86
- Figure 3-4. $\delta^{13}\text{C}$ content in marine sediment cores of Hudson Bay. Data from cores 5, 6, and 8 is adapted from Kuzyk et al. (2009a). Different grey scales reflect different cores. 87
- Figure 3-5. Grain size (% < 63 μm) (left) and surface sediment %OM content (right) controls on Anthropogenic Hg loadings. Open circles are cores located near river outlets (6 and 9), filled circles are all other cores with stable background Hg concentrations. ... 88

Figure 3-6. Relationships between Hg and OM content in background (left) and surface (right) sediments. Open circles represent cores located near river outlets, filled circles represent all remaining cores with steady background Hg concentrations..... 91

Figure 3-7. The relationship between Anthropogenic and Background Hg fluxes. Open circles represent cores located near river outlets, filled circles represent all remaining cores with steady background Hg concentrations..... 92

Figure 4-1. Box core locations and relative proportions of PC and RC fractions in marine sediments from Hudson Bay. White bars = PC, (PC = S1 + S2 + S3), black bars = RC. Highest and lowest surface values of TOC are indicated. Numbers refer to core designations in the text..... 107

Figure 4-2. Inventories of labile carbon in HB. Left panel, S2 Carbon Inventories normalized to RC Inventories. Right panel, S3 Carbon Inventories normalized to PC Inventories. Inventories were calculated for a 130 year period prior to sample collection. 111

Figure 4-3. S2/RC and $\delta^{13}\text{C}$ (‰) content in HB marine sediments..... 112

Figure 4-4. Determination of the mean HI in two groups of sediments of HB. 113

Figure 4-5. Van Krevelen-type diagrams of HB sediments. Solid black lines refer to classical kerogen maturation pathways..... 116

Figure 4-5. C:N ratios and RC content of HB sediments. Each point represents a single section from an individual core..... 117

Figure 4-7. Comparison of HI and OI with elemental measurements of marine OM. ... 119

Figure A-1. Vertical profile of Hg in sediments of Core 15..... 151

List of Common Abbreviations

AMDE	Atmospheric Mercury Depletion Event
DGM	Dissolved gaseous mercury
GEM	Gaseous elemental mercury
HB	Hudson Bay
HBS	Hudson Bay System
Hg	Mercury
HgD	Dissolved mercury
HgP	Particulate mercury
HgT	Total mercury
OC	Organic Carbon
OM	Organic Matter
PC	Pyrolizable Carbon
RC	Residual Carbon
RE	Rock Eval Analysis
RGM	Reactive gaseous mercury
TOC	Total Organic Carbon

Manuscript Claims

Chapter 2

Hare, A., Stern, G.A., Macdonald, R.W., Kuzyk, Z., Wang, F. 2008. Contemporary and preindustrial mass budgets of mercury in the Hudson Bay marine system: The role of lateral sediment recycling. *Science of the Total Environment*, 406(1-2):190-204

A. Hare collected and analyzed river and marine water samples for mercury data. A. Hare assisted Z. Kuzyk with sediment collection. A. Hare analyzed sediments for mercury data and wrote the manuscript with input from the co-authors.

Chapter 3

Hare, A.A., Stern, G.A., Kuzyk, Z.A., Macdonald, R.W., Johannessen, S., Wang F. Natural and anthropogenic mercury distribution in marine sediments from Hudson Bay, Canada.

A. Hare assisted Z. Kuzyk with sediment collection. A. Hare analyzed sediments for mercury data and performed the modeling of sediment inputs. A. Hare wrote the manuscript with input from the co-authors.

Chapter 4

Hare, A.A., Wang, F., Kuzyk, Z., Macdonald, R.W., Sanei, H, Stern, G.A. Biogeochemistry of organic matter in recent marine sediments from Hudson Bay, Canada.

A. Hare assisted Z. Kuzyk with sediment collection. A. Hare analyzed sediments for mercury data. H. Sanei provided analytical services for generating organic carbon data. A. Hare wrote the manuscript with input from the co-authors.

Outline of Thesis Chapters

This thesis is structured in a publication-based format with five chapters and one Appendix. The new research produced during this study is divided into three individual manuscripts that each composes one chapter. These chapters include their own introduction, materials and methods, results and discussion, and reference sections.

Chapter 1 provides the background and rationale for each of the three research sections, and addresses the issues: where the problem came from, why this is important, what is already known about the problem, what other approaches have been used to investigate the problem, what other research relevant to this study has been performed, and, why this particular method and location was chosen.

Chapter 2 investigates how Hg fluxes involving the Hudson Bay Marine System (HBS) have changed since industrialization. A compilation of mass budgets of Hg is produced for the contemporary and pre industrial periods by using a wide range of environmental measurements of Hg in the marine water column, sediments, and river waters. These budgets identify large industrial-era increases in a number of Hg fluxes to the HBS and reveal the size and importance of lateral sediment transport in contributing Hg to regions of offshore burial.

Chapter 3 investigates whether or not the marine sediments in Hudson Bay accurately reflect the history of anthropogenic Hg emissions in North America, and where the majority of anthropogenic Hg deposited to Hudson Bay has been captured. This study establishes that anthropogenic emissions to the atmosphere have a distinguishable impact on the Hg concentrations in marine sediments of Hudson Bay but

underlying natural processes in some areas enrich Hg to levels similar to that observed from anthropogenic activities. Furthermore, although large localized enrichments are observed in some areas, the overall modern pattern of spatial variability in Hg flux is similar to that during the pre industrial era.

Chapter 4 investigates the role that sedimentation plays in Hg capture by examining the type of organic mater in the HBS that most strongly governs Hg capture. It is written from an organic carbon perspective and uses Rock Eval analyses complementary to recent biogeochemical studies (Kuzyk et al., 2008a; Kuzyk et al., 2009a; Kuzyk et al., 2009b). The sources and classes of OM captured in Hudson Bay are identified and their distribution is described. The carbon fractions are then investigated for influence on Hg capture, and a unique relationship between Hg and reworked marine OM that appears largely due to the distinctive sedimentary dynamics of Hudson Bay is described.

Chapter 5 provides a synthesis of the three research chapters by compiling the new information provided by this thesis into a single discussion. New insight is obtained into the Hg dynamics of the HBS and directions for further Hg studies are identified. The implications of this work on the global Hg issue are discussed.

CHAPTER 1

General Introduction

1.0 Thesis Objectives

The objectives of this thesis are to characterize the magnitudes and temporal changes of the major environmental fluxes of mercury (Hg) to and from Hudson Bay, to explore the contributions of natural and anthropogenic processes to sediment Hg distribution, and to investigate the nature of particulate burial flux of Hg to the sediments.

1.1 Overview of the Mercury Issue

Hg is a potent vertebrate neurotoxin and a naturally occurring element that resides at low levels in nearly all parts of the abiotic and biotic components of the global environment. It naturally moves within and between these compartments by a wide range of processes and appears to have generally posed little threat to human or animal health prior to the industrialized era, also known as the Anthropocene (Crutzen, 2002). Currently, Hg is a global contaminant and a high priority concern in many regions of the earth, posing a health threat to a wide range of human populations (AMAP, 2009; Mergler et al., 2007; WHO, 2005). Its transformation from a largely benign trace metal to a contaminant of global concern is principally the result of human activities that have perturbed the natural geochemical cycle of Hg (Nriagu, 1984; Pacyna and Winchester, 1990).

1.2 Hg Exposure to Humans

Exposure to Hg can pose a serious threat to human health. Several chemical species of Hg are neurotoxins capable of disrupting nerve transmission, inhibiting nerve cell growth, and causing cell death (Atchison and Hare, 1994; Castoldi et al., 2001). Developing infants and children are particularly susceptible to Hg exposure due to higher tissue absorption rates of Hg and greater nerve growth (Goyer and Clarkson, 2001; O'Flaherty, 1998), sometimes displaying cognitive impairment and developmental delay in cases of chronic Hg exposure (Clarkson, 1997; Counter and Buchanan, 2004). In extreme cases, environmental exposure to high Hg concentrations has led to widespread neurological damage and death in children and adults in certain populations (Bakir et al., 1973; Rustam and Hamdi, 1974; Takeuchi et al., 1962). Nevertheless, large scale population studies have been inconsistent in their assessment of the relationship between environmental Hg exposure and neurological disorders, often finding no clear connection (Johansson et al., 2002; Mozaffarian and Rimm, 2006; Spurgeon, 2006). This is due in part to the difficulty in discerning neurological effects from Hg exposure that could also arise from multiple other conditions (Auger et al., 2005), as well as the heterogeneity of study designs (Mozaffarian and Rimm, 2006). As a result, the risk of negative health impacts from environmental Hg exposure has been largely established to arise from chronic exposure to Hg in specific foods consumed by susceptible populations (e.g. Auger et al., 2005; Grandjean et al., 1999; Grandjean et al., 2004; Grandjean et al., 2001; Ratcliffe et al., 1996; Steuerwald et al., 2000; van Wijngaarden et al., 2006). Such investigations have supported the establishment and refinement of guidelines at the

national and international level for exposure to dietary Hg intake (EPA, 2004; Health-Canada, 2004; WHO, 2003).

The primary route of Hg exposure to humans is through dietary consumption of pelagic fish and marine mammal species (Counter and Buchanan, 2004; Johansen et al., 2007; van Wijngaarden et al., 2006). These organisms more frequently contain high levels of Hg than other species because they exist at top trophic levels in food chains where a neurotoxic form of Hg called methyl Hg (MeHg) accumulates through the process of biomagnification. MeHg is more efficiently transferred between trophic levels than many other environmentally relevant Hg species (e.g. Hg(0), di-methyl Hg, HgCl₂, HgCl₄²⁻) because it strongly binds to thiol (reduced sulfur-containing) groups such as those on cysteine and glutathione amino acids, and is removed at lower rates than the respiration of consumed carbon. This results in its selective retention during the consumption and metabolism of biological tissues by organisms (Kainz et al., 2006; Reinfelder et al., 1998), leading to MeHg accumulation in individual organisms and increasing tissue concentrations with increasing trophic level (Watras et al., 1998). Consequently, MeHg accounts for nearly 100% of Hg in fish muscle and in the muscle and skin of Arctic marine mammals (Wagemann et al., 1998) and dietary guidelines for Hg consumption principally reflect tissue MeHg concentrations.

As a result of MeHg biomagnification, the danger of Hg toxicity in diet is strongly influenced by food chain structure and the age of the organisms consumed. Since marine ecosystems commonly exhibit more complex food webs than terrestrial ecosystems, top trophic level marine species exist at higher trophic levels than their terrestrial counterparts (Dietz et al., 2000). Consequently, human populations inhabiting

coastal regions frequently exhibit high tissue concentrations of Hg because they commonly consume marine organisms that exist at high trophic levels. This is particularly a factor in the Hg burdens of the Inuit people in Canada and Greenland because they frequently consume marine mammals which represent the highest trophic levels of a marine food chain (Chan and Receveur, 2000; Muckle et al., 2001; Wein et al., 1996). Some evidence also exists that environmental MeHg concentrations and the phytoplankton species composition can influence the uptake of MeHg into food webs and subsequently, its concentration in higher organisms (Mason et al., 1996; Morel et al., 1998), indicating that other biophysical parameters can govern MeHg body burdens as well. These issues have prompted governments and scientific studies involved in the Arctic to consider Hg one of the highest priority heavy metals of concern despite the known toxicity of other environmentally relevant metals such as cadmium and lead.

Marine concentrations of MeHg are primarily the result of MeHg production within the aquatic environment, rather than from direct anthropogenic emissions of MeHg and its subsequent transport and deposition. Chemical speciation studies of Hg emissions find that MeHg composes extremely small fractions of the total Hg emitted from natural and anthropogenic sources (Carpi, 1997; Galbreath and Zygarlicke, 1996; Pacyna and Pacyna, 2002; Pacyna et al., 2006; Park et al., 2008). Correspondingly low MeHg levels are found in the atmosphere (Gabriel et al., 2005) and in precipitation (Mason et al., 1992; Schroeder and Munthe, 1998; St.Louis et al., 1995) where they could be transported and deposited to remote environments. Rather, the amount of MeHg within most ecosystems is largely dependent on a variety of parameters such as anoxia, the activity of sulfate-reducing bacteria, temperature, and organic matter, sulfate and

sulfide concentrations (Hammerschmidt and Fitzgerald, 2006b; Hammerschmidt et al., 2008; Ogrinc et al., 2007; Sunderland et al., 2006). Recent studies show that in ocean systems, Hg methylation also occurs in the oxygenated, low sulfur and organic matter conditions of the water column, presumably from heterotrophic biological activity (Cossa et al., 2009; Sunderland et al., 2009). However, the connection between the total amount of Hg and the amount of MeHg in marine sediments is usually weak (e.g. (Hammerschmidt and Fitzgerald, 2006b; Kannan and Falandysz, 1998; Ogrinc et al., 2007)), thus rendering inorganic Hg distribution an ineffective predictor of where sediment MeHg concentrations are high.

The total amount of MeHg usually composes a very small fraction of the total Hg present in aquatic environments: less than 10 % in sediments (Delongchamp et al., 2009; Gilmour et al., 1998; Ogrinc et al., 2007), 10-20 % in open ocean waters (Cossa et al., 2009; Sunderland et al., 2009), and up to 30-40 % in some coastal Arctic waters (St. Louis et al., 2007). As a result, common environmental MeHg concentrations are below 5 pM in seawater (Cossa et al., 1997; Horvat et al., 2003; Mason et al., 1998; Mason and Sullivan, 1999), which is well below levels of toxicity. However, because of its capability to biomagnify, it becomes concentrated upwards of a million times from water concentrations to tissue concentrations of marine species (Baeyens et al., 2003; Francesconi and Lenanton, 1992; Hammerschmidt and Fitzgerald, 2006a).

1.3 Relevance of Environmental Inorganic Hg Studies

Although studies of inorganic Hg concentrations do not directly predict MeHg levels in biological tissues, knowledge of their spatial and temporal distribution provide

useful information that helps address many fundamental Hg-related concerns. For instance, on a global and long term scale, the increasing burdens of Hg in biota during the industrial era are reflected in the time line of anthropogenic additions of inorganic Hg to the environment. For example, Hg concentrations in the teeth of modern Norwegians is an order of magnitude higher than those in 12th century individuals (Eide et al., 1993) and Hg concentrations in the hair of modern Greenland residents is 3-fold or more that of residents from the 15th and 16th centuries (EEA, 2005). Similar observations have been made with a variety of marine animals such as beluga whales (Outridge et al., 2002), polar bears (Dietz et al., 2006), seals (Sun et al., 2006) and several species of seabirds (Thompson et al., 1992), all showing industrial era increases in Hg burdens compared to the preindustrial era. These observations are currently best explained by the large increase in the amount of Hg circulating through the Earth's surface ecosystems, because no known natural process such as climatic variability or changes in biological behaviour match these century-scale trends. Similarly, the natural variability of inorganic Hg distribution has also been invoked to explain regional differences in the Hg burdens of species from the same era (Renzoni et al., 1998; Wagemann et al., 1998). These types of studies imply that inorganic Hg can, to some extent, plausibly explain modern biological Hg levels, even though their response to inorganic Hg inputs depends on a variety of biogeochemical parameters (Munthe et al., 2007).

Inorganic Hg distribution and concentration also provides insight into the extent of human impact on the environment, and the effect of regulatory control measures designed to limit such impact. For example, evidence of the widespread contamination of remote environments by the atmospheric transport and deposition of anthropogenic Hg is

abundantly provided by trends of inorganic Hg capture by lake sediments (Bindler et al., 2001a; Bindler et al., 2001b; Fitzgerald et al., 2005; Fitzgerald et al., 1998; Hermanson, 1998; Lockhart et al., 1998), ice cores (Schuster et al., 2002) and peat bogs (Biester et al., 2002; Givelet et al., 2004). In some cases the effect of regulatory control measures can be observed in the history of steady or declining Hg fluxes that appear after a time period of increasing Hg emissions e.g. (Delongchamp et al., 2009; Johannessen et al., 2005; Lindeberg et al., 2007). Studies such as these provide important validation of legislation that curbs human emissions to the environment.

These reasons largely provide the impetus for inorganic Hg studies in remote environments. However, inorganic Hg itself is also toxic to organisms and sediment quality guidelines for inorganic Hg concentrations exist that permit a basic estimation of whether negative effects could be expected in benthic organisms inhabiting impacted sediments (Boyd et al., 1998; Burton, 2002; Hubner et al., 2009; Kamman et al., 2005).

1.4 Extent of Human Impact on the Global Circulation of Hg

Human activities in the industrialized era have strongly altered the dynamics of the global geochemical Hg cycle. Many industrial and commercial processes release large amounts of Hg from geological sources into the surface ecosystems of the earth where they significantly contribute to the total amount of Hg circulating in surface environments (Lindberg et al., 2009; Pacyna et al., 2006; Pirrone et al., 1996). The release of Hg in gaseous elemental (Hg(0)) and gaseous reactive (Hg(II)) forms to the atmosphere composes most of these emissions, followed by discharges into surface waters (Pacyna et al., 2006). For example, anthropogenic Hg fluxes to the atmosphere are currently

estimated at ~2.5 times natural emissions, and have increased the atmospheric Hg content by roughly 300 % over the last 130 years (Lamborg et al., 2002). The increased atmospheric Hg reservoir is reflected in increased atmospheric deposition of Hg, which is nearly 3-fold higher than pre industrial levels (Fitzgerald et al., 1998; Lamborg et al., 2002). Since the atmosphere is the major source of Hg to the global oceans, the impact on this environment has been a 25 % to 46 % increase in surface water Hg concentrations above preindustrial levels (Lamborg et al., 2002; Sunderland and Mason, 2007). Elevated atmospheric Hg deposition is also implicated in the large industrial era increases observed in the global soil reservoir of Hg (Han et al., 2002). The result of such large scale additions to the atmosphere, the pedosphere (soil system) and hydrosphere is large increases in the size of all major exchanges of Hg between ecosystems of the earth and their abiotic and biotic components (Lamborg et al., 2002; Mason and Sheu, 2002).

Although Hg is naturally removed from circulating at the earth's surface by sedimentation and water mass mixing into deep aquatic basins, this process appears no longer sufficient to maintain steady Hg levels in the oceans. This is particularly exemplified by recent models of the global Hg cycle that estimate deep water masses only export ~20 % to 30 % of incoming Hg to deep sediments (Lamborg et al., 2002; Mason and Sheu, 2002). Yet, while deep ocean exports of Hg via burial and exchange with other water masses remain near preindustrial levels, Hg inputs to these waters have increased nearly 2-fold (Lamborg et al., 2002). The imbalance between inputs and exports has resulted in a lag between changes in seawater and atmospheric Hg concentrations by decades to centuries. Consequently, surface and deep water masses are expected to continue increasing until they reach 80 % and 150 % over preindustrial

levels, respectively, considering only that atmospheric Hg emission remain at current levels (Sunderland and Mason, 2007). The eventual impact of anthropogenic Hg emissions on the global oceans could actually be much greater considering that recent predictions of global Hg emissions for the next mid-century range up to a 96 % increase in total global emissions (Streets et al., 2009). In the Arctic Ocean, sedimentation removes a greater proportion of incoming Hg than in the global oceans, but this system also loses far less Hg through evasion and receives reduced relative inputs from direct atmospheric deposition (Outridge et al., 2008). The balance of these fluxes further restricts the response of seawater Hg concentrations to changes in atmospheric concentrations. As a result, the Arctic Ocean is predicted to respond even slower than other oceans to changes in Hg emissions (Outridge et al., 2008).

1.5 Human Impact on Hg in Aquatic Sediments of North America

In North America, the extent of anthropogenic impact to aquatic ecosystems from elevated atmospheric Hg deposition has commonly been investigated by determining the historical and current Hg content in lake sediments. Based on these records, studies have demonstrated atmospheric anthropogenic Hg capture by many lakes in Canada (Hermanson, 1998; Lockhart et al., 1998; Lucotte et al., 1995; Muir et al., 2009), the U.S.A (Fitzgerald et al., 2005; Lorey and Driscoll, 1999a; Perry et al., 2005), and nearby in Greenland (Bindler et al., 2001b). These studies show nearly ubiquitous enrichments of Hg in sediments corresponding to deposition beginning in the late 19th or early 20th century, with the later enrichments appearing in more northern lakes (Lucotte et al., 1995). A latitudinal relationship also appears over very large regional distances, with

higher inputs of anthropogenic Hg occurring at more southerly latitudes and lower inputs at northern latitudes (Muir et al., 2009). Such studies have demonstrated the significance of human Hg emissions to Hg concentrations in freshwater systems, and provided the scientific basis for many progressive investigations of the impact of experimental Hg additions to lakes on the Hg concentrations in their biota (e.g. (Harris et al., 2007; Heyes et al., 2004).

The investigation of anthropogenic Hg impacts to marine sediments has received much less attention. Several studies have demonstrated the impact of anthropogenic Hg from point sources to coastal or estuarine sediments (Gagnon et al., 1997; Johannessen et al., 2005). These studies have demonstrated that anthropogenic Hg additions to marine systems are captured by the vertical particle flux and buried in marine sediments. However, the impact of atmospherically transported Hg to marine sediments has been much less clear because atmospheric Hg fluxes tend to be far smaller than those from point sources, being more diffusely added to the aquatic environment, and therefore are more susceptible to obscuring factors. Investigations of atmospheric anthropogenic Hg impact to marine sediments have thus far been unclear due to underlying geological variability (Asmund and Nielsen, 2000) and diagenetic mobilization of Hg (Gobeil et al., 1999).

1.6 Vertical Particle Flux of Hg

The connection between atmospheric and sedimentary Hg relies largely on the vertical transport of Hg from surface waters to the seafloor via particle flux. In the open ocean this relationship is reflected in the vertical distribution of Hg, which displays

evidence of both an atmospheric source and particle scavenging. The highest Hg levels in ocean waters are frequently found near the surface, and minimum levels within the central water column commonly increase with depth (Cossa et al., 2004; Cossa et al., 1997; Fitzgerald et al., 2007; Laurier et al., 2004; Mason et al., 1998; Mason and Sullivan, 1999). Atmospheric contributions of Hg to the ocean are primarily in the Hg(0) and inorganic Hg(II) forms, which actively cycle and interchange through various biological and photochemical processes. (Fitzgerald et al., 2007; Strode et al., 2007). Both Hg(0) and dissolved forms of Hg(II) such as HgCl_4^{2-} dominate the Hg reservoir in the ocean but Hg(0) is not particle reactive and is not removed from the water column via sedimentation. However, a small fraction of the Hg(II) is bound by particulate matter, which provides a platform for the transport and distribution of Hg both laterally and vertically (Cossa et al., 2004; Guentzel et al., 1996; Sunderland and Mason, 2007). Particulate Hg concentrations are very low in the ocean except near the coast and estuaries where particulate matter concentrations are higher (Coquery et al., 1995; Guentzel et al., 1996; Leitch et al., 2007; Mason et al., 2001). In offshore regions, some particulate Hg is regenerated into the dissolved phase by the decomposition of the particulate matter during its descent to the sediments, reducing the actual flux of Hg to the seafloor (Cossa et al., 1997). Correspondingly, the Hg flux to sediments is quite low in offshore regions, and represents only a small fraction of the total amount of Hg circulating in the ocean (Lamborg et al., 2002; Sunderland et al., 2009; Sunderland and Mason, 2007). Hg can also be extensively bound by colloids, commonly represented by mineral aggregations such as metal oxyhydroxides that are coated with organic matter and less than 1 μm in size. The proportion of Hg bound by colloids is highest in rivers

and estuaries and diminishes towards the open ocean but can still compose ~10 % to 50 % of the total dissolved Hg (Guentzel et al., 1996). Aggregation and settling of such colloidal materials can further contribute Hg to the sediments.

The composition of Hg-bearing particles in the marine water column is generally inferred from sedimentary relationships between Hg and various biogeochemical parameters. The spatial distribution of Hg in marine sediments is most frequently found associated with total organic carbon (TOC), implying a strong role of organic matter (OM) in transporting Hg to sediments (Hammerschmidt and Fitzgerald, 2006b; Hammerschmidt et al., 2008; Sunderland et al., 2006). The close association of OM with fine particulate materials also results in a relationship between sediment Hg concentrations and fine particle size (Barghigiani et al., 1996; Sunderland et al., 2006). However, in marine sediments with low TOC ($\sim < 1$ % by weight), poor spatial relationships with Hg concentrations have been observed, possibly due to a greater influence of inorganic Hg sources (Ogrinc et al., 2007; Trefey et al., 2007), or variable OM sources (Sunderland et al., 2006). In marine systems, the identity and relative importance of differing organic materials in transporting Hg has been largely unexplored, but similar to freshwater systems, is likely dominated by fulvic, humic and sulfur-containing compounds where these are present (Goulet et al., 2007). Some recent studies have used geochemical analyses to demonstrate that Hg in freshwater systems is scavenged preferentially by the S2 carbon fraction from Rock Eval pyrolysis, largely representing algal carbon (Outridge et al., 2007; Sanei and Goodarzi, 2006; Stern et al., 2009)

1.7 Relevance of Recent Scientific Investigations to this Study

Although there are numerous studies investigating abiotic Hg behaviour within various freshwater ecosystems of the Hudson Bay watershed, very few studies have previously investigated abiotic Hg in the Hudson Bay marine system. These few investigations are particularly relevant to this study of Hg in the Hudson Bay marine system. The earliest investigations of abiotic Hg in the Hudson Bay marine system appear to come from Lockhart et al. (Lockhart et al., 1998; 1995) who report two vertical Hg profiles in marine sediments from the eastern region of the Bay. Fluxes of Hg calculated from these cores range from 0.6 to 1.6 ng/cm²/yr and are comparable to the range of fluxes determined in this study and presented in Chapter 2. The fluxes of Hg from two rivers in the Hudson Bay watershed, the Churchill River and the Nelson River, were recently estimated by Kirk and St. Louis (2009) and provide a complimentary estimate to the fluxes reported in Chapter 2. Since this estimate was not available at the time of publication of the manuscript in Chapter 2 it is not included in that study. However, these fluxes are within a 2-fold range of the total Hg delivered to Hudson Bay from the same two rivers reported here. The difference in flux estimates is likely due to a different period of river sampling in that study, which included more frequent measurements during low-flow periods of the river. The sampling for the study presented here took place largely through the spring freshet period, during which time rivers tend to demonstrate higher Hg concentrations than at other times of the year (e.g. (Leitch et al., 2007)). Levels of Hg in marine zooplankton and marine fish have recently been provided by Pazerniuk (2007), who reported a comprehensive assessment of Hg levels in nearly the entire Hudson Bay food web. Notably, higher Hg concentrations were found in cod

inhabiting the western region of HB, potentially due to differences in the food web structure. Biotic Hg concentrations from Pazerniuk (2007) are used in Chapter 2 to estimate the total size of the biological Hg reservoir in HB. Recent biogeochemical studies are also particularly relevant to this study (Kuzyk et al., 2008a; Kuzyk et al., 2009a; Kuzyk et al., 2009b). These investigations have provided substantial information on the sediment and OM dynamic of HB, describing their sources, movement and distribution. The establishment of these basic geochemical factors has strongly supported, and is supported by, the Hg studies presented here.

1.8 Rationale for Hg studies in the Hudson Bay marine system

Hudson Bay presents an ideal location for marine Hg studies because of the demographics of its resident populations, its geographical location, and its underlying geology. The Hudson Bay region is populated by numerous small communities that consume large amounts of marine foods, including marine mammals, in their diet. This identifies them as a population at risk for negative health effects from Hg consumption based on World Health Organization guidelines (WHO, 2008). This situation is further compounded by the disproportionately high number of children and young mothers in the Arctic aboriginal population compared to the Canadian population (Van Oostdam et al., 2005), which compose the second type of population at risk to Hg exposure (WHO, 2008). These circumstances warrant careful attention to the Hg levels in the HBS because they could identify changing conditions of Hg that could manifest themselves as negative health impacts. Secondly, Hudson Bay is strongly linked to industrial human activities in central North America by its large watershed and proximity to highly populated areas.

Hudson Bay receives large freshwater inputs from a highly developed watershed and is therefore likely to display records of human Hg emissions. For example, several studies have previously demonstrated anthropogenic inputs of Hg to freshwater systems surrounding the HBS (Hermanson, 1998; Lockhart et al., 1998; Muir et al., 2009). Yet, Hudson Bay lies within a latitudinal gap in the study of Hg in North American marine systems, having been largely overlooked in past studies of Hg on this continent. Moreover, although river Hg fluxes to Hudson Bay do not currently appear to reflect anthropogenic Hg inputs (Hare et al., 2008), Hudson Bay is also the site of many proposed large scale industrial developments (hydroelectric reservoirs, mines) which could alter the local Hg dynamics through changes in freshwater runoff, flooding of land and reservoir creation, the introduction of point sources of Hg, and changes in the distribution of biota. The establishment of basic abiotic Hg measurements permits the assessment of ongoing human impacts to this environment. Thirdly, Hudson Bay represents geological conditions that are amenable to investigations of anthropogenic impacts. Hudson Bay appears to generally have low underlying geological contributions of Hg with relatively small natural variations in Hg concentrations that could otherwise obscure the anthropogenic Hg record.

Lastly, Hudson Bay is experiencing ongoing environmental changes linked to changing climate that could significantly alter the Hg cycle in HB. The appearance of new top trophic level, non ice-adapted marine mammal species in recent decades could potentially restructure the marine food web (Higdon and Ferguson, 2009), with uncertain consequences on the marine diets of local residents. Climate warming is similarly implicated in restructuring forage fish populations in HB, with concomitant dietary

changes in seabird populations (Gaston et al., 2003). Other observed changes in the Hudson Bay system that have been related to climate warming are an advancement of the tree line (Lescop-Sinclair and Payette, 1995), changing amounts of freshwater inputs (Déry et al., 2005) and changing patterns of ice distribution and timing, including a later freeze-up and earlier spring break-up (Gough et al., 2004). These transformations could have the potential to alter the regional Hg cycle by changing Hg fluxes from erosion, runoff, and potentially, increasing MeHg production in the vast wetlands composing large sections of its southern watershed.

1.9 References

- AMAP, 2009. AMAP Assessment 2009: Human Health in the Arctic., Arctic Monitoring and Assessment Programme, Oslo, Norway.
- Asmund, G. and Nielsen, S., 2000. Mercury in dated Greenland marine sediments. *Science of The Total Environment*, 245: 61-72.
- Atchison, W. and Hare, M., 1994. Mechanisms of methylmercury-induced neurotoxicity. *FASEB J.*, 8(9): 622-629.
- Auger, N., Kofman, O., Kosatsky, T. and Armstrong, B., 2005. Low-Level Methylmercury Exposure as a Risk Factor for Neurologic Abnormalities in Adults. *NeuroToxicology*, 26(2): 149-157.
- Baeyens, W., Leermakers, M., Papina, T., Saprykin, A., Brion, N., Noyen, J., De Gieter, M., Elskens, M. and Goeyens, L., 2003. Bioconcentration and Biomagnification of Mercury and Methylmercury in North Sea and Scheldt Estuary Fish. *Archives of Environmental Contamination and Toxicology*, 45(4): 498-508.
- Bakir, F., Damluji, S.F., Amin-Zaki, L., Murtadha, M., Khalidi, A., Al-Rawi, N.Y., Tikriti, S., Dhahir, H.I., Clarkson, T.W., Smith, J.C. and Doherty, R.A., 1973. Methylmercury Poisoning in Iraq. *Science*, 181(4096): 230-241.

- Barghigiani, C., Ristori, T. and Arenas, J.L., 1996. Mercury in marine sediment from a contaminated area of the northern Tyrrhenian Sea: <20 μm grain-size fraction and total sample analysis. *The Science of the Total Environment*, 192: 63-73.
- Bindler, R., Olofsson, C., Renberg, I. and Frech, W., 2001a. Temporal Trends in Mercury Accumulation in Lake Sediments in Sweden. *Water, Air, & Soil Pollution: Focus*, 1(3): 343-355.
- Bindler, R., Renberg, I., Appleby, P.G., Anderson, N.J. and Rose, N.L., 2001b. Mercury Accumulation Rates and Spatial Patterns in Lake Sediments from West Greenland: A Coast to Ice Margin Transect. *Environmental Science & Technology*, 35(9): 1736.
- Carpi, A., 1997. Mercury from Combustion Sources: A Review of the Chemical Species Emitted and Their Transport in the Atmosphere. *Water, Air, & Soil Pollution*, 98(3): 241-254.
- Castoldi, A.F., Coccini, T., Ceccatelli, S. and Manzo, L., 2001. Neurotoxicity and molecular effects of methylmercury. *Brain Research Bulletin*, 55(2): 197-203.
- Chan, H.M. and Receveur, O., 2000. Mercury in the traditional diet of indigenous peoples in Canada. *Environmental Pollution*, 110(1): 1-2.
- Clarkson, T.W., 1997. The Toxicology of Mercury. *Critical Reviews in Clinical Laboratory Sciences*, 34(4): 369-403.
- Cossa, D., Averty, B. and Pirrone, N., 2009. The origin of methylmercury in open Mediterranean waters. *Limnol. Oceanogr.*, 54(3): 837-844.
- Cossa, D., Cotte-Krief, M.-H., Mason, R.P. and Bretaudeau-Sanjuan, J., 2004. Total mercury in the water column near the shelf edge of the European continental margin. *Marine Chemistry*, 90(1-4): 21.
- Cossa, D., Martin, J.-M., Takayanagi, K. and Sanjuan, J., 1997. The distribution and cycling of mercury species in the western Mediterranean. *Deep Sea Research Part II: Topical Studies in Oceanography*, 44(3-4): 721.
- Counter, S.A. and Buchanan, L.H., 2004. Mercury exposure in children: a review. *Toxicology and Applied Pharmacology*, 198(2): 209-230.
- Crutzen, P.J., 2002. Geology of mankind. *Nature*, 415(3): 23.

- Delongchamp, T.M., Lean, D.R.S., Ridal, J.J. and Blais, J.M., 2009. Sediment mercury dynamics and historical trends of mercury deposition in the St. Lawrence River area of concern near Cornwall, Ontario, Canada. *Science of The Total Environment*, 407(13): 4095-4104.
- Déry, S.J., Stieglitz, M., McKenna, E.C. and Wood, E.F., 2005. Characteristics and trends of river discharge into Hudson, James, and Ungava Bays, 1964-2000. *Journal of Climate*, 18(14): 2540.
- Dietz, R., Riget, F., Born, E.W., Sonne, C., Grandjean, P., Kirkegaard, M., Olsen, M.T., Asmund, G., Renzoni, A., Baagoe, H. and Andreasen, C., 2006. Trends in Mercury in Hair of Greenlandic Polar Bears (*Ursus maritimus*) during 1892 - 2001. *Environmental Science & Technology*, 40(4): 1120-1125.
- Dietz, R., Riget, F., Cleemann, M., Aarkrog, A. and Johansen, P., 2000. Comparison of contaminants from different trophic levels and ecosystems. *The Science of the Total Environment*, 245: 221-231.
- EEA, 2005. *Environment and Health*, European Commission, Copenhagen.
- Eide, R., Wesenberg, G.R. and Fosse, G., 1993. Mercury in primary teeth in preindustrial Norway. *European Journal of Oral Sciences*, 101(1): 1-4.
- EPA, 2004. What you need to know about mercury in fish and shellfish. In: U.S.E.P. Agency (Editor).
- Fitzgerald, W.F., Engstrom, D.R., Lamborg, C.H., Tseng, C.M., Balcom, P.H. and Hammerschmidt, C.R., 2005. Modern and Historic Atmospheric Mercury Fluxes in Northern Alaska: Global Sources and Arctic Depletion. *Environ. Sci. Technol.*, 39(2): 557-568.
- Fitzgerald, W.F., Engstrom, D.R., Mason, R.P. and Nater, E.A., 1998. The case for atmospheric mercury contamination in remote areas. *Environ. Sci. Technol.*, 32: 1-7.
- Fitzgerald, W.F., Lamborg, C.H. and Hammerschmidt, C.R., 2007. Marine Biogeochemical Cycling of Mercury. *ChemInform*, 38(20).
- Francesconi, K.A. and Lenanton, R.C.J., 1992. Mercury contamination in a semi-enclosed marine embayment: Organic and inorganic mercury content of biota, and

- factors influencing mercury levels in fish. *Marine Environmental Research*, 33(3): 189-212.
- Gabriel, M.C., Williamson, D.G., Brooks, S. and Lindberg, S., 2005. Atmospheric speciation of mercury in two contrasting Southeastern US airsheds. *Atmospheric Environment*, 39(27): 4947-4958.
- Gagnon, C., Pelletier, E. and Mucci, A., 1997. Behaviour of anthropogenic mercury in coastal marine sediments. *Marine Chemistry*, 59: 159-176.
- Galbreath, K.C. and Zygarlicke, C.J., 1996. Mercury Speciation in Coal Combustion and Gasification Flue Gases. *Environmental Science & Technology*, 30(8): 2421-2426.
- Gaston, A., Woo, K. and JM, H., 2003. Trends in Forage Fish Populations in Northern Hudson Bay since 1981, as Determined from the Diet of Nestling Thick-Billed Murres *Uria lomvia*. *Arctic*, 56(3): 227 - 233.
- Gilmour, C., Riedel, G.S., Ederington, M.C., Bell, J.T., Gill, G.A. and Stordal, M.C., 1998. Methylmercury concentrations and production rates across a trophic gradient in the northern Everglades. *Biogeochemistry*, 40(2): 327-345.
- Gobeil, C., Macdonald, R.W. and Smith, J.N., 1999. Mercury Profiles in Sediments of the Arctic Ocean Basins. *Environ. Sci. Technol.*, 33(23): 4194-4198.
- Gough, W., Cornwell, A. and Tsuji, L., 2004. Trends in Seasonal Sea Ice Duration in Southwestern Hudson Bay. *Arctic*, 57(3): 299-305.
- Goulet, R.R., Holmes, J., Page, B., Poissant, L., Siciliano, S.D., Lean, D.R.S., Wang, F., Amyot, M. and Tessier, A., 2007. Mercury transformations and fluxes in sediments of a riverine wetland. *Geochimica et Cosmochimica Acta*, 71(14): 3393-3406.
- Goyer, R.A. and Clarkson, T.W., 2001. Toxic effects of metals. In: C.D. Klaassen (Editor), *Casarett & Doull's Toxicology: The Basic Science of Poisons*. 6th Edition. McGraw-Hill, pp. 822-826.
- Guentzel, J.L., Powell, R.T., Landing, W.M. and Mason, R.P., 1996. Mercury associated with colloidal material in an estuarine and an open-ocean environment. *Marine Chemistry*, 55(1-2): 177-188.

- Hammerschmidt, C. and Fitzgerald, W., 2006a. Bioaccumulation and Trophic Transfer of Methylmercury in Long Island Sound. *Archives of Environmental Contamination and Toxicology*, 51(3): 416-424.
- Hammerschmidt, C.R. and Fitzgerald, W.F., 2006b. Methylmercury cycling in sediments on the continental shelf of southern New England. *Geochimica et Cosmochimica Acta*, 70(4): 918.
- Hammerschmidt, C.R., Fitzgerald, W.F., Balcom, P.H. and Visscher, P.T., 2008. Organic matter and sulfide inhibit methylmercury production in sediments of New York/New Jersey Harbor. *Marine Chemistry*, 109(1-2): 165-182.
- Han, F.X., Banin, A., Su, Y., Monts, D.L., Plodinec, J.M., Kingery, W.L. and Triplett, G.E., 2002. Industrial age anthropogenic inputs of heavy metals into the pedosphere. *Naturwissenschaften*, 89(11): 497.
- Hare, A., Stern, G.A., Macdonald, R.W., Kuzyk, Z.Z. and Wang, F., 2008. Contemporary and preindustrial mass budgets of mercury in the Hudson Bay Marine System: The role of sediment recycling. *Science of The Total Environment*, 406(1-2): 190.
- Harris, R.C. et al., 2007. Whole-ecosystem study shows rapid fish-mercury response to changes in mercury deposition. *Proceedings of the National Academy of Sciences*, 104(42): 16586-16591.
- Health-Canada, 2004. *Mercury: Your Health and the Environment: A Resource Tool*.
- Hermanson, M.H., 1998. Anthropogenic Mercury Deposition to Arctic Lake Sediments. *Water, Air, and Soil Pollution*, 101: 309-321.
- Heyes, A., Krabbenhoft, D.P., Mason, R.P. and Gilmour, C., 2004. Spatial and temporal dynamics of Hg methylation in a boreal wetland: results from METALLICUS. *Materials and Geoenvironment*, 51(2): 1052.
- Higdon, J.W. and Ferguson, S.H., 2009. Loss of Arctic sea ice causing punctuated change in sightings of killer whales (*Orcinus orca*) over the past century. *Ecological Applications*, 19(5): 1365-1375.
- Horvat, M., Kotnik, J., Logar, M., Fajon, V., Zvonaric, T. and Pirrone, N., 2003. Speciation of mercury in surface and deep-sea waters in the Mediterranean Sea. *Atmospheric Environment*, 37(Supplement 1): 93-108.

- Johannessen, S., Macdonald, R.W. and Eek, K.M., 2005. Historical Trends in Mercury Sedimentation and Mixing in the Strait of Georgia, Canada. *Environ. Sci. Technol.*, 39: 4361-4368.
- Johansen, P., Mulvad, G., Pedersen, H.S., Hansen, J.C. and Riget, F., 2007. Human accumulation of mercury in Greenland. *Science of The Total Environment*, 377(2-3): 173-178.
- Johansson, N., Basun, H., Winblad, B. and Nordberg, M., 2002. Relationship between mercury concentration in blood, cognitive performance, and blood pressure, in an elderly urban population. *BioMetals*, 15(2): 189-195.
- Kirk, J.L. and St. Louis, V.L., 2009. Multiyear Total and Methyl Mercury Exports from Two Major Sub-Arctic Rivers Draining into Hudson Bay, Canada. *Environmental Science & Technology*, 43(7): 2254.
- Kuzyk, Z.A., Gofii, M.A., Stern, G.A. and Macdonald, R.W., 2008. Sources, pathways and sinks of particulate organic matter in Hudson Bay: Evidence from lignin distributions. *Marine Chemistry*, 112(3-4): 215.
- Kuzyk, Z.A., Macdonald, R.W., Johannessen, S.C., Gobeil, C. and Stern, G.A., 2009a. Towards a Sediment and Organic Carbon Budget for Hudson Bay. *Marine Geology*, 264: 190-208.
- Kuzyk, Z.A., Macdonald, R.W., Tremblay, J. and Stern, G., 2009b. Elemental and stable isotopic constraints on river influence and patterns of nitrogen cycling and biological productivity in Hudson Bay. *Continental Shelf Research*, Submitted.
- Lamborg, C.H., Fitzgerald, W.F., O'Donnell, J. and Torgersen, T., 2002. A non-steady-state compartmental model of global-scale mercury biogeochemistry with interhemispheric atmospheric gradients. *Geochimica et Cosmochimica Acta*, 66(7): 1105.
- Laurier, F.J.G., Mason, R.P., Gill, G.A. and Whalin, L., 2004. Mercury distributions in the North Pacific Ocean--20 years of observations. *Marine Chemistry*, 90(1-4): 3.
- Leitch, D.R., Carrie, J., Lean, D., Macdonald, R.W., Stern, G.A. and Wang, F., 2007. The delivery of mercury to the Beaufort Sea of the Arctic Ocean by the Mackenzie River. *Science of The Total Environment*, 373(1): 178.

- Lescop-Sinclair, K. and Payette, S., 1995. Recent advance of the Arctic treeline along the eastern coast of Hudson Bay. *J. Ecology*, 83: 929-936.
- Lindeberg, C., Bindler, R., Bigler, C., Ros, eacute, n, P. and Renberg, I., 2007. Mercury Pollution Trends in Subarctic Lakes in the Northern Swedish Mountains. *AMBIO: A Journal of the Human Environment*, 36(5): 401-405.
- Lockhart, W.L., Wilkinson, P., Billeck, B.N., Danell, R.A., Hunt, R.V., Brunskill, G.J., Delaronde, J. and St. Louis, V., 1998. Fluxes of mercury to lake sediments in central and northern Canada inferred from dated sediment cores. *Biochemistry*, 40: 163 - 173.
- Lockhart, W.L., Wilkinson, P., Billeck, B.N., Hunt, R.V., Wagemann, R. and Brunskill, G.J., 1995. Current and Historical Inputs of Mercury to High-Latitude Lake in Canada and to Hudson Bay. *Water, Air, and Soil Pollution*, 80(603-610).
- Lorey, P. and Driscoll, C.T., 1999. Historical Trends of Mercury Deposition in Adirondack Lakes. *Environmental Science & Technology*, 33(5): 718.
- Lucotte, M., Mucci, A., Hillaire-Marcel, C., Pichet, P. and Grondin, A., 1995. Anthropogenic mercury enrichment in remote lakes of northern Québec (Canada). *Water, Air, & Soil Pollution*, 80(1): 467-476.
- Mason, R.P., Reinfelder, J.R. and Morel, F.M.M., 1996. Uptake, Toxicity, and Trophic Transfer of Mercury in a Coastal Diatom. *Environmental Science & Technology*, 30(6): 1835-1845.
- Mason, R.P., Rolffhus, K.R. and Fitzgerald, W.F., 1998. Mercury in the North Atlantic. *Marine Chemistry*, 61(1-2): 37.
- Mason, R.P. and Sheu, G.P., 2002. Role of the ocean in the global mercury cycle *Global Biogeochem. Cycles*, 16(4): 1093.
- Mason, R.P. and Sullivan, K.A., 1999. The distribution and speciation of mercury in the South and equatorial Atlantic. *Deep-Sea Research II*, 46: 937-956.
- Mergler, D., Anderson, H., Chan, L., Mahaffey, K., Murray, M., Sakamoto, M. and Stern, A., 2007. Methylmercury Exposure and Health Effects in Humans: A Worldwide Concern. *AMBIO: A Journal of the Human Environment*, 36(1): 3-11.

- Morel, F.M.M., Kraepiel, A.M.L. and Amyot, M., 1998. The Chemical Cycle and Bioaccumulation of Mercury. *Annual Review of Ecology and Systematics*, 29(1): 543-566.
- Mozaffarian, D. and Rimm, E.B., 2006. Fish Intake, Contaminants, and Human Health: Evaluating the Risks and the Benefits. *JAMA*, 296(15): 1885-1899.
- Muckle, G., Ayotte, P., Dewailly, E., Jacobson, S.W. and Jacobson, J.L., 2001. Determinants of Polychlorinated Biphenyls and Methylmercury Exposure in Inuit Women of Childbearing Age. *Environmental Health Perspectives*, 109(9): 957-963.
- Muir, D.C.G., Wang, X., Yang, F., Nguyen, N., Jackson, T.A., Evans, M.S., Douglas, M., Kock, G., Lamoureux, S., Pienitz, R., Smol, J.P., Vincent, F. and Dastoor, A., 2009. Spatial Trends and Historical Deposition of Mercury in Eastern and Northern Canada Inferred from Lake Sediment Cores. *Environ. Sci. Technol.*, 43: 4802-4809.
- Munthe, J., Bodaly, R.A., Branfireun, B.A., Driscoll, C.T., Gilmour, C.C., Harris, R., Horvat, M., Lucotte, M. and Malm, O., 2007. Recovery of Mercury-Contaminated Fisheries. *AMBIO: A Journal of the Human Environment*, 36(1): 33-44.
- Nriagu, J.O., 1984. Changing metal cycles and human health, Dahlem Konferenzen. Springer-Verlag, Berlin.
- O'Flaherty, E.J., 1998. Physiologically based models of metal kinetics. *Critical Reviews in Toxicology*, 28: 271-317.
- Ogrinc, N., Monperrus, M., Kotnik, J., Fajon, V., Vidimova, K., Amouroux, D., Kocman, D., Tessier, E., Zizek, S. and Horvat, M., 2007. Distribution of mercury and methylmercury in deep-sea surficial sediments of the Mediterranean Sea. *Marine Chemistry*, 107: 31-48.
- Outridge, P., Macdonald, R.W., Wang, F., Stern, G. and Dasoor, A.P., 2008. A mass balance inventory of mercury in the Arctic Ocean. *Environmental Chemistry*, 5: 89-111.
- Outridge, P.M., Hobson, K.A., McNeely, R. and Dyke, A., 2002. A comparison of modern and preindustrial levels of mercury in the teeth of Beluga in the

- Mackenzie delta, Northwest Territories, and Walrus at Igloodok, Nunavut, Canada. *Arctic*, 55(2): 123-132.
- Outridge, P.M., Sanei, H., Stern, G.A., Hamilton, P.B. and Goodarzi, F., 2007. Evidence for Control of Mercury Accumulation Rates in Canadian High Arctic Lake Sediments by Variations of Aquatic Primary Productivity. *Environ. Sci. Technol.*, 41(15): 5259-5265.
- Pacyna, E.G. and Pacyna, J.M., 2002. Global Emission of Mercury from Anthropogenic Sources in 1995. *Water, Air, & Soil Pollution*, 137(1): 149-165.
- Pacyna, E.G., Pacyna, J.M., Steenhuisen, F. and Wilson, S., 2006. Global anthropogenic mercury emission inventory for 2000. *Atmospheric Environment*, 40(22): 4048-4063.
- Pacyna, J.M. and Winchester, J.W., 1990. Contamination of the global environment as observed in the Arctic. *Palaeogeography, Palaeoclimatology, Palaeoecology*, 82: 149-157.
- Park, K.S., Seo, Y.C., Lee, S.J. and Lee, J.H., 2008. Emission and speciation of mercury from various combustion sources. *Powder Technology*, 180(1-2): 151.
- Pazerniuk, M., 2007. Total and Methyl Mercury Levels in Hudson Bay Zooplankton: Spatial Trends and Processes, University of Manitoba, Winnipeg.
- Perry, E., Norton, S.A., Kamman, N.C., Lorey, P.M. and Driscoll, C.T., 2005. Deconstruction of Historic Mercury Accumulation in Lake Sediments, Northeastern United States. *Ecotoxicology*, 14(1): 85-99.
- Renzoni, A., Zino, F. and Franchi, E., 1998. Mercury Levels along the Food Chain and Risk for Exposed Populations. *Environmental Research*, 77(2): 68-72.
- Rustam, H. and Hamdi, T., 1974. Methyl Mercury Poisoning in Iraq. *Brain*, 97: 499-510.
- Sanei, H. and Goodarzi, F., 2006. Relationship between organic matter and mercury in recent lake sediment: The physical-geochemical aspects. *Applied Geochemistry*, 21: 1900-1912.
- Schuster, P.F., Krabbenhoft, D.P., Naftz, D.L., Cecil, L.D., Olson, M.L., Dewild, J.F., Susong, D.D., Green, J.R. and Abbott, M.L., 2002. Atmospheric Mercury Deposition during the Last 270 Years: A Glacial Ice Core Record of Natural and

- Anthropogenic Sources. *Environmental Science & Technology*, 36(11): 2303-2310.
- Spurgeon, A., 2006. Prenatal methylmercury exposure and developmental outcomes: review of the evidence and discussion of future directions. *Environmental Health Perspectives*, 114(2): 307-312.
- St. Louis, V., Hintelmann, H., Graydon, J.A., Kirk, J.L., Barker, J., Dimock, B., Sharp, M.J. and Lehnerr, I., 2007. Methylated Mercury Species in Canadian High Arctic Marine Surface Waters and Snowpacks. *Environmental Science & Technology*, 41(18): 6433-6441.
- Stern, G., Sanei, H., Roach, P., Delaronde, J. and Outridge, P., 2009. Historical interrelated variations of mercury and aquatic organic matter in lake sediment cores from a sub-arctic lake in Yukon, Canada; further evidence toward the algal-mercury scavenging hypothesis. *Environmental Science and Technology*, in press.
- Streets, D.G., Zhang, Q. and Wu, Y., 2009. Projections of Global Mercury Emissions in 2050. *Environmental Science and Technology*, 43: 2983-2988.
- Strode, S.A., Jaegle', L., Selin, N.E., Jacob, D.J., Park, R.J., Yantosca, R.M., Mason, R.P. and Slemr, F., 2007. Air-sea exchange in the global mercury cycle. *Global Biogeochem. Cycles*, 21.
- Sun, L., Yin, X., Liu, X., Zhu, R., Xie, Z. and Wang, Y., 2006. A 2000-year record of mercury and ancient civilizations in seal hairs from King George Island, West Antarctica. *Science of The Total Environment*, 368(1): 236.
- Sunderland, E.M., Gobas, F.A., Branfireun, B.A. and Heyes, A., 2006. Environmental controls on the speciation and distribution of mercury in coastal sediments. *Marine Chemistry*, 102: 111-123.
- Sunderland, E.M., Krabbenhoft, D.P., Moreau, J.W., Strode, S.A. and Landing, W.M., 2009. Mercury sources, distribution, and bioavailability in the North Pacific Ocean: Insights from data and models. *Global Biogeochem. Cycles*, 23.
- Sunderland, E.M. and Mason, R.P., 2007. Human impacts on open ocean mercury concentrations. *Global Biogeochem. Cycles*, 21.
- Takeuchi, T., Morikawa, N., Matsumoto, H. and Shiraishi, Y., 1962. A pathological study of Minamata disease in Japan. *Acta Neuropathologica*, 2(1): 40-57.

- Thompson, D.R., Furness, R.W. and Walsh, P.M., 1992. Historical changes in mercury concentrations in the marine ecosystem of the north and north-east Atlantic ocean as indicated by seabird feathers, *Journal of Applied Ecology*. Blackwell Publishing Limited, pp. 79-84.
- Trefey, J.H., Trocine, R.P., McElvaine, M.L., Rember, R.D. and Hawkins, L.T., 2007. Total mercury and methylmercury in sediments near offshore drilling sites in the Gulf of Mexico. *Environ. Geol.*, 53: 375-385.
- Van Oostdam, J. et al., 2005. Human health implications of environmental contaminants in Arctic Canada: A review. *Science of The Total Environment*, 351-352: 165-246.
- van Wijngaarden, E., Beck, C., Shamlaye, C.F., Cernichiari, E., Davidson, P.W., Myers, G.J. and Clarkson, T.W., 2006. Benchmark concentrations for methyl mercury obtained from the 9-year follow-up of the Seychelles Child Development Study. *NeuroToxicology*, 27(5): 702-709.
- Wagemann, R., Trebacz, E., Boila, G. and Lockhart, W.L., 1998. Methylmercury and total mercury in tissues of arctic marine mammals. *The Science of The Total Environment*, 218(1): 19-31.
- Watras, C.J., Back, R.C., Halvorsen, S., Hudson, R.J.M., Morrison, K.A. and Wentz, S.P., 1998. Bioaccumulation of mercury in pelagic freshwater food webs. *Science of The Total Environment*, 219(2-3): 183-208.
- Wein, E.E., Freeman, M.M. and Makus, J.C., 1996. Use of Preference for Traditional Foods among the Belcher Island Inuit. *Arctic*, 49(3): 256-264.
- WHO, 2003. *Elemental Mercury and Inorganic Mercury Compounds: Human Health Aspects*, World Health Organization, Geneva, Switzerland.
- WHO, 2005. *World Health Organization Policy Paper: Mercury in Health Care*, World Health Organization, Geneva, Switzerland.
- WHO, 2008. *Guidance for identifying populations at risk from mercury exposure*, World Health Organization, Geneva, Switzerland.

CHAPTER 2

Contemporary and Preindustrial Mass Budgets of Mercury in the Hudson Bay Marine System: The Role of Sediment Recycling

Abstract

Based on extensive sampling of the rivers, troposphere, seawater and sediments, mercury (Hg) mass budgets are constructed for both contemporary and preindustrial times in the Hudson Bay Marine System (HBS) to probe sources and pathways of Hg and their responses to the projected climate change. The contemporary total Hg inventory in the HBS is estimated to be 98 t, about 1 % of which is present in the biotic systems and the remainder in the abiotic systems. The total contemporary Hg influx and outflux, around 6.3 t/yr each, represent a 2-fold increase from the preindustrial fluxes. The most notable changes are in the atmospheric flux, which has gone from a nearly neutral (0.1 t/yr) to source term (1.5 t/yr), increased river inputs (which may also reflect increased atmospheric deposition to the HBS watershed) and in the sedimentary burial flux which has increased by 2.4 t/yr over preindustrial values, implying that much of the modern Hg loading entering this system is buried in the sediments. The capacity to drive increased Hg loading from the atmosphere to sediment burial may be supported by the resuspension of an extraordinarily large flux (120 t/yr) of shallow-water glacial sediments uncontaminated by anthropogenic Hg, which could scavenge Hg from the water column before being transported to the deeper accumulative basins. Under the projected climate warming in the region, the rate of the sediment recycling pump will likely increase due to

enhanced Hg scavenging by increasing biological productivity, and thus strengthen atmosphere-ocean Hg exchanges in the HBS.

2.0 Introduction

The sub-Arctic HBS, including Hudson Bay, Foxe Basin, and Hudson Strait (Figure 2-1), is the largest inland sea in the world with a total surface area of 1.24×10^6 km². It contains the most southerly penetration of Arctic marine water, and supports the most southern Arctic marine ecosystems in the world (Stewart and Lockhart, 2005). Exhibiting a general counter-clockwise circulation around its margin, the coastal freshwater corridor of the HBS is fed by large riverine inputs (carbon, freshwater) from a vast watershed in the heart of North America, and is the important location for primary production and higher trophic levels (seals, belugas, polar bears) of the marine ecosystem. The HBS is also highly susceptible to climate change and is projected to become ice-free for most of the year if the current warming trend continues (Gagnon and Gough, 2005; Gough and Wolfe, 2001). Despite its location in the vanguard of polar change, the HBS and its potential response to global change has been largely overlooked by most scientific endeavours until recently.

Similar to mammals from the Beaufort Sea of the Arctic Ocean, marine mammals from the HBS in recent years have been found to contain very high Hg concentrations. For example, beluga whales from the Arviat region of western Hudson Bay averaged 10.1 µg/g (wet weight) Hg in liver, 3.5 µg/g in kidney, 0.9 µg/g in muscle, and 0.3 µg/g in muktuk (Lockhart et al., 2005; Stern and Lockhart, 2007), near or well above the recommended 0.5 µg/g Canadian guideline for human consumption (CFIA, 2001).

Similar Hg levels are found in beluga from other regions of Hudson Bay (Lockhart et al., 2005; Stern and Lockhart, 2007), raising concerns for both the health of the animals and the northern residents who consume these tissues as part of their traditional diet.

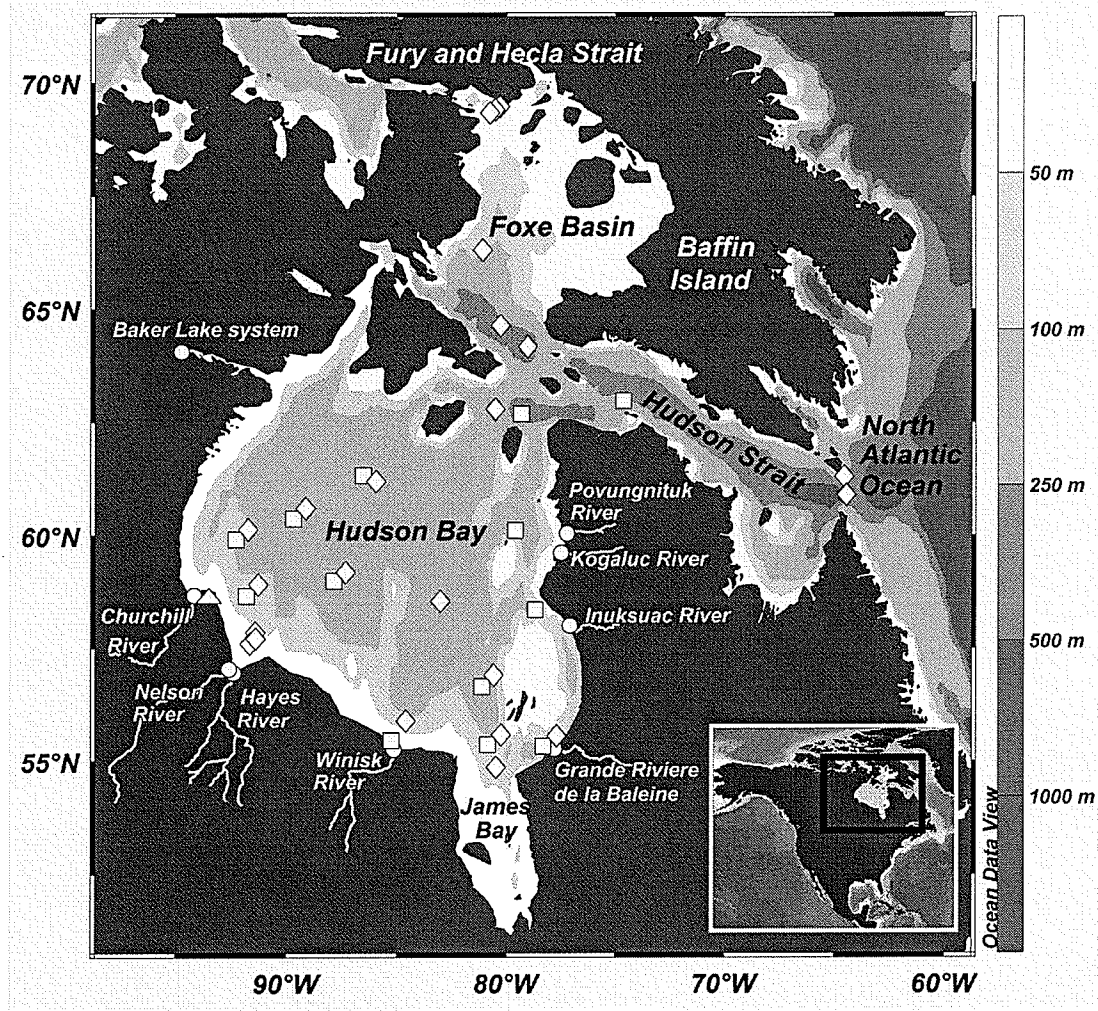


Figure 2-1. Hydrographical components and bathymetry of the Hudson Bay system, showing the sampling locations for rivers (circles), marine waters (diamonds), marine sediment cores (squares), and air (triangle). The map was created using Ocean Data View (<http://odv.awi.de>).

The relative importance of sources and processes underpinning Hg bioaccumulation in marine mammals of the HBS remains unclear. Hg sources include

local geological background and human activities, while possible pathways include coastal erosion, regional and global long-range transport via the atmosphere, oceans, and rivers. Processes complicating this picture include bioaccumulation and biomagnification within food webs as well as transport of Hg along migratory pathways by the biota themselves, e.g., (Blais et al., 2007). As part of the Canadian-led ArcticNet research program, extensive studies have recently been conducted on most of these pathways in the HBS. Based on this work, we present here the first mass budgets for Hg in the HBS for both contemporary and preindustrial times. The value of such mass budgets, which have been constructed for the global ocean (Lamborg et al., 2002; Mason and Sheu, 2002; Sunderland and Mason, 2007), the Mediterranean Sea (Rajar et al., 2007), and most recently the Arctic Ocean (Outridge et al., 2008), is that they provide the context within which major pathways and reservoirs of Hg can be assigned and compared, and time frames over which such reservoirs might be changed. Ultimately, a mass budget can be used to address the question of how Hg trends in marine mammals relate to human disturbance of the regional and global Hg cycle.

2.1 Experimental Methods

2.1.1 Study Area

The HBS in this study includes all the marine waters enclosed by the North American mainland and Baffin Island (Figure 2-1, Table 2-1), similar to the definition used by Saucier et al. (Saucier et al., 2004). Three directly connected basins are included: Hudson Bay (including James Bay), Foxe Basin, and Hudson Strait. Limited exchange between the HBS and the global oceans occurs in Foxe Basin and Hudson Strait. Arctic

Ocean water enters Foxe Basin through Fury and Hecla Strait and then enters Hudson Bay primarily along the west coast. Surface currents circulate within Hudson Bay cyclonically and then exit into Hudson Strait where they continue along a southern boundary current to the North Atlantic Ocean. Some North Atlantic and Arctic Ocean water enters along the northern shore of Hudson Strait where it re-circulates and mixes with water exiting Hudson Bay, before re-entering the North Atlantic Ocean (Straneo and Saucier, 2008). Most of the exchange between the HBS and the North Atlantic Ocean occurs in the upper 100 m (Drinkwater, 1988); only a small amount of North Atlantic water contributes to deeper water masses of the HBS.

Table 2-1. The Hudson Bay Marine System as defined in this study

Constituents	Surface Area (10³ km²)^a	Volume (10³ km³)^a	Mean depth (m)^a
Hudson Bay (including James Bay)	841	86	103
Foxe Basin	205 ^b	15 ^c	75 ^c
Hudson Strait	194	35	178
Entire HBS	1240 ^d	137 ^d	-
Arctic Ocean (excluding HBS)	9540	13000	1360
Global Ocean	362000	1350000	3730

^a Jakobsson (2002).

^b Calculated from the difference between the entire HBS and the other constituents.

^c Estimated from Jakobsson (2002).

^d Sum of all the constituents.

The HBS spans nearly 20° of latitude and borders four distinct terrestrial ecozones (south to north: Hudson Plains, Taiga Shield, Southern Arctic, Northern Arctic), while all marine waters fall within the same marine ecozone (Arctic

Archipelago) (Marshall et al., 1996; Wiken, 1986). However, surface temperatures and salinities are moderately warmer and fresher, respectively, in James Bay and to a lesser extent, the eastern and southern coasts, compared to the remainder of the HBS (Stewart and Lockhart, 2005). Correspondingly, the distribution of terrestrial and marine biota follows latitudinal gradients. The extensive HBS watershed ($> 3.7 \times 10^6 \text{ km}^2$), delivers approximately $940 \text{ km}^3/\text{yr}$ of water from the North American continent, of which $650 \text{ km}^3/\text{yr}$ empties directly into Hudson Bay (Déry et al., 2005; Straneo and Saucier, 2008). Consistent bathymetry (Figure 2-1) with few upwelling regions supports the stability of these freshwater inputs and promotes the establishment of a brackish surface layer throughout Hudson Bay, and to a lesser extent, Hudson Strait. The majority of Foxe Basin does not stratify due to shallow water depth and high wind stress.

The HBS is also the largest body of water in the world to experience a cryogenic cycle that includes completely ice covered (late winter: December - May) and completely open water (late summer: August – November) periods (Saucier et al., 2004). During the ice covered period, small intermittent leads open up between land-fast ice and mobile pack ice, near islands, and in Hudson Strait.

Mean daily air temperatures range from -30° C to -20° C in January and 7° C to 15° C in July, in northern and southern regions of the HBS, respectively (Environment Canada National Climate Data and Information Archive; <http://www.ec.gc.ca>. Accessed on April 11, 2008). Snowfall exceeds rainfall throughout Hudson Bay by nearly an order of magnitude and both types of precipitation follow latitudinal and longitudinal gradients with higher precipitation in the south and east, and less precipitation in the north and west. Maximum mean annual rainfall (494 mm) and snowfall (257 cm) in the HBS peak

in the south and east, respectively. The lowest rainfall (102 mm) and snowfall (183 cm) occur in the north-west region of the HBS.

Mass balance budgets of water and sediment in the HBS are shown in Table 2-2. Whereas the influx and outflux of water in the HBS are relatively well established (Déry et al., 2005) (Straneo and Saucier, 2008), very limited data are available for the sediment fluxes in the HBS. The sediment influxes and outfluxes in Table 2-2 represent the first effort in establishing a sediment mass balance budget for the HBS; the details are described in the footnotes of the table and discussed in the corresponding sections below. The most striking feature in the sediment budget is the extraordinarily large flux (120 t/yr) of resuspended sediment in the HBS, which is expected to play a major role in Hg dynamics in the HBS.

2.2.2 Water Sampling and Analysis of Hg

River and marine sampling locations are shown in Figure 2-1. Marine water samples were collected during three separate cruises in the late summer and fall (August to November), 2005 to 2007 from onboard the Canadian Research Icebreaker CCGS *Amundsen* using regular 18-L Niskin-style PVC sample bottles attached to a remotely controlled rosette water sampler. Sample depths were determined based on real-time measurements of water salinity and temperature during the rosette downcast. River water samples were collected from 2005 to 2007 during high (Nelson and Hayes Rivers and Baker Lake system), high and low (Churchill) and low flow (Kogaluc, Povirmituq, Winisk, Great Whale and Nastapoca Rivers) periods. Rivers were sampled at their confluence with Hudson Bay using a 5-L Teflon coated Niskin bottle (General Oceanics,

Miami, FL) or by hand using trace metal sampling techniques. Unfiltered water samples were collected at all marine and river sites for measurement of total Hg (HgT), while at some locations pre-cleaned and pre-tested filter cups (Nalgene, Rochester, NY) or a peristaltic pump with Polypro GH filters (Gelman) and a Teflon filter head were used to collect dissolved Hg (HgD) samples. HgD is operationally defined here as the Hg remaining in the sample after filtration through a 0.45 μm pore-size filter. Replicate samples and procedural field blanks were collected at each sampling site.

Hg samples were stored in 50-mL new, unused sterile Falcon polypropylene tubes (VWR) routinely batch-tested for background Hg levels by incubating several tubes from each package with ultra-pure MilliQ water and ultra-pure HCl (JT Baker, Phillipsburg NJ) for several hours, and analyzing the Hg content in the water. All tubes tested showed Hg concentrations below the detection limit (0.04 ng/L). Samples were preserved with 0.5% v/v ultra-pure HCl in the field within 2 hr of collection and refrigerated until analysis. The clean-hands-dirty-hands trace metal sampling techniques (Fitzgerald, 1999) were followed strictly to minimize potential contamination of samples.

The analysis of Hg in seawater samples was performed by cold-vapour atomic fluorescence spectroscopy (CVAFS) on a Tekran 2600 Hg analyzer in Class 10-1000 clean-rooms at the metal-free, Ultra-Clean Trace Elements Laboratory (UCTEL) of the University of Manitoba, following U.S. EPA Method 1631 as described previously (Leitch et al., 2007). Certified reference materials (CRMs) ORMS-3 (certified river water; National Research Council of Canada) and BCR-579 (certified coastal seawater; Institute for Reference Materials and Measurements, European Union) were used for quality control by analyzing one CRM and two analytical blanks per batch of 12 samples.

CRM results were within 10 % of the certified value (n > 35). Further laboratory QA/QC was carried out twice per year as part of the inter-laboratory comparison program under the Collaborative Mercury Research Network (COMERN) and the Metals in the Human Environment Research Network (MITHE-RN).

Sample replicates with a coefficient of variation < 10 % and from sampling events with procedural field blanks < 10 % of the replicated sample mean have been considered in this study; replicates not meeting these criteria have been excluded from further analysis. All fresh and marine water Hg values represent replicated field sample means.

Table 2-2. Water and sediment fluxes of the Hudson Bay System

Constituents	Flux		
	Low	High	Best Estimate
Water (km ³ /yr) ^a			
Riverine	892	948 ^b	940
Precipitation-Evaporation	10	50	30
Oceanic			
Arctic (Fury and Hecla Strait)	1300	3200	2200
Net Atlantic (Hudson Strait)	3170	6300	-3170
Water Inputs - Outputs			0
Sediment (10 ⁶ t/yr)			
Riverine ^c	8.2	11.4	10.2
Atmospheric ^d	0.71	0.77	0.74
Coastal erosion	18 ^e	27.5 ^f	18 ^e
Net oceanic ^g			< -1
Re-suspension ^h			120
Sedimentation ⁱ	-78	-216	-147
Sediment Inputs – Outputs			~0

(Positive and negative numbers denote additions to and losses from the system, respectively)

^a Straneo and Saucier (2008), unless otherwise specified.

^b Shiklomanov and Shiklomanov (2003)

^c Suspended sediment concentrations primarily from Environment Canada (2004),; also Nelson River data from Baker (1989), G. McCullough (pers. communication),; Nunavut data from Jefferies et al. (1994). Estimated Rupert, Broadback and Nottaway River fluxes (d'Anglejan, 1980) scaled to total runoff for east James Bay region. Estimated Great Whale River fluxes (Hudon et al., 1996) scaled to total runoff for Quebec region.

^d Prorated from the dry deposition flux range of 570 mg/m²/yr to 624 mg/m²/yr for aeolian material in the Arctic Ocean (Stein and Macdonald, 2004) to the total surface area of the HBS.

^e Prorated from a thermal erosion rate of ~1000 t/yr/km in eastern Hudson Bay (Zevenhuizen et al., 1994) to a total of ~18310 km of the Hudson Bay shoreline that has at least some unconsolidated coastal cliffs (Martini, 1986; Stewart and Lockhart, 2005).

^f Based on the mean thermal erosion rate of the Laptev and East Siberian Seas (Grigoriev et al., 2004)

^g Assuming a maximum suspended sediment concentration of 1 mg/L in seawater.

^h Estimated from the difference of total sediment influx and outflux. See the text for details.

ⁱ Estimated from applying the mean and the standard deviation of the sedimentation rate (0.12 ± 0.07 g/cm² yr) to 10 % of the total HBS surface area.

2.2.3 Sediment Sampling and Analysis of Hg

Marine sediment samples were collected from 13 box cores taken in 2005 from onboard the CCGS *Amundsen* using a box corer with a surface collection area of 0.1 m² and a maximum penetration depth in the seafloor of 50 cm (Figure 2-2). Coring locations were determined by using bathymetry and sub-bottom profiling data from a Knudsen K320R sub-bottom profiler and a Kongsberg-Simrad EM300 to select areas with sufficient sediment accumulation. Upon retrieval any standing water on top of the core was drained slowly and sub-sectioning began within 1 hr of collection. Between 14 and 20 sub-sections were collected per core at a vertical resolution of 1 cm (top 10 cm), 2 cm (10 – 20 cm depths) or 5 cm (20 cm downwards) after discarding material in contact with the box core walls. Each layer was collected separately using acetone-cleaned stainless steel hand tools, homogenized in stringently pre-cleaned 500 mL I-Chem glass jars (VWR) and immediately sub-sampled for Hg and supporting chemical parameters. Sediment samples were frozen at -20 °C immediately after sub-sampling and transported frozen to the laboratory where they remained in storage at -30 °C until freeze drying. Freeze dried sediments were subsequently stored in the dark at room temperature.

Hg was extracted from freeze dried sediments by closed vessel microwave digestion with HNO₃ following U.S EPA Method 3051 on a Microwave Assisted Reaction System (MARS; CEM Corporation, NC, U.S.A). The digestants were diluted and analyzed by CVAFS following the same procedure described above for water samples. Procedural blanks, analytical replicates and the CRM MESS-3 (marine sediments) from the NRCC were digested and analyzed with each group of samples in the same manner for QA/QC purposes. Analytical accuracy was within 7.7 % of the certified value for Hg concentration (n = 36). All sediment Hg values represent analytical replicate means.



Figure 2-2. Collection of a box core and preparation for sectioning. Top Left: After the box core has been lowered quickly to the sediments at ~ 1 m/s and penetrates the sediments up to 50 cm deep, a swing arm closes the bottom of the box core and it is retrieved slowly by a winch onto the ship deck. Bottom Left: Careful removal of the box core from the frame preserves the vertical structure of the sediments. Right: One face of the box core is removed and all sediment in contact with the box core walls is discarded before sectioning of the core begins.

2.2.4 Atmospheric Monitoring of Hg

Gaseous elemental mercury (GEM) in the lower troposphere was monitored throughout May 2005 to May 2007 near the Churchill Northern Studies Center (CNSC; 58.74 °N, 93.82 °W), Churchill, Manitoba with an automated Tekran 2537A instrument with a zero-air generator and an air intake located 5 m above the ground. From March to October 2006 reactive gaseous mercury (RGM) and particulate mercury (pHg) were also monitored at the same site with an automated Tekran 1130/1135/2537A system. GEM measurements were taken every 5 min, and RGM and pHg measurements every 2 hr. Internal calibration of instruments occurred every 23 hr and external calibrations were performed bimonthly throughout most of the sampling period.

2.2.5 Evasion of Dissolved Gaseous Mercury

The magnitude of the ocean-atmosphere exchange of Hg(0) was estimated using a two-layer thin-film model similar to that used by (Poissant et al., 2000). This model estimates the net Hg(0) flux between the ocean and atmosphere based on the concentration gradients of Hg(0) in the air and water, Henry's Law constant and the mass transfer coefficient of Hg in water, and takes the general form:

$$F = -k_w(RT[GEM] / KH - [DGM]) \quad (1)$$

where F = flux ($\text{ng/m}^2 \text{ s}$), k_w = mass transfer velocity of Hg in the thin film on the water side, R = the ideal gas law constant ($\text{atm/m}^3 \text{ mol K}$), $[GEM]$ = gaseous elemental Hg concentration in air (ng/m^3), $[DGM]_w$ = dissolved gaseous elemental Hg

concentration in water (ng/m³), and KH = Henry's Law constant (atm/mol m³). The value of kw may be determined according to the method of (Liss and Merlivat, 1986) (for wind speeds between 3.6 and 13 m/s):

$$k_w = 2.8 \times 10^{-6} (2.8U_{10} - 9.6)(Sc_{Hg}/600)^{-0.5} \quad (2)$$

where U₁₀ is the wind speed at 10 m above the sea surface and Sc_{Hg} is the Schmidt number of Hg which is described by

$$Sc_{Hg} = \eta T / \rho DT, \quad (3)$$

where ηT = the dynamic viscosity of water at temperature T (K), ρ = the density of water (g/cm³) and DT = the diffusivity of Hg(0) in water (cm²/s) where

$$DT = D_{298.15} \times (T / 298.15) \times (\eta_{298.15} / \eta T) \quad (4)$$

2.2.6 Ancillary Data

Ancillary water mass parameters (salinity, temperature, pressure) were collected from the CCGS *Amundsen* using a Sea-Bird CTD that simultaneously measured the water column during the rosette cast for sample collection. Data from the CTD was rigorously analyzed with SBE Data Processing 5.37 software.

2.3 Results

2.3.1 Hg in the Marine Waters of the HBS

Marine water column HgT concentrations were measured throughout the HBS in all three basins and in regions of marine water mass exchange with the Arctic Ocean and North Atlantic Ocean. The overall average HgT measured in the HBS was 0.77 ± 0.35 ng/L (mean \pm s.d., $n = 124$), higher than that reported in the North Atlantic (0.48 ± 0.32 ng/L; Mason et al. 1998). This is likely due to the shallow depth of the HBS which is essentially a mediterranean sea. In particular, as shown in Figure 2-1, the majority of the measurements were sited in the shallow coastal corridor of Hudson Bay and within the offshore entrainment of river water (surface salinity 23 - 28). Consequently, differences were observed between the basins composing the HBS.

The lowest mean HgT levels in the HBS were observed in Foxe Basin (Figure 2-3A), averaging 0.48 ± 0.07 ng/L. This value is similar to that measured in waters from the Canadian Arctic Archipelago (0.47 ± 0.1 ng/L), which is the source of marine water to this basin. No obvious vertical gradients were found in the Hg profiles in this shallow water column of Foxe Basin (mean water depth ca. 75 m). Upper (25 m) and lower (64 m) depths at the east end of Fury & Hecla Strait displayed similar HgT levels (0.44 ± 0.04 ng/L and 0.48 ± 0.02 ng/L, respectively) which most likely can be attributed to intense mixing in the narrow and shallow channel; temperature and salinity distributions indicated that this water was well mixed and represented a nearly homogenous unit. Similar observations of a well mixed water column and vertical Hg profiles were observed in central and southern Foxe Basin, where HgT measured 0.49 to 0.59 ng/L.

Dissolved Hg measured at two stations in Foxe Basin accounted for 83 – 87 % of HgT implying that HgP composes a very small fraction of the Hg content in this basin despite close contact with the sediments.

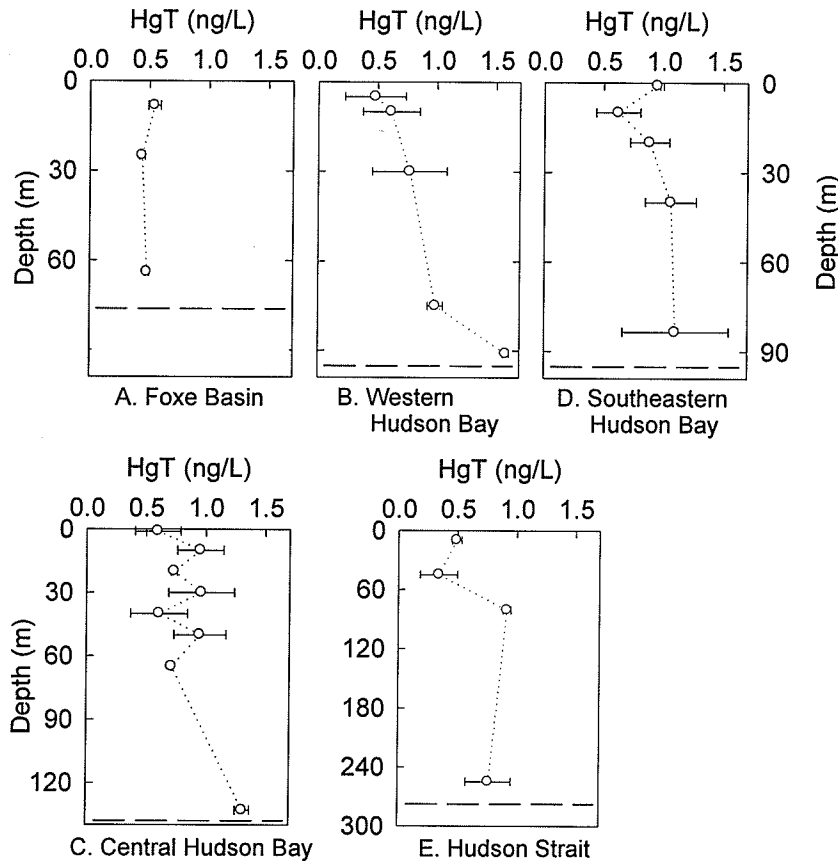


Figure 2-3. Regional depth profiles of HgT concentrations in the HBS. Each region is composed of 3 to 5 stations (n = 2 to 8 per depth). Error bars are standard deviations of the mean; dashed line represents the approximate depth of the region.

Higher mean HgT levels were measured in Hudson Bay than in the other basins (0.82 ± 0.36 ng/L; Figure 2-3B-D). In contrast to Foxe Basin, vertical stratification is extensive in Hudson Bay and a surface mixed layer (SML; as defined by Kara et al., (2000)) depth averaging 20 m was determined based on CTD data. Regional profiles demonstrated lower HgT concentrations in surface waters compared to deeper waters and highest HgT levels were observed in at depths near the sediment surface. Overall, HgT

concentrations within the SML of Hudson Bay (0.66 ± 0.31 ng/L) differed from those in the deeper layer (0.97 ± 0.34 ng/L) based on a two-tailed t-test ($p = 0.002$), suggesting vertical flux or benthic influence in establishing the Hg distribution. At three stations in central Hudson Bay, HgD was measured and accounted for 75 – 90 % of HgT. Despite its greater water depth, temperature and salinity profiles in Hudson Strait did not demonstrate a consistent surface mixed layer. Mean HgT values in Hudson Strait (0.64 ± 0.34 ng/L; Figure 2-3E) were between those measured in Hudson Bay and Foxe Basin.

Currents in Hudson Strait import North Atlantic water but the majority does not penetrate Hudson Bay or Foxe Basin. Rather, most imported North Atlantic water recirculates in Hudson Strait and mixes with outflowing Hudson Bay and Foxe Basin water before leaving along the southern Hudson Strait coast (Straneo and Saucier, 2008). The estimated marine output to the North Atlantic from the HBS is close to 0.1 Sv ($3170 \text{ km}^3/\text{yr}$) (Table 2-2) (Drinkwater, 1988; Straneo and Saucier, 2008). A cross section of HgT measured at the east end of Hudson Strait showed a mean HgT concentration of 0.57 ± 0.17 ng/L in the upper 100 m, which composes the primary region of marine water advection from the HBS. Using the net outflow through Hudson Strait to the North Atlantic of 3170 km^3 annually and a mean HgT concentration of 0.57 ng/L, the net oceanic Hg outflux to the Atlantic Ocean was estimated to be 1.7 ± 0.5 t/yr.

2.3.2 Oceanic Hg Fluxes to the HBS

Water mass exchange between the global ocean and the HBS occurs only through Fury and Hecla Strait and Hudson Strait (Figure 2-1). Currents in Fury and Hecla Strait transport up to 0.1 Sv into Foxe Basin during the summer and 0.04 Sv during the winter

(Drinkwater, 1988); an average oceanic influx of Arctic marine water of 0.07 Sv (or 2200 km³ /yr) is used in this study (Straneo and Saucier, 2008) (Table 2-2). Water export through Fury and Hecla Strait is negligible according to currently available measurements. By using measurements of Hg_T made along a cross section of Fury and Hecla Strait (0.45 ± 0.04 ng/L) and the net annual inflow of 2200 km³, the annual oceanic flux of Hg through this strait is calculated to be 1 ± 0.1 t/yr.

2.3.3 Air-sea Exchange of Hg

Atmospheric fluxes of Hg include wet and dry deposition of Hg(II) in the forms of RGM and pHg, and evasional flux of Hg(0). In the Arctic, deposition is enhanced by atmospheric mercury depletion events (AMDEs) that occur during polar sunrise when GEM is oxidized photochemically to RGM and subsequently deposited to the surface environment (Schroeder et al., 1998). The occurrence of AMDEs in the HBS has been reported in Kuujjuarapik, QC (Poissant and Pilote, 2003) and Churchill, MB (Kirk et al., 2006). However, increasing evidence suggests that the majority of AMDE-deposited Hg(II) in snow packs is photo-reduced and re-emitted back to the atmosphere (Dommergue et al., 2003; Kirk et al., 2006; Lalonde et al., 2002). The net contribution of the AMDEs to the Hg load to the polar marine ecosystem depends in part on the difference between Hg deposited to the snow pack and that deposited to the edge of the ice pack or polynyas where it could enter the water column and be exposed to different redox mechanisms than on the snow surface. Thus, the net contribution of AMDEs to the polar marine ecosystems remains a subject of debate.

The Global and Regional Atmospheric Heavy Metals Model (GRAHM) (Parisa et al., 2004) has been used to predict atmospheric Hg deposition specifically to Arctic and sub-Arctic regions, including the HBS. It estimated a total atmospheric Hg flux of 13.6 t/yr, including dry and wet Hg(II) deposition and Hg(0) evasion, and the contribution of the AMDEs. In contrast, recent global simulations based on the GEOS-Chem model, which includes a comprehensive assessment of both atmospheric deposition and Hg(0) exchange, suggest a much lower net atmospheric flux to the HBS region ranging from 0.3 to 3.5 t/yr (Strode et al., 2007).

Direct measurements on Hg(II) deposition and Hg(0) evasion have also been made at Churchill, MB. The total Hg contribution of spring melt (net wet + dry deposition in winter/spring including net AMDE loadings to the HBS has been estimated by Kirk et al. (2006) who used HgT concentrations in the snow pack on coastal sea-ice to suggest that only $0.21 \pm 0.17 \mu\text{g}/\text{m}^2$ is added annually during the spring, which is equivalent to 0.26 ± 0.2 t/yr.

The wet-only deposition of Hg in summer and fall has been measured from an automated station in Churchill which collected a Hg flux of $1.41 \mu\text{g}/\text{m}^2 \text{ yr}$ (Sanei et al., 2007), equivalent to 1.75 t/yr if scaled to the entire HBS. Since northern regions receive considerably less precipitation than southern regions, this is likely an over-estimate for the wet-only Hg deposition in summer and fall to the HBS.

No data are available on the dry deposition of Hg in the HBS region. However, the Arctic Ocean receives between 570 and 624 $\text{mg}/\text{m}^2/\text{yr}$ of aeolian particulate inputs, equivalent to 5.7 Mt/yr over its $9555 \times 10^3 \text{ km}^2$ surface area (Stein and Macdonald, 2004). Assuming a similar deposition rate in the HBS and a Hg concentration in Arctic

airborne dust similar to uncontaminated soils (0.06 ug/g d.w) (Bodek et al., 1988), an estimate of 0.015 ± 0.001 t/yr of Hg can be derived for dry deposition during summer and fall in the HBS.

Oceanic flux of Hg(0) demonstrates seasonal and latitudinal gradients throughout the global ocean, implying the importance of Hg(0) production via photo-catalytic and biological processes (Strode et al., 2007). The range of evasion in the HBS may be estimated by using evasion rates in the North Atlantic Ocean ($11 \mu\text{g}/\text{m}^2/\text{yr}$), (Mason et al., 1998) and the Arctic shelves ($4.76 \mu\text{g}/\text{m}^2/\text{yr}$), (Cossa et al., 1996) as the upper and lower boundaries, respectively, for the HBS. Based on free ocean-atmosphere exchange 5 months annually due to sea-ice cover (Saucier et al., 2004), these rates suggest 2.5 to 5.7 t/yr of Hg(0) is transferred from the ocean to the atmosphere by evasion.

Evasion may also be estimated using the method of Liss and Merlivat (1986). Although no data have been reported on DGM in the HBS, DGM measurements from the North Atlantic and Arctic Oceans and the Canadian Arctic Archipelago typically average 30 – 35 pg/L (Poulain et al., 2007; Temme et al., 2005), while our real-time GEM measurements in the lower troposphere of Churchill average $1.4 \text{ ng}/\text{m}^3$. The remaining environmental parameters required for Equation (1) have been provided by Saucier et al. (2004) specifically for the HBS. Considering a mean annual air temperature directly above the sea of $1.5 \text{ }^\circ\text{C}$, a mean annual wind speed at 10 m above the sea surface of 5 m/s, and a mean sea-surface salinity of 30 (Saucier et al., 2004), Equation (1) yields an evasion rate of $5.9 \mu\text{g}/\text{m}^2/\text{yr}$. This value is similar to the global average evasion rate of $7.2 \mu\text{g}/\text{m}^2/\text{yr}$ (Mason and Sheu, 2002) and falls between Arctic and North Atlantic rates. Assuming a similar period of free ocean-atmosphere exchange as above, evasion would

account for 3.0 t/yr of Hg(0) flux from the ocean to the atmosphere in the HBS. The mean annual flux of Hg(0) from the above two independent approaches is thus 3.7 ± 1.7 t/yr.

The net atmospheric Hg exchange to the HBS can then be calculated as:

$$\begin{aligned} \text{Net atmospheric exchange} &= \text{Net wet and dry deposition during winter and spring} \\ &+ \text{wet and dry deposition during summer and fall} \\ &- \text{evasion} \\ &= (0.26 \pm 0.2) + (1.75) + (0.015 \pm 0.001) - (3.7 \pm 1.7) = -1.7 \pm 1.7 \text{ t/yr} \quad (6) \end{aligned}$$

The measurement-based approach thus suggests that the atmosphere could be a net sink for Hg in the HBS ($-3.4 - 0$ t/yr). Combining the modeled and measurement-based approaches results in a large range in the estimate of the atmospheric contribution of Hg to the HBS on the order of -3.4 to 13.6 t/yr.

2.3.4 Riverine Hg Flux to the HBS

Measurements of Hg were made in 9 rivers that deliver a mean cumulative discharge of $243 \text{ km}^3/\text{yr}$ of freshwater to Hudson Bay (26 % of the total riverine discharge to the HBS) and represent all four bordering ecozones. HgT concentrations ranged from 0.72 ng/L to 3.47 ng/L (Table 2-3), averaging $2.07 \pm 0.92 \text{ ng/L}$, which is slightly above the average of 58 small rivers of the eastern seaboard of the U.S.A. ($1.8 \pm 1.3 \text{ ng/L}$; Peckenham et al., 2003) and considerably lower than that in the Mackenzie River ($7.2 \pm 4.3 \text{ ng/L}$) (Leitch et al., 2007).

A strong correlation between HgT concentration and annual freshwater discharge was observed across all rivers except for the two largest (Nelson River and Baker Lake

system) ($r^2 = 0.92$, $p < 0.001$; Figure 2-4), implying that different mechanisms regulate HgT levels in small and medium compared to large rivers in this system. A moderate correlation was also found between mean HgT concentration and latitude of the river mouth ($r^2 = 0.63$, $p = 0.019$; Figure 2-4), excluding the Churchill River for which large scale water diversion occurs. Accordingly, ecozone (i.e., geology, vegetation and climate) appeared to influence HgT levels; rivers draining the southern Hudson Plains (Churchill, Nelson, Hayes, and Winisk) exhibited significantly higher concentrations of 2.75 ± 0.56 ng/L, compared to 1.21 ± 0.36 ng/L for rivers draining the Southern Arctic (Baker Lake, Nastapoca, Kogaluc, and Povungnituk) ($p = 0.01$).

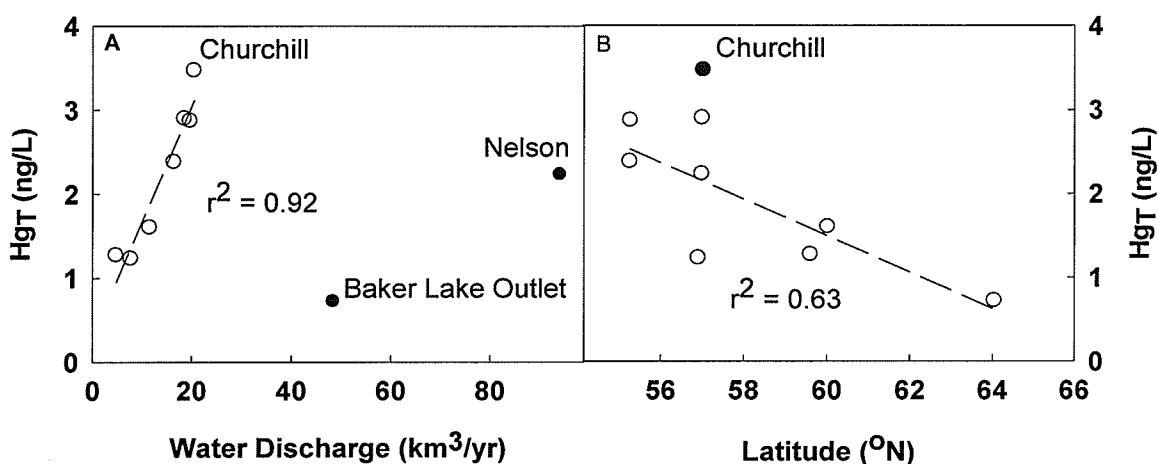


Figure 2-2. Relationships between the HgT concentration in river water and A) the water discharge, and B) the latitude of the river mouth. The rivers identified by the filled circles were excluded from the analysis.

Dissolved Hg (HgD, $<0.45 \mu\text{m}$) concentrations were determined in 6 of the 9 HBS rivers. HgD accounted for 85 % of HgT in the Nelson River, while the Hayes River demonstrated the lowest fraction of HgD (63 %) (Table 2-3). Overall, HgD predominated in the water column of the rivers measured, composing 63 to 96 % of HgT. Individual HgD fluxes range from 5 to 179 kg/yr among the rivers measured, while HgT fluxes

range from 6 kg/yr to 210 kg/yr (Table 2-3). Considering the sediment discharge in Table 2-3, this implies mean annual HgP in the range of 0.002 to 0.07 mg/kg and HgP fluxes on the order of 1 to 31 kg/yr.

The estimated cumulative annual river discharge to the HBS ranges from 892 km³/yr (Straneo and Saucier, 2008) to 948 km³/yr (Shiklomanov and Shiklomanov, 2003). Déry et al. (2005) observed that the cumulative total annual discharges from 42 rivers entering Hudson Bay and Hudson Strait varied by $\pm 22\%$ over a 36 year period. By using a cumulative annual discharge of 940 km³/yr after Straneo and Saucier (2007) and assuming similar variability throughout the HBS as for Hudson Bay, the range of Hg concentrations in the sampled rivers gives an annual HgT flux of 1.9 ± 1.0 t/yr (Table 2-3).

Table 2-3. Riverine Hg fluxes to the Hudson Bay System

Rivers	Discharge		Hg concentration (ng/L)			Hg flux (kg/yr)		
	Water ^a (km ³ /yr)	Sediment ^b (10 ⁶ t/yr)	HgD	HgP ^c	HgT	HgD	HgP ^c	HgT
Povungnituk	11.6	-	1.13	0.47	1.6	13	5.5	19
Kogaluc	4.9	-	1.05	0.22	1.27	5	1.1	6.2
Nastapoca	7.9	-	-	-	1.23	-	-	10
Grande Baleine	19.8	0.1d	2.28	0.59	2.87	45	11	57
Winisk	16.5	0.2d	-	-	2.38	-	-	39
Hayes	18.6	-	1.83	1.07	2.9	34	20	54
Nelson	94.2	0.74	1.9	0.33	2.23	179	31	210
Churchill	20.6	0.18	3.34	0.13	3.47	69	2.7	71
Baker Lake Outflow	48.5	-	-	-	0.72	-	-	35
Sub-total	243							501
All HBS rivers ^e	940							1940
Other Arctic Rivers:								
Mackenzie ^f	330	125	2.77	3.68	7.18	530	1640	2170

Ob ^g	405	16.5	0.56	-	-	530	820	1350
Lena ^g	525	17.6	1	-	-	1150	2900	4050
Yenisei ^g	626	5.9	0.3	-	-	410	310	720

^a Déry et al. (2005).

^b AMAP (1998).

^c Estimated from the difference between HgT and HgD.

^d Environment Canada (2004).

^e Prorated to the total water discharge.

^f Leitch et al. (2007).

^g Coquery et al. (1995).

(HgD: dissolved Hg; HgP: Particulate Hg; HgT: total Hg)

2.3.5 Coastal Erosion Hg Flux to the HBS

Although sub-aerial coastal erosion is an important source of sediment and hence probably Hg to most of the Arctic shelf seas (e.g., Grigoriev et al., 2004; Outridge et al., 2008), we expect that the supply rates of this process are much smaller along the rapidly emerging coastline of Hudson Bay; the present emergence rate is about 0.01 m/yr around the southern part of the Bay (Begin et al., 1993). Thermal erosion of permafrost along coastal cliffs is the only major driver for the erosion, and thus observed average annual erosion rates, even in susceptible areas, are relatively low (e.g., 0.6 m/yr - Zevenhuizen et al., 1994; compare with average coastal retreat rates of ~ 3 m/yr in the Arctic shelf seas - Grigoriev et al., 2004). Zevenhuizen et al. (1994) reported a sediment supply rate of about 1000 t/yr km due to thermal erosion along a 15 km stretch of coastline in eastern Hudson Bay, where the coastal cliffs contained 60 % fine-grained soils (Zevenhuizen et al., 1994). This rate of sediment supply is comparable to what occurs along rocky and non-icy coasts in the Arctic shelf seas (Grigoriev et al., 2004). Pro-rating this supply rate to the portion of the Hudson Bay shoreline that has at least some unconsolidated coastal cliffs (~18310 km; Martini, 1986; Stewart and Lockhart, 2005), we estimate a total

coastal erosion sediment supply of 18×10^6 t/yr (Table 2-2). An upper limit of 27.5 t/yr can be derived if we apply the mean thermal erosion rate of the Laptev and East Siberian Seas (Grigoriev et al. 2004). Applying an average Hg concentration of 14 ng/g as observed from deep portions of the HBS sediment cores (see below), the total Hg flux due to sub-aerial coastal erosion is estimated to be 0.25 – 0.38 t/yr.

2.3.6 Mercury Removal by Sedimentation

Sediment cores were obtained at 13 locations of the HBS (Figure 2-1), of which 11 were sited in Hudson Bay and 2 in Hudson Strait. Hg concentrations throughout the cores ranged from 8 to 54 ng/g (dry weight, d.w.), while surface sediment HgT was 30.3 ± 12.3 ng/g. Higher HgT was observed in surface layers compared to deeper layers in 9 of 13 cores, with the remainder demonstrating near-vertical profiles of Hg.

Sedimentation rates derived from ^{210}Pb data were 0.11 ± 0.07 g/cm²/yr in Hudson Bay and 0.12 ± 0.09 g/cm²/yr in Hudson Strait (Kuzyk et al., 2009a). No data are available for Foxe Basin, however with much of the northern part of the Basin less than 50 m deep and a major region of ice scour (Ingram and Prinsenber, 1998), it is unlikely that Foxe Basin is a permanent sink for sediments except in the southern Foxe Channel where depths reach > 200 m.

Although the derived sedimentation rates for Hudson Bay and western Hudson Strait fall within the range observed for the Arctic Ocean shelves (Stein and Macdonald, 2004), the cores were generally sited in or near areas where regional sedimentation maps developed from seismic data (Hendersen, 1989; Josenhans et al., 1988) show at least pockets of sediment accumulation. Postglacial sediments are indeed scarce in the central

part of Hudson Bay, and instead glacial sediments and glacial till are exposed across wide areas of the seafloor (Hendersen, 1989; Hill et al., 1999; Josenhans et al., 1988). Thus, the area of seafloor presently capturing the sedimentary Hg flux is much less than the total seafloor surface area. High-resolution seismic reflection data and core data also suggested that the deposition of post-glacial sediments was very limited in Hudson Strait (Andrews et al., 1994). Using the regional sedimentation map for Hudson Bay (Josenhans et al., 1988), we estimate that the area of post-glacial sedimentation is only $\sim 82600 \text{ km}^2$, or 10 % of the total surface area of Hudson Bay. Using an equivalent area of sediment capture for the remainder of the HBS and an average sedimentation rate for those cores collected in or near a significant mapped depositional area ($0.12 \pm 0.07 \text{ g/cm}^2/\text{yr}$) and the corresponding mean surface Hg concentration ($30.8 \pm 12.3 \text{ ng/g}$) yields a total sediment burial flux of $147 \pm 69 \times 10^6 \text{ t/yr}$ and a Hg flux of $4.5 \pm 3.2 \text{ t/yr}$.

2.3.7 Mercury Recycling via Sediment Resuspension

The total sediment burial flux ($147 \times 10^6 \text{ t/yr}$) is clearly not supported by the known external sediment sources to the Bay (river inputs $\sim 10 \times 10^6 \text{ t/yr}$, coastal erosion $\sim 18 \times 10^6 \text{ t/yr}$; Table 2-2), which implies a significant recycling component due to resuspension and lateral transport, as previously suggested by Henderson (1989) and Josenhans et al. (1988). Postglacial isostatic rebound in Hudson Bay means that unconsolidated material from tidal flats and shallow subtidal areas are constantly subjected to wave-base, storm surge and tidal current erosion (Zevenhuizen et al., 1994). Fine material, which is relatively abundant in coastal deposits ($\sim 60\%$; Zevenhuizen et al., 1994) because of deposition during the period of inundation of the postglacial Tyrrell

Sea, is thereby potentially available for transport to deeper areas. The sediment budget of the HBS is balanced by assuming a supply by resuspension of about 120×10^6 t/yr (Table 2-2). This quantity does not seem unreasonable considering that, at the present rate of isostatic rebound (0.01 m/yr in southern Hudson Bay; Bégin et al., 1993), four times as much sediment is potentially available for transport from the coastal area (0-20 m depth zone) of southern Hudson Bay alone (an area of about 46,900 km²).

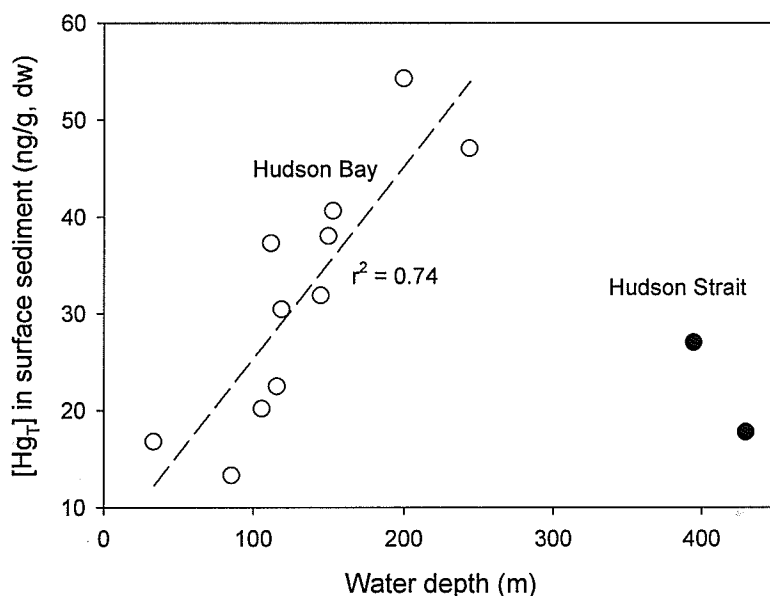


Figure 2-5. Relationship between the Hg_T concentration in surface sediment (top 1 cm) and the water depth.

Assuming the Hg concentration in these coastal materials, which are largely glacial, is similar to the deep sections of the sediment cores (~14 ng/g, which is equivalent to the mean Hg concentration in surface sediments in shallow areas – Figure 2-5), a recycled sedimentary Hg flux due to resuspension and lateral transport is estimated to be 1.7 t/yr.

Little is known about the total biotic Hg inventory in HBS. Table 2-4 presents current standing stock estimates and biotic Hg concentration data, which suggests a total biotic Hg pool of around 1 t. The largest biotic pool of Hg is found in phytoplankton, which contains 0.93 t of Hg throughout the entire HBS. About 40 kg of Hg is present in marine mammals, 70 % of which is in beluga whales. This is followed by fish and zooplankton which contain roughly 30 and 11 kg of Hg, respectively.

Table 2-4. Calculations of Biotic Hg Inventory in the HBS

Organisms	Population (x 1000)		Mean mass (kg)	Biomass		HgT (µg/g)	HgT Mass (kg)
	Range	Estimate		Total (10 ⁶ t)	% with Hg		
Beluga Whales	57.5 – 108.6 ^a	80.2	900	0.0722	40	1 ^b	28.9
Narwhal	2.2 – 9.9 ^c	5.1	1250	0.0638	40	1 ^d	2.6
Polar Bears	3.26 – 5.01 ^e	4.14	350	0.0145	40	0.1 ^f	0.058
Walrus	-	6.0 ^g	1000	0.06	40	0.1 ^h	0.24
Ringed Seal	-	516 ⁱ	57	0.294	40	0.5 ^d	5.9
Bearded Seal	-	84 ^j	225	0.189	40	0.5 ^k	3.8
Fish	-	-	-	0.294 ^l	100	0.1 ^m	29.4
Zooplankton	-	-	-	2.67 ⁿ	100	0.004 ^m	10.7
Phytoplankton	-	-	-	18.6 ^o	100	0.05 ^p	930
Total							1010

^a 95 % confidence limit (P. Richard, Department of Fisheries and Oceans Canada, unpublished data)

^b Lockhart et al. (2005)

^c (COSEWIC, 2004); (Richard, 1998)

^d (Wagemann et al., 1998)

^e (Aars et al., 2006); (Lunn et al., 1997)

^f (AMAP, 2005)

^g (COSEWIC, 2006)

^h (Born et al., 1981)

ⁱ (Smith, 1975)

^j Canadian Arctic Resources Committee (<http://www.carc.org/pubs/v19no3/2.htm>; accessed on April 14, 2008)

^k estimated as equal to ringed seals

^l estimated from (Outridge et al., 2008)

^m Pazerniuk (2007)

ⁿ Harvey et al. (Harvey et al., 2001), and the zooplankton density in Foxe Basin equal to half that in Hudson Bay

^o (Jones and Anderson, 1994; Roff and Legendre, 1986)

^p (Poulain et al., 2007)

2.4 Discussion

2.4.1 Contemporary Mercury Mass Budgets in the HBS

Current estimates of Hg fluxes to the HBS are associated with uncertainties due to the dynamic nature of the system and limited data. Strengths of these budgets, however, are that the components have been independently estimated and are supported by a relatively wide coverage of new Hg measurements. As shown in Table 2-5, the greatest uncertainty lies in the net atmospheric flux term because modeling and field data produce a wide range (-3.4 to 13.6 t/yr). Despite these uncertainties, it is reasonable to assume that Hg levels in the HBS are near steady-state but increasing slowly since the preindustrial time, as suggested for the Arctic Ocean and global oceans (Lamborg et al., 2002; Mason and Sheu, 2002; Outridge et al., 2008). If the estimated anthropogenic enrichment factor since industrialization for the global (25 %) or North Atlantic (57 %) oceans (Sunderland and Mason, 2007) can be applied to the HBS, the abiotic inventory of Hg would have been increasing at a rate of 0.13 or 0.23 t/yr, respectively. Based on these numbers, a “best estimate” of the net atmospheric flux is calculated to be ~1.5 t/yr, which is between the upper limit of the measurement-based estimate (0 t/yr; Equation (6)) and the modeled result from the GEOS-CHEM (0.3 – 3.5 t/yr)(Strode et al., 2007).

The estimates and the expected ranges of the Hg fluxes in the HBS, summarized in Table 2-5, can be schematically represented in a contemporary Hg mass budget for the

HBS (Figure 2-6B). The total Hg inventory in the HBS is 98 t, about 1 % of which (1 t) is present in the biotic systems and the rest in the abiotic systems. Annual Hg inputs and outputs are 6.3 and 6.2 t/yr, respectively. The net atmospheric deposition (1.5 t/yr), river transport (1.9 t/yr), and resuspension (1.7 t/yr) are the major sources of Hg to the HBS and similar in magnitude, while oceanic influx from the Arctic Ocean follows at roughly half the magnitude (1 t/yr), and coastal erosion contributes a negligible Hg flux to the HBS (0.25 t/yr). Sedimentation is the dominant removal mechanism of Hg at 4.5 t/yr, and oceanic outflux to the North Atlantic Ocean accounts for a remaining 1.7 t/yr.

Table 2-5. Estimates of contemporary and historic mercury fluxes to the HBS

Flux	Contemporary			Preindustrial
	Low	High	Best estimate	
Net Atmospheric	-3.4 ^a	13.6 ^b	1.5 ^c	0.1 ^d
Oceanic				
Arctic	0.9 ^e	1.1 ^e	1.0 ^e	0.7 ^f
Net North Atlantic	-1.2 ^g	-2.2 ^g	-1.7 ^g	-1.25 ^f
Riverine	0.9 ^h	2.9 ^h	1.9 ^h	0.6 ⁱ
Erosion	0.25 ^j	0.38 ^k	0.25 ^j	0.25 ^j
Sedimentation	-1.3 ^l	-7.7 ^l	-4.5 ^l	-2.1 ^m
Resuspension	-	-	1.7 ⁿ	1.7 ⁿ
Total			~0.1 ^o	~0 ^p

^a lower boundary from the measurement-based calculation (Equation (6)).

^b upper boundary from the GRHAM model (Ariya et al., 2004).

^c estimated by assuming the Hg inventory in the HBS is increasing at a rate similar to that for the North Atlantic Ocean (Sunderland and Mason, 2007).

^d estimated by assuming the preindustrial HBS was at steady-state.

^e based on the [HgT] range in Fury and Hecla Strait.

^f from the mean anthropogenic enrichment factor of the North Atlantic Oceans (Sunderland and Mason 2007).

^g based on the [HgT] range at the east end of Hudson Strait

^h based on the range of [HgT] and a $\pm 22\%$ variability in the annual water discharge of the rivers (Déry et al., 2005).

ⁱ assuming the preindustrial suspended sediment contained 60 ng/g Hg, similar to the uncontaminated surface soils (Bodek et al., 1988).

^j estimated from the thermal erosion rate of 1000 t/yr/km (Zevenhuizen et al., 1994); see the text for details.

^k estimated from the coastal retreat rate of 3 m/yr for Arctic shelf seas (Grigoriev et al., 2004).

^l Estimated from the mean and the standard deviation of Hg in surface sediments and the sediment flux shown in Table 2-2.

^m estimated from the mean Hg concentration from the deeper layers of the sediment cores and the sediment flux shown in Table 2-2.

ⁿ estimated from the mean Hg concentration from the deeper layers of the sediment cores and the resuspension sediment flux shown in Table 2-2.

^o assuming an anthropogenic enrichment factor of Hg in the HBS since the preindustrial time is similar to that in the North Atlantic Ocean (Sunderland and Mason, 2007).

^p assuming the Hg in the HBS was at steady state during preindustrial time.

The Hg residence time in the entire water column of the HBS is ~15 years, which is in good agreement with the residence time of deep water in Hudson Bay (Pett and Roff, 1982), and the Hg residence time in the upper layer (200 m) of the Arctic Ocean (15 years; Outridge et al., 2008). In a surface mixed layer of 25 m in Hudson Bay (total abiotic Hg of 13.9 t), the Hg residence time is calculated to be about 2 years, similar to the predicted residence time of the surface water layer in Hudson Bay (1-2 years) (Ingram and Prinsenbergh, 1998) and higher than that estimated for Hg on the global ocean shelves (8 months) (Cossa et al., 1996).

2.4.2 Preindustrial Mercury Mass Budget in the HBS

The Hg distribution patterns in the HBS sediment cores also allow us to propose a preindustrial Hg mass budget based on sediment fluxes of >150 years ago (i.e., at sediment depths where excess ²¹⁰Pb has decayed away and before the onset of the anthropocene). Most sediment cores displayed an enrichment of Hg in the surface layer (~ 30 - 40 ng/g), but decline to ~ 10 - 15 ng/g in deep layers. Hg concentrations in

sediments from Hudson Strait where there is little recent sedimentation are also very low (~ 20 ng/g), further indicating that the pre-industrial sediment (i.e., deep layers in depositional areas of Hudson Bay, and sediment in non-depositional Hudson Strait) contain low Hg material similar to glacial deposits.

Assuming that sediment capture by the basins of the HBS has remained unchanged over the past 200 years, a Hg content of 14 ng/g in deep sediment layers implies a preindustrial Hg burial rate of 2.1 t/yr in the HBS. Sunderland and Mason (2007) recently estimated that anthropogenic activities have increased surface global ocean and North Atlantic Ocean Hg reservoirs by 25 % and 57 %, respectively. Given similar increases in the HBS this implies a preindustrial Hg influx from the Arctic Ocean of 0.6 and 0.8 t/yr, an outflux to the Atlantic Ocean of 1.1 and 1.4 t/yr, and a total pre-industrial abiotic inventory of Hg in the HBS of 62 and 78 t, respectively. The pre-industrial riverine Hg flux can be estimated from the suspended sediment flux of the rivers (10.2×10^6 t/yr) by assuming the Hg concentration in the suspended sediment is equal to that in uncontaminated soils (60 ng/g; Bodek et al., 1988), which result in a riverine Hg flux of 0.6 t/yr. With the assumption of steady-state conditions for Hg in the pre-industrial HBS, the pre-industrial net atmospheric Hg flux is nearly neutral (0.1 t/yr). The pre-industrial Hg fluxes and Hg mass budget are summarized in Table 2-5 and Figure 2-6A.

2.4.3 Sedimentary Capture and Control of Hg in the HBS

From preindustrial to contemporary times, the most notable changes in the Hg budget are the increase in direct net atmospheric deposition (0.1 to 1.5 t/yr), river

transport (0.6 to 1.9 t/yr), and the sedimentary burial flux (2.1 to 4.5 t/yr). It is important to consider that increased atmospheric deposition to the watershed is also probably responsible for increased river transport of Hg, rather than direct geologic or anthropogenic developments. The observation that sediment Hg burial can account for the majority of the Hg additions implies that much of the modern Hg loading entering this system via air or river is buried in the sediments. Figure 2-6 describes a potential mechanism to bury Hg in the HBS, supported by a unique set of circumstances where shallow-water glacial sediments are resuspended and transported to the deeper accumulative basins, possibly in a series of progressive resuspension-sedimentation cycles.

The access to these glacial coastal sediments by resuspension processes is assured in the long term by post-glacial isostatic rebound which continues presently at up to 0.01 m/yr (Bégin et al., 1993), especially along the southern HBS coast. The particularly large sediment flux involved in resuspension transport (120 t/yr; Table 2-2) is likely not directly connected to atmospheric Hg inputs. Instead, particle producing processes in the HBS (i.e., autochthonous production) could scavenge Hg and deliver it to depth as found in global oceans (e.g., Mason and Sheu, 2001), where it becomes entrained into the resuspension transport pathway. It is possible that these connected processes transport Hg from the water into the basin sink in such a way as to support increased modern atmospheric Hg deposition in the HBS in much the same way as proposed for POPs by Dachs et al. (2002).

Several lines of evidence suggest that such a sediment recycling pump is likely at work in the HBS. First, the remarkable sedimentary flux of Hg recorded in the sediments

of the HBS indicates that this system captures, and does not export, Hg inputs. This process is supported by substantial resuspension of sediments along the vast shallow southern coasts, which must occur in the absence of extraordinarily large unknown sources of sediment to the HBS. Secondly, despite the close proximity of riverine and coastally eroded inputs, sediments in the southern HBS have lower Hg concentrations than those in the deep water locations. Correspondingly, intensively studied areas along the southern HBS coast have revealed that ice scour and wave action remove surficial Holocene sediments, thereby transporting old material from the shallow regions to depositional basins. Finally, while there has been a 2-to-5-fold estimated increase in the global atmospheric Hg reservoir (Fitzgerald et al., 1998; Sunderland and Mason, 2007), the global ocean lags significantly (Sunderland and Mason, 2007), due to the dominance of GEM in the atmosphere which partitions weakly to water and has low reactivity. AMDEs after polar sunrise might provide the means for rapid Hg deposition but much of that Hg(II) is deposited onto the frozen ground (snow and ice) where it is rapidly photoreduced and re-emitted to the atmosphere leaving a negligible net effect (Kirk et al., 2006).

2.4.4 Sensitivity to Climate Change

A variety of climate models have indicated that the HBS is very sensitive to changes in global climate, with the most susceptible environmental characteristic being the sea ice, e.g., (Gagnon and Gough, 2005; Gough and Wolfe, 2001; Saucier and Dionne, 1998). While the inter-annual variability in sea ice thickness and duration in this system is underlain by decadal-scale changes related to the North Atlantic Oscillation and

the El-Niño/Southern Oscillation (ENSO) (Mysak et al., 1996), evidence exists that climate is also changing spatial and temporal sea ice dynamics. Over the last three decades the ice-free period in south east Hudson Bay has increased by three days per decade due to earlier dates of break-up (Gough et al. 2004). A cascade of effects from the change in sea ice conditions is plausible considering its leading influence on Hg processes (e.g., air-sea exchange, wave-driven sediment resuspension rates) in the HBS. A detailed analysis has recently been given by Outridge et al. (2008) on the sensitivity and response of Hg biogeochemistry in the Arctic Ocean to the projected climate change. Although the net effect on a Hg balance is difficult to predict due to positive influences on both source and sink terms, most Hg processes are likely to be amplified, increasing the total amount of Hg mobilized between the system components. The difference between the sum of the contemporary and preindustrial Hg source budgets described in Table 2-5 (6.3 t and 3.4 t, respectively) suggest that such a trend has already occurred; a warming climate will support this development.

While atmosphere and river contributions to the HBS are considerably dynamic over long time periods (Figure 2-6A and B), rivers represent a larger relative influence than in other marine systems. Since river Hg fluxes are also dynamic over short time scales (e.g., seasonal; Leitch et al. 2007) and responsive to watershed development (e.g., damming) (Bodaly et al., 1984), they present a substantial Hg transport pathway to the HBS that is subject to disturbance by climate change as well as intensive human activities (e.g., irrigation, chemical contamination, damming). River transport of Hg to the ocean is also influenced indirectly by atmospheric deposition to catchments. Their impact on Hg dynamics in oceans appears most significant in near-shore and estuarine regions (e.g., see

Sunderland and Mason, 2007) which tend to be favoured in Arctic marine ecosystems by large animals like belugas (Stewart and Lockhart, 2005).

Although increasing Hg fluxes can be expected from rivers and coastal erosion in the sub-Arctic HBS, the large sedimentary flux process will continue to be a key to understanding system response. Shortening the sea ice cover season, and increasing temperature and nutrient input (from the vast HBS watershed or from enhanced upwelling and mixing) may also contribute to the vertical flux of Hg in the marine water column, strengthening the connection between the resuspension process and sedimentary deposition.

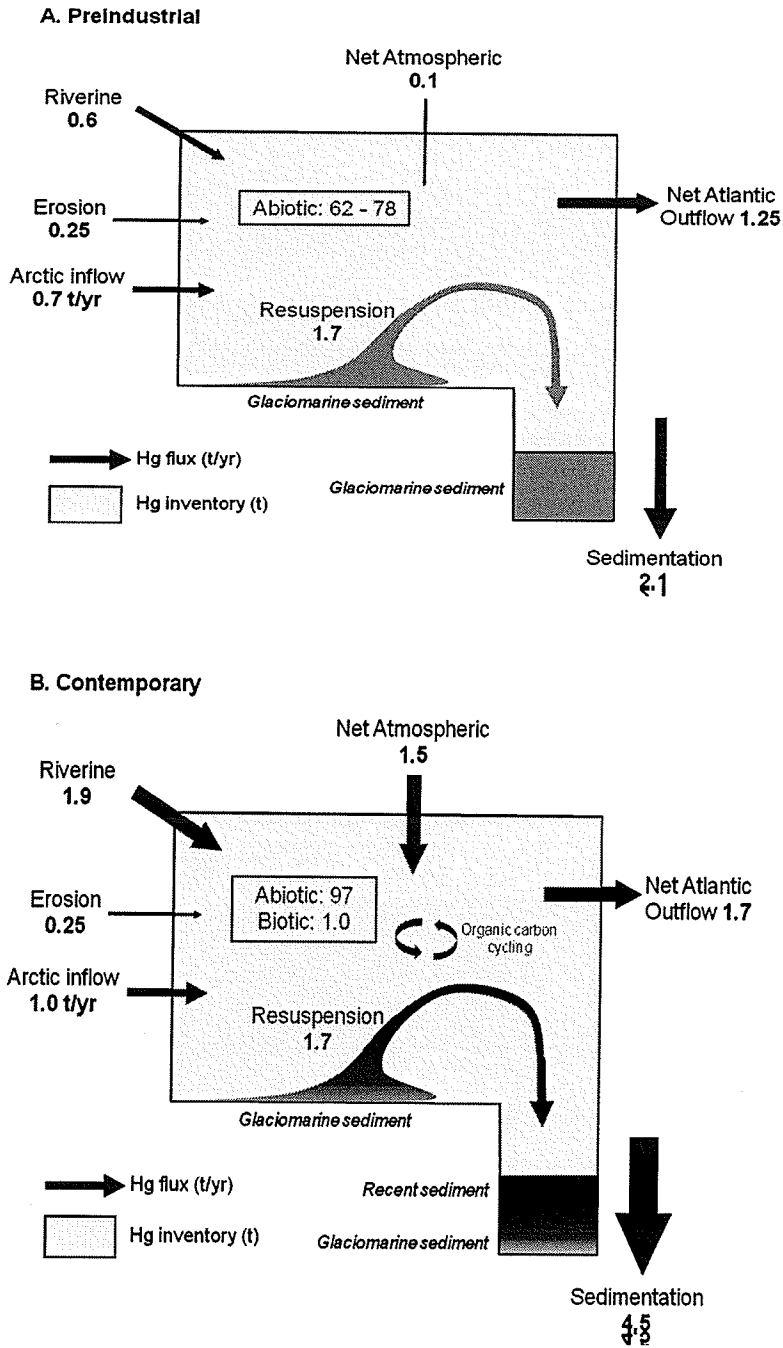


Figure 2-6. Mass balance model for Hg in the HBS for A) preindustrial and B) contemporary times.

2.5 Conclusion

The global ocean model suggests that the net atmospheric Hg flux to the North Atlantic Ocean (including the Arctic and HBS) is close to neutral (i.e., deposition \approx evasion) (Sunderland and Mason, 2007). While this seems to be the case for the HBS in preindustrial times, the atmosphere has become an increasingly important source of Hg in the contemporary HBS. The increasing Hg deposition from the atmosphere is within the capacity of the system to collect and bury in marine sediments and consequently, increased Hg inputs do not directly correspond to increased transport from the HBS to the global oceans. The strength of sedimentary control in the HBS is supported by unique circumstances that present large regions of shallow coastal sediments to wave, ice and tidal forces through sustained isostatic post-glacial rebound along the southern coast. Unconsolidated glacial sediments in near-shore regions are removed from the boundary margin to deeper, depositional areas and potentially provide an additional mechanism for scavenging Hg from the water column.

The present work represents the first attempt in scaling all the possible Hg fluxes in the HBS toward a better understanding of the fate and effect of Hg in the system. Further work is warranted to refine and reduce the uncertainty associated with each of the individual flux terms. Nevertheless, the mass budget calculations suggest that the internal aquatic processes, particularly the sediment recycling processes, may have a stronger control of Hg dynamics in this marine environment experiencing isostatic rebound. The interplay of these processes and their responses under a changing climate is likely the ultimate driver for the Hg bioaccumulation in the HBS marine ecosystems.

2.6 References

- Aars, J., Lunn, N.J. and Derocher, A.E.E., 2006. Proceedings of the Fourteenth Working Meeting of the IUCN/SSC Polar Bear Specialist Group, Gland, Switzerland.
- AMAP, 1998. Arctic Pollution Issues, Arctic Monitoring and Assessment Program, Oslo, Norway.
- AMAP, 2005. AMAP Assessment 2002: Heavy Metals in the Arctic., Oslo, Norway.
- Andrews, J.T., Tedesco, K., Briggs, W.M. and Evans, L.W., 1994. Sediments, sedimentation rates, and environments, southeast Baffin shelf and northwest Labrador Sea, 8-26 ka. *Canadian Journal of Earth Sciences*, 31(1): 90-103.
- Ariya, P.A., Dastoor, A.P., Amyot, M., Schroeder, W.H., Barrie, L., Anlauf, K., Raofie, F., Ryzhkov, A., Davignon, D., Lalonde, J. and Steffen, A., 2004. The Arctic: A sink for mercury. *Tellus, Series B: Chemical and Physical Meteorology*, 56(5): 397-403.
- Begin, Y., Berube, D. and Gregoire, M., 1993. Downward Migration of Coastal Conifers as a Response to Recent Land Emergence in Eastern Hudson Bay, Québec. *Quaternary Research*, 40(1): 81-88.
- Blais, J.M., Macdonald, R.W., Mackay, D., Webster, E., Harvey, C. and Smol, J.P., 2007. Biologically mediated transport of contaminants in aquatic systems. *Environmental Science and Technology*, 41: 1075-1084.
- Bodaly, R.A., Hecky, R.E. and Fudge, R.J.P., 1984. Increases in fish mercury levels in lakes flooded by the Churchill River diversion, northern Manitoba. *Canadian Journal of Fisheries and Aquatic Sciences*, 41(4): 682-691.
- Bodek, I., Lyman, W., Reehl, W. and Rosenblatt, D., 1988. Environmental inorganic chemistry: properties, processes, and estimation methods. .
- Born, E.W., Kraul, I. and Kristensen, T., 1981. Mercury, DDT and PCB in the Atlantic walrus (*Odobenus rosmarus rosmarus*) from the Thule District, North Greenland. *Arctic*, 34(3): 255-260.
- CFIA, 2001. Product Inspection Program, Canadian Guidelines for Chemical Contaminants and Toxins in fish and Fish Products. In: C.F.I. Agency (Editor), Ottawa, ON.

- Coquery, M., Cossa, D. and Martin, J.M., 1995. The distribution of dissolved and particulate mercury in three Siberian estuaries and adjacent Arctic coastal waters. *Water, Air, & Soil Pollution*, 80(1): 653.
- COSEWIC, 2004. Assessment and Update Status Report on the Narwhal *Monodon monoceros* in Canada, Committee on the Status of Endangered Wildlife in Canada, Ottawa, ON, Canada.
- COSEWIC, 2006. Assessment and Update Status Report on the Atlantic Walrus *Odobenus rosmarus* in Canada, Committee on the Status of Endangered Wildlife in Canada, Ottawa, ON, Canada.
- Cossa, D., Coquery, M., Gobeil, C. and Martin, J.M., 1996. Mercury fluxes at the ocean margins
Global and Regional Mercury Cycles: Sources, Fluxes and Mass Balances: 229 - 247.
- d'Anglejan, 1980. Effects of seasonal changes on the sedimentary regime of a subarctic estuary, Rupert Bay (Canada). *Sediment Geology*, 26: 51-68.
- Dachs, J., Lohmann, R., Ockenden, W.A., MÃ©janelle, L., Eisenreich, S.J. and Jones, K.C., 2002. Oceanic biogeochemical controls on global dynamics of persistent organic pollutants. *Environmental Science and Technology*, 36(20): 4229-4237.
- DÃ©ry, S.J., Stieglitz, M., McKenna, E.C. and Wood, E.F., 2005. Characteristics and trends of river discharge into Hudson, James, and Ungava Bays, 1964-2000. *Journal of Climate*, 18(14): 2540.
- Dommergue, A., Ferrari, C.P., Poissant, L., Gauchard, P.A. and Boutron, C.F., 2003. Diurnal cycles of gaseous mercury within the snowpack at Kuujuarapik/Whapmagoostui, QuÃ©bec, Canada. *Environmental Science and Technology*, 37(15): 3289.
- Drinkwater, K.F., 1988. On the Mean and Tidal Currents in Hudson Strait. *Atmos. Ocean.*, 26(2): 252-266.
- Fitzgerald, W., 1999. Clean hands, dirty hands: Clair Patterson and the aquatic biogeochemistry of mercury. In: C.I. Davidson (Editor), *Clean Hands, Clair Patterson's Crusade Against Environmental Lead Contamination*. Nova Science, Commack, NY, pp. 119-137.

- Fitzgerald, W.F., Engstrom, D.R., Mason, R.P. and Nater, E.A., 1998. The case for atmospheric mercury contamination in remote areas. *Environ. Sci. Technol.*, 32: 1-7.
- Gagnon, A.S. and Gough, W.A., 2005. Climate Change Scenarios for the Hudson Bay Region: An Intermodel Comparison. *Climatic Change*, 69(2): 269.
- Gough, W.A. and Wolfe, E., 2001. Climate Change Scenarios for Hudson Bay, Canada, from General Circulation Models. *Arctic*, 54(2): 142-148.
- Grigoriev, V., Rachold, V., Hubberten, H.W. and Schirmeister, L., 2004. Organic carbon input to the Arctic seas through coastal erosion. In: R. Stein and R.W. Macdonald (Editors), *The Organic Carbon Cycle in the Arctic Ocean*. Springer, Berlin, pp. 41-44.
- Harvey, M., Therriault, J.C. and Simard, N., 2001. Hydrodynamic control of late summer species composition and abundance of zooplankton in hudson bay and hudson strait (canada). *Journal of Plankton Research*, 23(5): 481-496.
- Hendersen, P., 1989. Provenance and Depositional Facies of Surficial Sediments in Hudson Bay, A Glaciated Epeiric Sea. 287 + xvii.
- Hill, P.R., Simard, A. and HÃ©quette, A., 1999. High-resolution seismic stratigraphy of late Quaternary deposits in Manitounouk Sound, northern Quebec: Effects of rapid postglacial emergence. *Canadian Journal of Earth Sciences*, 36(4): 549-563.
- Hudon, C., Morin, R., Bunch, J. and Harland, R., 1996. Carbon and nutrient output from the Great Whale River (Hudson Bay) and a comparison with other rivers around Quebec. *Canadian Journal of Fisheries and Aquatic Sciences*, 53(7): 1513-1525.
- Ingram, R. and Prinsenberg, S.J., 1998. Coastal Oceanography of Hudson Bay and Surrounding Eastern Canadian Arctic Waters *The Sea*, 11: 835-861.
- Jeffries, J., Carey, J. and Swyripa, M., 1994. Riverine inputs of contaminants. In: J.L. Murray and R.G. Shearer (Editors), *Synopsis of research conducted under the 1993/94 Northern Contaminants Program*. Indian and Northern Affairs Canada, Ottawa, Canada, pp. 117-127.
- Jones, E. and Anderson, L., 1994. Northern Hudson Bay and Foxe Basin: Water Masses, Circulation and Productivity. *Atmosphere-Ocean*, 32(2): 361-374.

- Josenhans, H., Balzer, S., Henserson, P., Nielson, E., Thorliefson, H. and Zevenhuizen, J., 1988. Preliminary seismostratigraphic and geomorphic interpretations of the Quaternary sediments of Hudson Bay, Geological Survey of Canada.
- Kara, A.B., Rochford, P.A. and Hurlburt, H.E., 2000. Efficient and accurate bulk parameterizations of air-sea fluxes for use in general circulation models. *Journal of Atmospheric and Oceanic Technology*, 17(10): 1421-1438.
- Kirk, J.L., St.Louis, V.L. and Sharp, M.J., 2006. Rapid Reduction and Reemission of Mercury Deposited into Snowpacks during Atmospheric Mercury Depletion Events at Churchill, Manitoba, Canada. *Environ. Sci. Technol.*, 40(24): 7590-7596.
- Kuzyk, Z.A., Macdonald, R.W., Johannessen, S.C., Gobeil, C. and Stern, G.A., 2009. Towards a Sediment and Organic Carbon Budget for Hudson Bay. *Marine Geology*, 264: 190-208.
- Lalonde, J.D., Poulain, A.J. and Amyot, M., 2002. The Role of Mercury Redox Reactions in Snow on Snow-to-Air Mercury Transfer. *Environ. Sci. Technol.*, 36(2): 174-178.
- Lamborg, C.H., Fitzgerald, W.F., O'Donnell, J. and Torgersen, T., 2002. A non-steady-state compartmental model of global-scale mercury biogeochemistry with interhemispheric atmospheric gradients. *Geochimica et Cosmochimica Acta*, 66(7): 1105.
- Leitch, D.R., Carrie, J., Lean, D., Macdonald, R.W., Stern, G.A. and Wang, F., 2007. The delivery of mercury to the Beaufort Sea of the Arctic Ocean by the Mackenzie River. *Science of The Total Environment*, 373(1): 178.
- Liss, P.S. and Merlivat, L., 1986. Air-sea gas exchange rates: Introduction and synthesis. In: P. Buat-Menard (Editor), *The role of air-sea exchange in geochemical cycling*. D. Reidel, Dordrecht, pp. 113-127.
- Lockhart, W.L., Stern, G.A., Wagemann, R., Hunt, R.V., Metner, D.A., DeLaronde, J., Dunn, B., Stewart, R.E.A., Hyatt, C.K., Harwood, L. and Mount, K., 2005. Concentrations of mercury in tissues of beluga whales (*Delphinapterus leucas*) from several communities in the Canadian Arctic from 1981 to 2002. *Science of The Total Environment*, 351-352: 391.

- Lunn, N.J., Stirling, I., Andriashek, D. and Kolenosky, G.B., 1997. Re-estimating the size of polar bears population in western Hudson Bay. *Arctic*, 50(3): 234-240.
- Marshall, I.B., Scott Smith, C.A. and Selby, C.J., 1996. A national framework for monitoring and reporting on environmental sustainability in Canada. *Environmental Monitoring and Assessment*, 39(1): 25-38.
- Martini, I.P., 1986. Chapter 7 Coastal Features of Canadian Inland Seas, Elsevier Oceanography Series. Elsevier, pp. 117-142.
- Mason, R.P., Rolffhus, K.R. and Fitzgerald, W.F., 1998. Mercury in the North Atlantic. *Marine Chemistry*, 61(1-2): 37.
- Mason, R.P. and Sheu, G.P., 2002. Role of the ocean in the global mercury cycle *Global Biogeochem. Cycles*, 16(4): 1093.
- Mysak, L.A., Ingram, R.G., Wang, J. and Van Der Baaren, A., 1996. The anomalous sea-ice extent in Hudson Bay, Baffin Bay and the Labrador Sea during three simultaneous NAO and ENSO episodes. *Atmosphere - Ocean*, 34(2): 313-343.
- Outridge, P., Macdonald, R.W., Wang, F., Stern, G. and Dasoor, A.P., 2008. A mass balance inventory of mercury in the Arctic Ocean. *Environmental Chemistry*, 5: 89-111.
- Parisa, A.A., Dastoor, A.P., Amyot, M., Schroeder, W.H., Barrie, L., Anlauf, K., Raofie, F., Ryzhkov, A., Davignon, D., Lalonde, J. and Steffen, A., 2004. The Arctic: a sink for mercury. *Tellus B*, 56(5): 397-403.
- Pazerniuk, M., 2007. Total and Methyl Mercury Levels in Hudson Bay Zooplankton: Spatial Trends and Processes, University of Manitoba, Winnipeg.
- Pett, R.J. and Roff, J.C., 1982. Some observations and deductions concerning the deep waters of Hudson Bay (James Bay). *Naturaliste Canadien*, 109(4): 767-774.
- Poissant, L., Amyot, M., Pilote, M. and Lean, D., 2000. Mercury Water-Air Exchange over the Upper St. Lawrence River and Lake Ontario. *Environ. Sci. Technol.*, 34(15): 3069-3078.
- Poissant, L. and Pilote, M., 2003. Time series analysis of atmospheric mercury in Kuujuarapik/Whapmagoostui (Quebec). In: C. Boutron and C. Ferrari (Editors), *Journal De Physique. IV : JP. XII International Conference on Heavy Metals in the Environment*, Grenoble, pp. 1079.

- Poulain, A.J., Ni Chadhain, S.M., Ariya, P.A., Amyot, M., Garcia, E., Campbell, P.G.C., Zylstra, G.J. and Barkay, T., 2007. A potential for mercury reduction by microbes in the High Arctic. *Appl. Environ. Microbiol.*: AEM.02701-06.
- Rajar, R., Cetina, M., Horvat, M. and Zagar, D., 2007. Mass balance of mercury in the Mediterranean Sea. *Marine Chemistry*, 107(1): 89-102.
- Richard, P.R., 1998. Hudson Bay Narwhal, Stock Status Report E5-44. In: F.a.O. Canada (Editor), Ottawa, ON, Canada, pp. 4 pp.
- Roff, J.C. and Legendre, L., 1986. Physico-chemical and biological oceanography of Hudson Bay. In: I.P. Martini (Editor), *Canadian Inland Seas*. Elsevier, New York, pp. 265-291.
- Sanei, H., Outridge, P., Wang, F., Fishback, L. and Armstrong, D., 2007. Preliminary results from a year's monitoring of Hg in wet deposition at Churchill, Manitoba, Northern Contaminants Program Annual workshop, Lake Louise, AB, Canada.
- Saucier, F., Senneville, S., Prinsenber, S., Roy, F., Smith, G., Gachon, P., Caya, D. and Laprise, R., 2004. Modelling the sea ice-ocean seasonal cycle in Hudson Bay, Foxe Basin and Hudson Strait, Canada. *Climate Dynamics*, 23: 303-326.
- Saucier, F.J. and Dionne, J., 1998. A 3-D coupled ice-ocean model applied to Hudson Bay, Canada: The seasonal cycle and time-dependent climate response to atmospheric forcing and runoff. *J. Geophys. Res.*, 103.
- Schroeder, W.H., Anlauf, K.G., Barrie, L.A., Lu, J.Y., Steffen, A., Schneeberger, D.R. and Berg, T., 1998. Arctic springtime depletion of mercury. *Nature*, 394(6691): 331.
- Shiklomanov, I.A. and Shiklomanov, A.I., 2003. Climatic Change and the Dynamics of River Runoff into the Arctic Ocean. *Water Resources*, 30(6): 593-601.
- Smith, T.G., 1975. Ringed seals in James Bay and Hudson Bay: population estimates and catch statistics. *Arctic*, 28: 179-182.
- Stein, R. and Macdonald, R., 2004. *The Organic Carbon Cycle in the Arctic Ocean*. Springer-Verlag Berlin Heidelberg, 363 + xix pp.
- Stern, G. and Lockhart, L., 2007. Mercury in beluga and walrus from the Canadian Arctic: status in 2006/07. In: I.A.a.N.D.o. Canada (Editor), *Synopsis of research*

- conducted under the 2006-2007 Northern Contaminants Program, Ottawa, pp. 226-242.
- Stewart, D.L. and Lockhart, W.L., 2005. An overview of the Hudson Bay marine ecosystem. *Can. Tech. Rep. Fish. Aquat. Sci.*, 2586: vi + 487 p.
- Straneo, F. and Saucier, F.J., 2008. The Arctic-Subarctic exchange through Hudson Strait. *Arctic-subarctic ocean fluxes*. Springer-Verlag, Dordrecht, The Netherlands.
- Strode, S.A., Jaegle', L., Selin, N.E., Jacob, D.J., Park, R.J., Yantosca, R.M., Mason, R.P. and Slemr, F., 2007. Air-sea exchange in the global mercury cycle. *Global Biogeochem. Cycles*, 21.
- Sunderland, E.M. and Mason, R.P., 2007. Human impacts on open ocean mercury concentrations. *Global Biogeochem. Cycles*, 21.
- Temme, C., Baukau, J., Schneider, B., Aspino, K., Fain, X. and Ferrari, C., 2005. Air-water exchange of mercury in the North Atlantic Ocean during Arctic summer, XIII International Conference on Heavy Metals in the Environment, Rio de Janeiro.
- Wagemann, R., Trebacz, E., Boila, G. and Lockhart, W.L., 1998. Methylmercury and total mercury in tissues of arctic marine mammals. *The Science of The Total Environment*, 218(1): 19-31.
- Wiken, E.B., 1986. Terrestrial ecozones of Canada. *Ecological Land Classification Series No. 19*: 26 pp. + map.
- Zevenhuizen, J., Amos, C.L., Asprey, K., Michaud, Y., Ruz, M.H. and Sutherland, T., 1994. The sediment budget of Manitounuk Sound, Southeastern Hudson Bay, Geological Survey of Canada, Ottawa, Canada.

CHAPTER 3

Natural and Anthropogenic Mercury Distribution in Marine Sediments from Hudson Bay, Canada

Abstract

Twelve marine sediment cores from Hudson Bay, Canada, were collected to investigate the contribution of atmospherically-transported mercury (Hg) to total sedimentary Hg loads and its impact on the natural spatial variability of sediment Hg in an Arctic/sub-Arctic marine system. Based on a 2-layer sediment mixing model, the historical Hg deposition to most of the cores reflects the known history of atmospheric Hg deposition in North America, with an onset of increased anthropogenic Hg emissions in the late 1800s and early 1900s and a reduction of Hg deposition in the mid- to late-1900s. Although surface enrichment factors for Hg suggest that anthropogenic activities have enhanced Hg fluxes 1.3 to 2.1 fold within cores, those cores reflecting anthropogenic trends display modern surface Hg concentrations largely within the range found in pre-industrial sediments across the Bay. A strong relationship between Hg and organic matter (OM) capture has preserved the preindustrial spatial pattern of Hg distribution across HB sediments throughout the industrial era and demonstrates that the vertical particle flux largely explains the response of sediments to changes in atmospheric Hg levels. However, two offshore cores demonstrate long periods of steadily increasing Hg concentrations commencing well before the onset of industrialization. Based on $\delta^{13}\text{C}$,

these changing concentrations may be due to increasing deposition of marine organic matter at that time.

3.0 Introduction

Lake sediments often record variations in atmospheric deposition of mercury (Hg), permitting reconstruction of the chronology of anthropogenic Hg emissions to the atmosphere from sediment cores (e.g., Lorey and Driscoll, 1999; Perry et al., 2005). While enhanced sediment loadings from post-industrial increases in atmospheric Hg are evident in many Arctic lakes (Bindler et al., 2001; Fitzgerald et al., 2005; Lockhart et al., 1998; Muir et al., 2009), Outridge et al. (2005) recently proposed an alternative hypothesis linking Hg enrichments in some Arctic lake sediments to recent increases in autochthonous primary productivity driven by increasing temperatures. Such observations highlight the importance of considering internal biogeochemical processes when interpreting Hg trends derived from Arctic sediment cores.

In contrast to lakes, the marine environment has seen few sediment-core studies applied to the question of enhanced post-industrial Hg loadings in the Arctic. Marine sediments provide an ultimate sink for anthropogenic Hg (Mason et al., 1994; Mason and Sheu, 2002), and coastal and estuarine sediments have been shown to reflect reliably the timing of transient, point source inputs of Hg (Gagnon et al., 1997; Gobeil and Cossa, 1993; Johannessen et al., 2005; Smith and Schafer, 1999). However, relating marine sediment core data to the chronology of atmospheric Hg deposition is not straightforward due to the complex dynamics of production and sedimentation of particles in the marine environment. The sedimentary record may be related to flux of Hg from the atmosphere,

but it also depends on particulate capture of Hg, transport and burial of particles, and the mobility over time of Hg in the sediments. In marine systems, long-range particle transport by currents, a long residence time for Hg in the water column, and benthic mixing may obscure the depositional history of atmospheric Hg. In Arctic systems, sea ice can further intercept and redistribute particles and Hg. Several studies in the remote Arctic have demonstrated surface Hg enrichments in coastal (Asmund and Nielsen, 2000) and offshore (Gobeil et al., 1999) marine sediments, but to what extent these enrichments reflect anthropogenic contributions is not clear.

Canada's Hudson Bay (HB) provides an opportunity to investigate the processes of Hg capture in a large marine system and the influence of elevated atmospheric Hg deposition to sediments observed over the last ca. 150 years (Swain et al. 1992). Lake sediment cores (Hermanson, 1998; Lockhart et al., 1998; Muir et al., 2009) and two previous cores from HB (Lockhart et al., 1998) indicate that the Bay and its watershed are subject to atmospheric deposition of anthropogenic Hg. The coastlines of the Bay contain no known industrial point sources, and a coupled sediment and Hg mass-balance model suggests that most of the particulate Hg is trapped within the Bay (Hare et al., 2008). Furthermore, there is a basic understanding of the supply, transport and sinks for sediment and organic carbon in HB (Kuzyk et al., 2008; Kuzyk et al., 2009a). In this paper we evaluate the contribution of anthropogenic, atmospheric Hg flux to Hudson Bay marine sediments and identify the local and regional processes (particle production, transport, and sedimentation) important for shaping patterns of marine sediment Hg within Hudson Bay.

3.1 Experimental Methods

3.1.1 Study Site

Hudson Bay is a large, shallow, sub-Arctic marine basin almost enclosed by the North American continent and extending from nearly 50 °N to 65 °N (Figure 3-1). Much of the seafloor appears non-depositional, with glacial till outcropping near the surface (Josenhans et al., 1988). However, depositional pockets scattered throughout the basin provide long-term sinks for sediment, organic carbon (OC) and Hg (Hare et al., 2008; Kuzyk et al., 2009a).

Although numerous small communities (population < 2000) are located along the HB coast, the area has no history of large-scale commercial or industrial development. A few gold mines, hydroelectric developments and pulp and paper mills operate away from the coast, but appear to contribute little, if any, Hg to the marine system (Hare et al., 2008; Kirk and St. Louis, 2009).

3.1.2 Sample Collection

Marine sediment box cores were collected from 11 locations in HB and one at the confluence with Foxe Channel (Figure 3-1) during the 2005 ArcticNet cruise aboard the *CCGS Amundsen* and sectioned as described previously (Hare et al., 2008). These cores represent relatively shallow depths, a wide range of sedimentation rates and mixing depths, and low organic carbon content (Table 3-1).

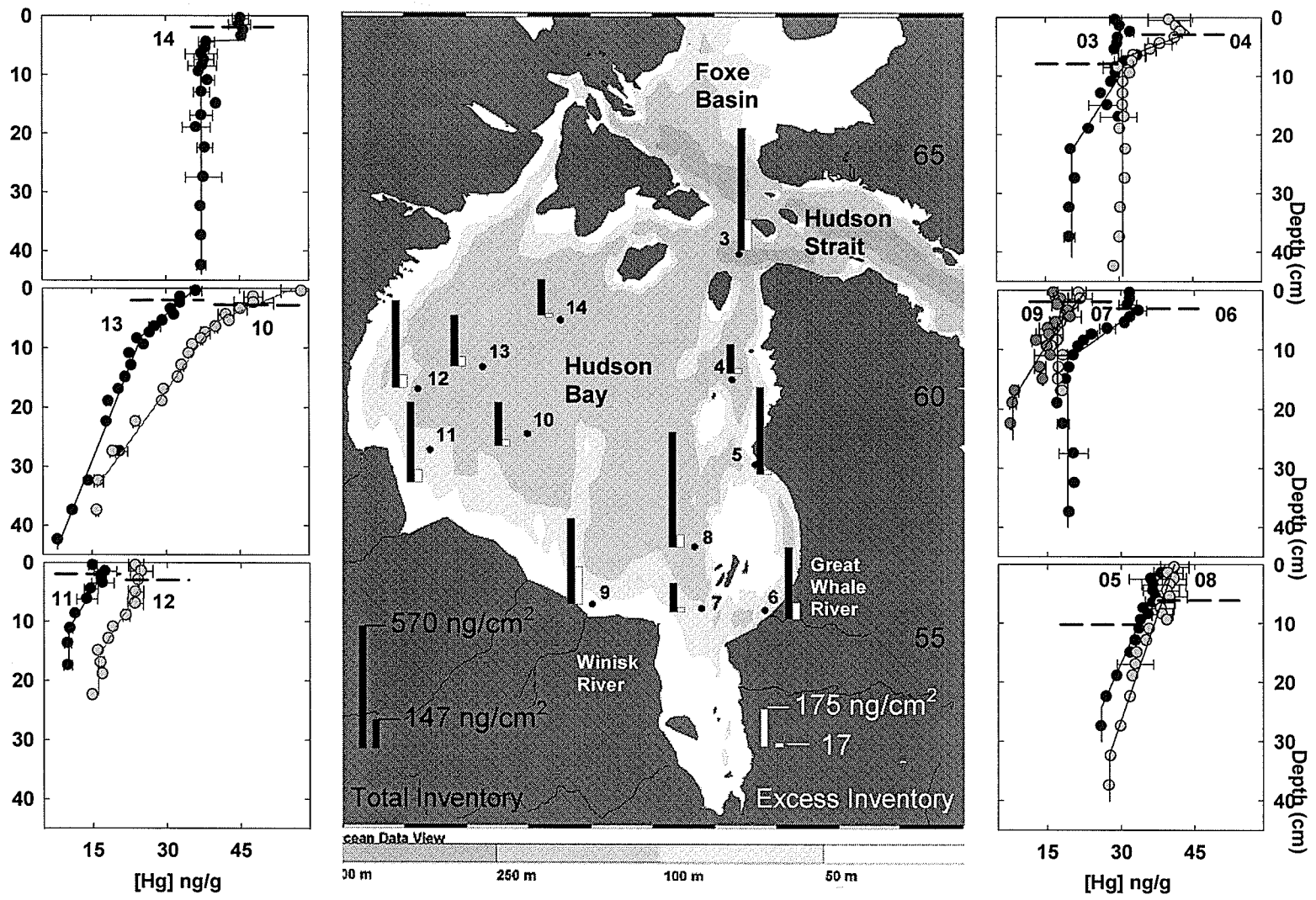


Figure 3-1. Sediment core locations, Hg concentrations and inventories. Graphs: circles and lines are measured and modeled Hg concentrations, respectively; horizontal error bars are the range or standard deviation (n = 2 to 5); dashed lines represent the depth of the surface mixed layer. Map: circles represent core locations, bars represent Hg inventories (see legends).

Table 3-1. Basic physical parameters of Hudson Bay sediment cores.

Core	Water depth (m) ^a	Surface Grain size ^a % < 63 µM	Sedimentation rate	
			g/cm ² /yr ^a	cm/yr
3	395	94	0.17	0.18
4	153	96	0.03	0.05
5	112	97	0.10	0.13
6	119	99	0.12	0.13
7	106	88	0.05	0.05
8	150	100	0.13	0.17
9	34	76	0.23	0.16
10	200	99	0.04	0.06
11	86	81	0.22	0.15
12	116	87	0.16	0.15
13	145	93	0.08	0.07
14	244	100	0.03	0.05

^a Core 3: 2-3 cm deep section, all other cores: 1-2 cm deep section

3.1.3 Sample Analyses

Mercury was extracted from freeze-dried sediments by closed-vessel microwave digestion with HNO₃ following U.S EPA Method 3051 on a Microwave Assisted Reaction System (MARS V, CEM). The digestants were analyzed in the Ultra-Clean Trace Elements Laboratory (UCTEL) at the University of Manitoba by Cold Vapour Atomic Fluorescence Spectrophotometry (CVAFS) on a Tekran 2600 Mercury Analyzer according to U.S. EPA Method 1631, as described previously (Leitch et al., 2007). Procedural blanks, analytical replicates (n = 2 to 5 for >50% of samples) and certified reference materials MESS-3, ORMS-3 (National Research Council of Canada) and BCR-579 (Institute for Reference Materials and Measurements of Belgium) provided QA/QC throughout the analyses. Analytical accuracy was within 7.7% of the certified value for Hg concentration (n = 36). All sediment Hg concentrations represent salt-corrected, dry weight values produced by

removing the mass of salt calculated from the water content of each layer and the salinity of the bottom water at the nearest station. Salt correction factors ranged from 1.01 to 1.09. $\delta^{13}\text{C}$ analyses were performed on an isotope mass spectrometer, as reported by Kuzyk et al. (2009b) Grain-size measurements were determined for one surficial layer in each core (core 3: 2-3 cm, all other cores: 1-2 cm) in a Beckman Coulter LS200 laser diffraction grain size analyzer, following organic matter removal with extended peroxidation.

Sediment geochronologies and a mixing rate for each core were determined using ^{210}Pb activity and verified with ^{137}Cs as previously reported (Kuzyk et al., 2009a). The intrinsic time resolution, determined by dividing the surface mixed layer (SML) by the sedimentation rate, ranged from 13 years on the southern and south western coasts to 58 years in the north east (Table 3-3). Surface mixed layers (SMLs) range from 0 to 10 cm and reflect the biological activity and TOC content of sediments (Kuzyk et al., 2009a).

3.1.4 Hg Inventories

Total Hg inventories were calculated by integrating the mass of Hg in each layer over the entire sediment core, and excess Hg inventories were determined as the difference between the total Hg inventories and inventories produced using background Hg concentrations.

3.1.5 Modeling of Hg Flux Histories

Hg flux histories were modeled in MATLAB with a two-layer sediment mixing model previously applied to transient Hg inputs to coastal marine sediments (Johannessen et al., 2005). Hg profiles were reproduced with a combination of input functions representing time periods with steady Hg concentrations and time periods with linearly increasing Hg concentrations in the incident particles. The modeled Hg fluxes start from background Hg concentrations and increase according to the modeled Hg concentration, the core-specific linear sedimentation rate, and diffusive mixing rates (Tables 3-1 and 3-2). A second input function for each core corresponding to a second change in Hg concentration was included when necessary to reproduce the observed profile. Such changes in Hg flux were adjusted to match the observed vertical profiles by manipulating the Hg concentration, the date of onset and the time over which an input signal lasted. The resulting Hg flux histories represent the simplest input functions that reproduce the observed sediment Hg profiles. Model fits were most sensitive to the timing and magnitude of changing Hg concentrations and less sensitive to the rate of increase or decrease. Model fits matched the observed profiles within 5 to 25 years of the indicated onset dates (Table 3-2), which is well within the intrinsic time resolution of the cores (Table 3-4).

3.2 Lateral and Vertical Variations of Hg in HB Sediments

Sediment Hg concentrations range from 8 to 58 ng/g ($n = 225$) (Figure 3-1), which is near the low end of those observed in sediments from the interior Arctic Ocean (10 to 120 ng/g, Gobeil et al., 1999), the Beaufort Shelf (1 to 130 ng/g,

Macdonald and Thomas, 1991), and the Greenland coast (4 to 280 ng/g, Asmund and Nielsen, 2000). Such low Hg concentrations are consistent with coastal glacial deposits in HB supplying sediments to the offshore region through resuspension and lateral transport (Kuzyk et al., 2009). These glacial materials appear to be characterized by low Hg concentrations and consequently dilute surface sediment concentrations relative to systems dominated by modern sediment sources (Hare et al., 2008).

Table 3-2. Input functions for modeled Hg flux histories.

Core	First input function (ng/g)	Time period (year)	Second input function (ng/g)	Time Period (yr)	r ²
3	20.3 + 0.14/yr	1880-1945	29.4 + 0.02/yr	1945-2005	0.84
4	30.7 + 0.16/yr	1870-1955	43.5 - 0.07/yr	1955-2005	0.96
5	26 + 0.07/yr	1820-2005 ^a	-	-	0.93
6	19.2 + 0.22/yr	1915-1975	32.2	1975-2005	0.96
7	17.1 + 0.05/yr	1885-2005	-	-	0.84
8	27.6 + 0.07/yr	1815-2005 ^a	-	-	0.96
9	8 + 0.12/yr	1890-1980	18.8 - 0.08/yr	1980-2005	0.84
10	16 + 0.055/yr	1480-1915 ^a	39.925 + 0.18/yr	1915-2005	0.97
11	10.1 + 0.11/yr	1930-1990 ^a	16.7 - 0.1/yr	1990-2005	0.96
12	16.1 + 0.11/yr	1900-1975	24.35	1975-2005	0.96
13	8.1 + 0.035/yr	1410-1895 ^a	25.075 + 0.1/yr	1895-2005	0.97
14	37.3 + 1.65/yr	1920-1925	45.55	1925-2005	0.91

^aInitial time period begins at deepest layer and represents and uppermost onset date for the Hg flux.

Reasonably constant background Hg concentrations can be identified in the lower portions of all cores (open boxes in Figure 3-2), except in cores 10 and 13 where Hg concentrations continually decrease downward throughout the cores. In all other cores, background Hg depths were checked with a transient pulse of Hg run through the mixing model for each core for 130 years, which represents the Anthropocene in a global Hg budget by Lamborg et al. (2006). Background Hg

concentrations are determined from the mean Hg concentrations in layers unaffected by a transient pulse of Hg mixed downwards for 130 years, present in all remaining cores except core 11. Mean Hg concentrations in the background sediment ranged from 8 to 37.7 ng/g and are strongly correlated with surface Hg concentrations ($r^2 = 0.91$), suggesting that processes controlling the spatial distribution of Hg have been consistent from preindustrial to modern times. Surface sediment Hg concentrations in HB are highest offshore (cores 10 and 14) and in the east (cores 4, 5, 8) and lowest along the southern and western coasts (cores 7, 9, 11 and 12). This pattern generally reflects the fraction of silt and clay ($\% < 63 \mu\text{m}$) in surface sediment layers ($r^2 = 0.73$, $p < 0.01$), and is consequently also a function of water depth ($r^2 = 0.68$, $p < 0.01$), except in Core 3 which is located at much greater depth in Foxe Channel and receives additional ice-rafted materials originating in the shallow Foxe Basin (Kuzyk et al., 2008).

Vertical sediment Hg profiles generally show the lowest concentrations at the bottoms of the cores and highest concentrations at or near the surface (Figure 3-2). Hg profiles fall into 3 categories: (1) generally steadily increasing Hg concentrations to the surface (cores 10 and 13), (2) stable background Hg concentrations with mid-core increases towards the surface and nearly constant concentrations in the surface layers (cores 3, 4, 5, 6, 7, 8, 9, 11, 12), and (3) a mid-core shift to higher Hg concentrations at the surface (core 14). Hg concentrations in the cores generally maintain their rank order throughout their length except for cores 10 and 13, which contain low concentrations at depth and high concentrations at the surface, relative to the other cores. The vertical variations in Hg profiles in most of the cores can be

explained by Hg input histories that reflect the historical pattern of anthropogenic Hg emissions from the industrial era. Model results closely fit all the observed profiles ($r^2 = 0.84$ to 0.96) (solid lines in Figure 3-1) and produce dates of onset of increasing Hg fluxes that correspond closely to historical timelines of atmospheric Hg emissions implied from North American lake sediments (Table 3-3). The optimal input functions for modeled Hg depositional histories are given in Table 3-2.

Table 3-3. Observed and modeled onset of major changes in Hg flux in sediments from North America and Greenland.

Hudson Bay Marine Sediment cores	Major or Mean Hg flux increase (yr)	Stable or declining flux	Intrinsic Time Resolution (yr)
3	1880	1945	44
4	1870 ^a	1955	58
6	1915	1975	23
7	1885	-	39
9	1890	1980	13
11	-	1990	13
12	1900	1975	20
Mean	1890	1970	
Lake Region			n
Mid-latitude ^b	1900	-	13
Mid-latitude	1900	1975 - 2000	5
Maine ^c	1900	-	6
Maine	1885	1995	1
Maine	1910	-	1
Subarctic ^b	1920		14
Subarctic	1920	1990	3
Quebec ^d	1930	-	8
Hudson Bay ^e	1870	-	1
Canadian Arctic ^b	1950	-	18
Greenland ^f	1900	-	1
Greenland	1900	1980	1

^a Dates before 1875 (130 years prior to sample collection) exceed the working limit of the ²¹⁰Pb dating method

^b Muir et al. 2009

^c Perry et al. (2005)

^d Lucotte et al. (1995)

^e Hermanson, 1998

^f Bindler et al. (2001b)

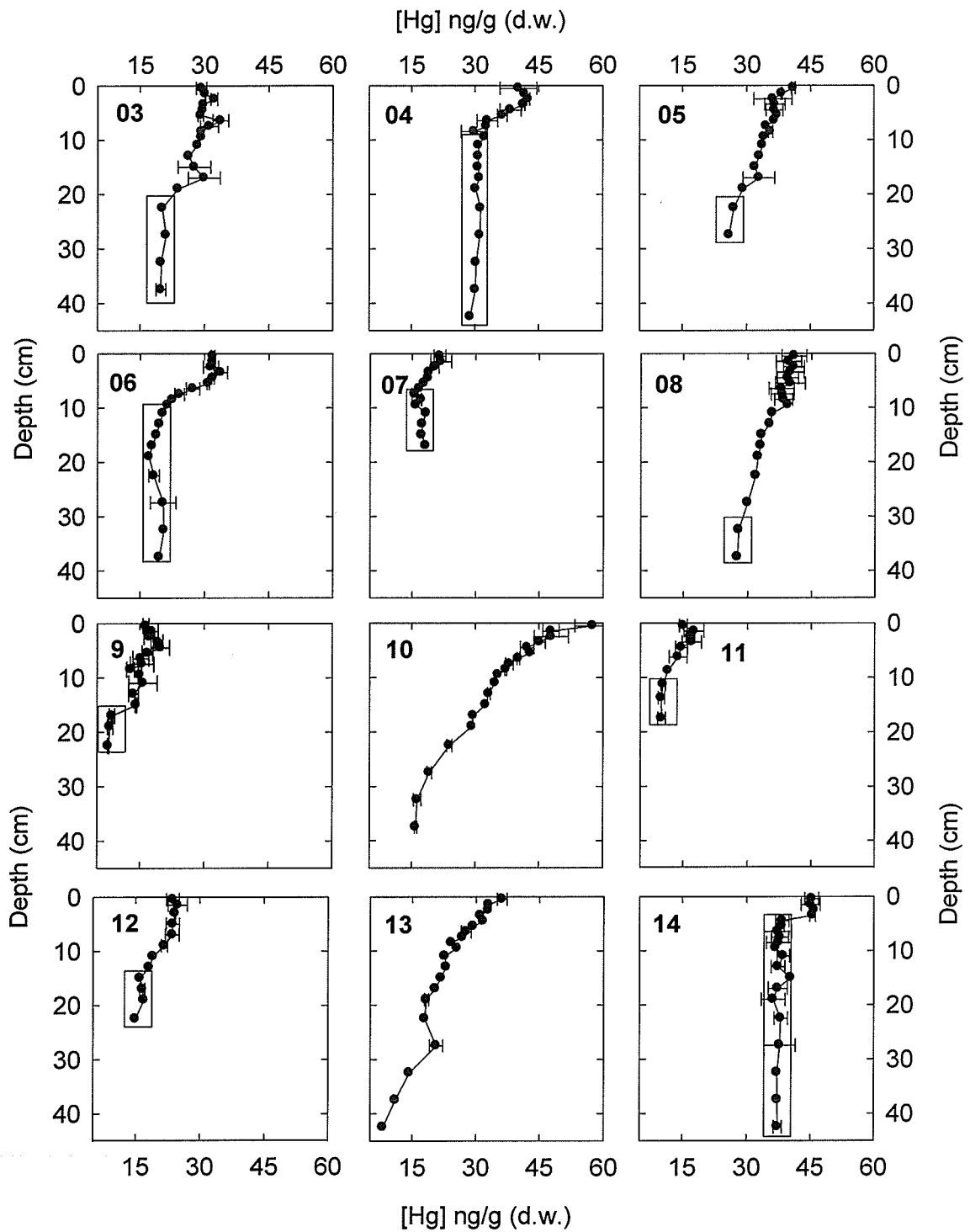


Figure 3-2. Vertical profiles of Hg concentrations in marine sediment cores taken from Hudson Bay. Open boxes represent background Hg layers.

Table 3-4. Hg concentrations, fluxes and surface enrichments in Hudson Bay sediment cores.

Core	Hg concentration (ng/g d.w.)			Modeled Hg flux (ng/cm ² /yr)			SEF ³
	Surface	Bground ¹ /Bottom	Anthro ²	Surface	Bground ¹ /Bottom	Anthro ²	
3	29.3	20.3	10.3	5.1	3.4	1.7	1.4
4	40.2	30.7	10.1	1.4	1.0	0.3	1.3
5	40.9	26.5	12.5	3.9	2.7	1.3	1.5
6	31.9	19.2	13.2	3.7	2.2	1.5	1.7
7	21.5	17.1	6.0	1.2	0.9	0.3	1.3
8	40.9	27.7	13.2	5.3	3.6	1.7	1.5
9	16.4	8.0	8.8	3.9	1.9	2.0	2.1
10 ^c	57.6	16.0	-	2.5	0.7	1.3	(3.6)
11 ^d	15.0	10.1	-	3.3	2.2	-	(1.5)
12	23.7	16.1	8.3	3.9	2.6	1.7	1.5
13 ^c	36.2	8.1	-	2.7	0.6	-	(4.5)
14	45.3	37.7	-	1.4	1.2	-	(1.2)

¹ Bground = Background

² No steady background Hg concentrations observed. Fluxes are base on the deepest Hg concentration.

³ SEF: Surface Enrichment Factor

3.3 Atmospheric Contribution to Sedimentary Hg

Mercury flux histories derived from the modeled input functions in over half the HB cores (3, 4, 6, 7, 9, 11 and 12) closely track the history of anthropogenic Hg emissions to the North American atmosphere, beginning to increase during the late 19th century and declining in recent decades (Lindberg et al., 2007). The modeled years for onset of increasing Hg fluxes range from 1870 to 1930 (mean: 1890) and for steady or declining Hg fluxes from 1945 to 1990 (mean: 1968) (Table 3-1). These dates correspond well with the onset of increasing and decreasing atmospheric Hg deposition observed from lake sediment records from North America and Greenland (increasing: 1870 to 1950, decreasing: 1970 to 2000, Table 3-1) and demonstrate that

the surface sediment enrichments in these cores can be explained by anthropogenic Hg emissions.

Cores 5 and 8 demonstrate deep surface mixed layers (Figure 3-1) and high biological activity (Kuzyk et al., 2009), indicating that a high degree of mixing occurs in these sediments. Hg fluxes consistently increase from deep layers that somewhat exceed the depths reached by inputs to these sediments 130 y.a. (Table 3-2). Evidence of a disturbed contaminant timeline is apparent from previous analyses of core 8 sediment (Kuzyk et al., 2009) and in a nearby core from another study (Lockhart et al., 1998), which both demonstrate the presence of ^{137}Cs below modeled depths corresponding to its initial date of release into the environment. These results suggest that anthropogenic Hg is present but not well modeled in these cores (Fig 3-1, Table 3-2).

3.4 Non-atmospheric Contributions to Sedimentary Hg

The Hg flux histories in cores 10 and 13 cannot be entirely explained by anthropogenic Hg additions to the atmosphere during industrial times. Although rates of increasing Hg fluxes in the upper portions of these cores can be explained by increasing Hg inputs around 1895 to 1915 (Table 3-2) the trend is clearly established well before the onset of the industrial era (Figure 3-1). The Hg enrichments in these cores from the deepest layer to the uppermost depths that cannot be impacted by early industrial-era inputs, based on the core-specific sedimentation and mixing parameters, ranges from 2.4 to 3-fold. These enrichments are higher than the 1.5-fold increase in the upper layers that could be affected by industrial-era deposition. Yet contaminant

timelines appear reasonably intact because anthropogenic lead content, determined by isotope ratios, demonstrates a timeline consistent with anthropogenic industrial activity by appearing at roughly the correct time period (1845 to 1930) in these cores (Kuzyk et al. 2009). However, biological mixing and other diagenetic processes are improbable explanations for these deep Hg enrichments based on the SML depths and the limited mobility of Hg in similar investigations (Delongchamp et al., 2009; Gagnon et al., 1997; Gobeil and Cossa, 1993).

Rather, a trend of increasingly heavy $\delta^{13}\text{C}$ signatures of the sedimentary organic matter (OM) appears synchronous with increasing Hg concentrations over the length of cores 10 and 13 (Figure 3-3). Increasing $\delta^{13}\text{C}$ indicates that sediments in the northwest/north-central part of HB have experienced increasing deposition of marine OM, relative to terrestrial OM, over the last few centuries. This pattern suggests that changes in particle composition and, specifically, particle source (terrigenous vs. marine), underlie the pre-industrial and continued progressive Hg increases in these cores. Increasing inputs of marine OM might produce increasing Hg concentrations in the sediment cores by conveying to the sediments increasing amounts of Hg scavenged from the water column. Based on $\delta^{13}\text{C}$ and C/N data from these cores (Kuzyk et al. 2009), the flux of marine-derived carbon in cores 10 and 13 increases by 3.7 and 2.0 times, respectively, which is proportional to the increase in total Hg flux over the same depths (3.6 and 2.0, respectively). This observation implies that marine OM represents a greater source of Hg than does the terrigenous or glacial material. In contrast to cores 10 and 13, the other cores show no matching down core correspondence between $\delta^{13}\text{C}$ and Hg concentrations (Figure 3-4).

Core 14 showed a relatively constant Hg concentration prior to an abrupt increase that may be explained by a change in Hg concentrations in incoming material around 1925, and steady Hg concentrations since that time. Based on the sampling resolution and the linear sedimentation rate, this change could have occurred over a period of 20 years. The modeled input function in core 14 cannot be assigned confidently to either anthropogenic or natural processes. $\delta^{13}\text{C}$ remains stable and does not suggest changing inputs of marine OM (Figure 3-4). Calculation of Hg flux suggests that the absolute change in the Hg flux above the background flux was small ($\sim 0.25 \text{ ng/cm}^2/\text{yr}$), due to the very low sedimentation rate at this site ($0.03 \text{ g/cm}^2/\text{yr}$, Table 3-1).

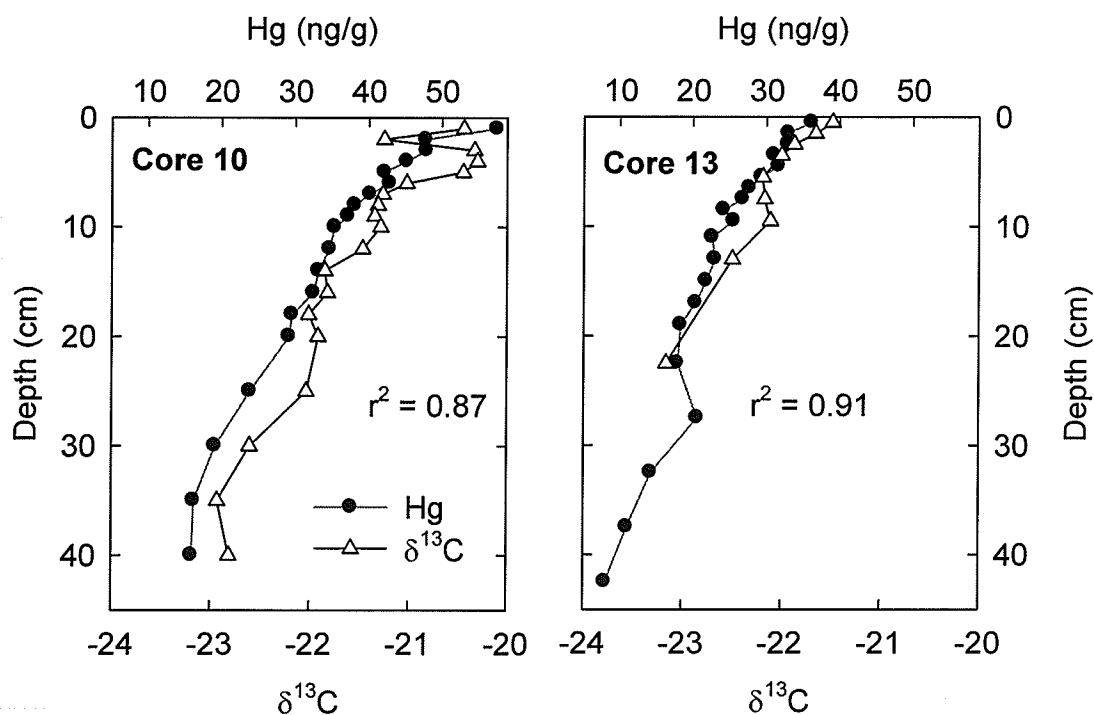


Figure 3-3. Co-variation of Hg and $\delta^{13}\text{C}$ Hg in two offshore cores (cores 10 and 13). Vertical error bars represent the intrinsic time resolution of each core.

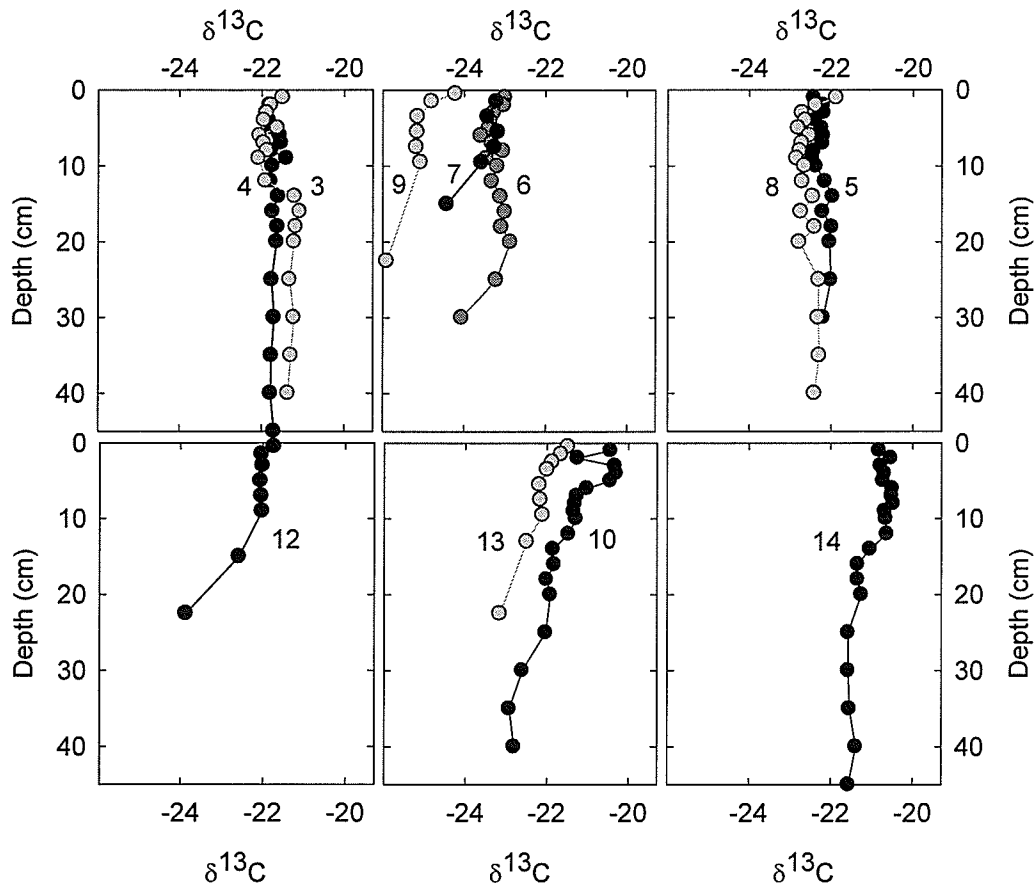


Figure 3-4. $\delta^{13}\text{C}$ content in marine sediment cores of Hudson Bay. Data from cores 5, 6, and 8 is adapted from Kuzyk et al. (2009a). Different grey scales reflect different cores.

3.5 Anthropogenic Hg loadings, Sediment Hg Fluxes and Surface Enrichment Factors

The anthropogenic Hg load on incoming particulate matter can be estimated by subtracting background Hg concentrations from modeled surface Hg concentrations, which represent the Hg concentration on incoming particles rather than in the sediment surface mixed layer. Anthropogenic loadings on the incident particles range from 6 to 13.2 ng/g and are strongly positively related to the fine grain size fraction ($r^2 = 0.89$) (Figure 3-5). Anthropogenic loadings on incident particles are

also related to OM ($r^2 = 0.62$) (Figure 3-5), implying that fine organic materials enhance anthropogenic Hg inputs to the sediments. Highly river-influenced surface sediments from cores 6 and 9 are exceptions to these relationships, with greater than expected anthropogenic Hg loads in view of their relatively coarser texture or low OC content. This is possibly due to distinct scavenging efficiencies from their different source materials or to greater winnowing of Hg from the nearby Winisk and Great Whale River watersheds (Figure 3-1).

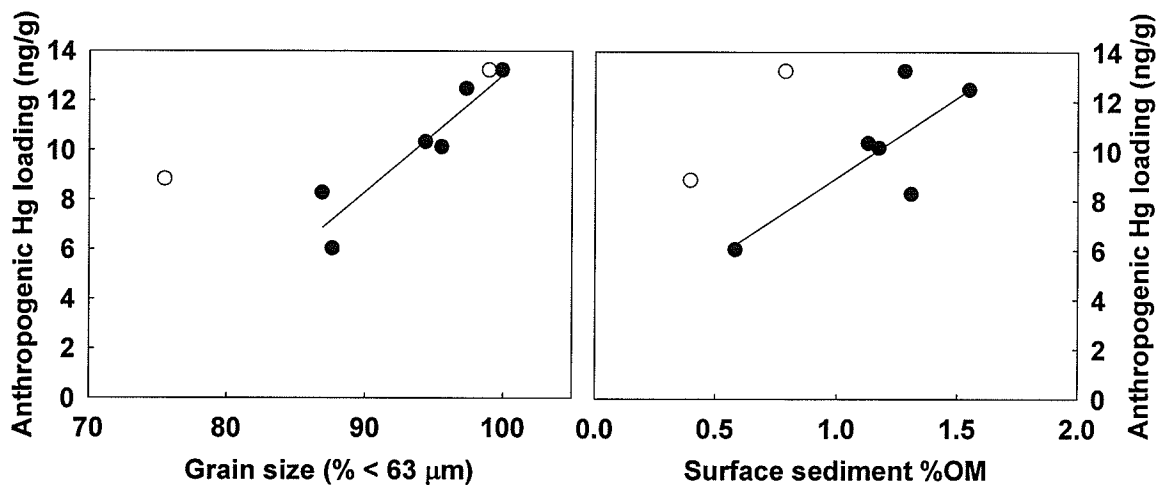


Figure 3-5. Grain size (% < 63 μm) (left) and surface sediment %OM content (right) controls on Anthropogenic Hg loadings. Open circles are cores located near river outlets (6 and 9), filled circles are all other cores with stable background Hg concentrations.

An estimate of the preindustrial scavenging can be produced by examining the relationship between background Hg concentrations and the OM content, which does not inherently contain Hg. A high degree of correlation between %OC and background Hg concentrations ($r^2 = 0.72$) implies the Hg present is essentially dependent on OC contributions to the sediments (Figure 3-6). This relationship considerably improves to $r^2 = 0.92$ if excluding core 3, which may contain different

sedimentary source materials from Foxe Basin (Kuzyk et al, 2009). In either case, the slope of the regression nearly passes through the origin, implying that matrix Hg is essentially absent (Figure 3-6). This is consistent with little evidence for significant geological sources of Hg to the HB basin in previous studies (Hare et al., 2008, Stewart and Lockhart, 2005). If OM is the major Hg ligand on particulate matter then the background Hg concentrations largely represent the effect of preindustrial scavenging. Under this scenario, the Anthropogenic Hg loadings then represent the increase in industrial-era scavenging, although a larger y-intercept between the modeled surface Hg concentrations and surface %OM could also indicate a larger modern contribution of matrix Hg. However, evidence of consistent sedimentation rates and particle size distribution in most of the cores (Kuzyk et al., 2009) suggest recent changes in matrix Hg contributions are unlikely. The relationship is considerably weaker ($r^2 = 0.55$) and the uncertainty in the intercept greater, likely because of greater heterogeneity in OM preservation in the surface oxic sediment layers relative to the stability of OM at background depths. Rather, the positive values of Anthropogenic Hg loadings suggest that more Hg is currently being scavenged than prior to industrialization, either through compositional changes in the incoming particulate matter or through increased Hg availability from higher atmospheric deposition.

Modeled surface Hg fluxes range from 1.2 to 5.3 ng/cm²/yr, while background sediment Hg fluxes range from 0.9 to 3.6 ng/cm²/yr (Table 3-4). The variation among the fluxes to different cores is largely the result of differences in sedimentation rate (7.7 fold; Table 3-1), because the differences in anthropogenic Hg concentrations are

much smaller (2.2-fold; Table 3-4). Under the assumption of constant sedimentation rates in each core, the background Hg fluxes may be subtracted from the modeled surface fluxes to identify the anthropogenic component of modern Hg fluxes. Anthropogenic Hg fluxes calculated in this way range from 0.3 to 2.0 ng/cm²/yr across HB, also primarily depending on variation in the sedimentation rate, which is roughly twice that of anthropogenic Hg concentrations. Correspondingly, anthropogenic and background Hg fluxes are strongly related ($r^2 = 0.99$) (Figure 3-7), specifically across the cores not located next to river outlets, where different controls on anthropogenic loadings are apparent (Figure 3-5). The dominance of sedimentation rate in controlling the variance in anthropogenic Hg fluxes indicates that variation in Hg supply is a comparatively smaller determinant of the spatial distribution of Hg fluxes in HB, and that the underlying sorting of particles remains a primary driver for spatial Hg distribution in this system. As a result, the preindustrial distribution of Hg capture has largely been preserved throughout the industrial era except in cases where compositional changes have occurred in sedimenting particles (i.e., cores 10 and 13).

Assuming constant sedimentation rates, the elevated modern Hg fluxes must arise from higher Hg concentrations on the incident particles or increased proportions of Hg-bearing particles. Consequently, in view of the compositional change in sedimenting particles in cores 10 and 13 that is reflected in consistently increasing proportions of marine carbon (Figure 3-3), we attribute the dramatic increase in Hg fluxes throughout the last several centuries in these cores (estimated from the deepest layer sampled at $\gg 130$ y.a., 0.6 to 0.7 ng/cm²/yr) to increased Hg-bearing materials.

In contrast, the cores with Hg flux histories synchronous with the history of anthropogenic Hg emissions may more accurately reflect increased Hg concentrations on incident particles since they display no evidence of compositional changes, at least in carbon source (Figure 3-4).

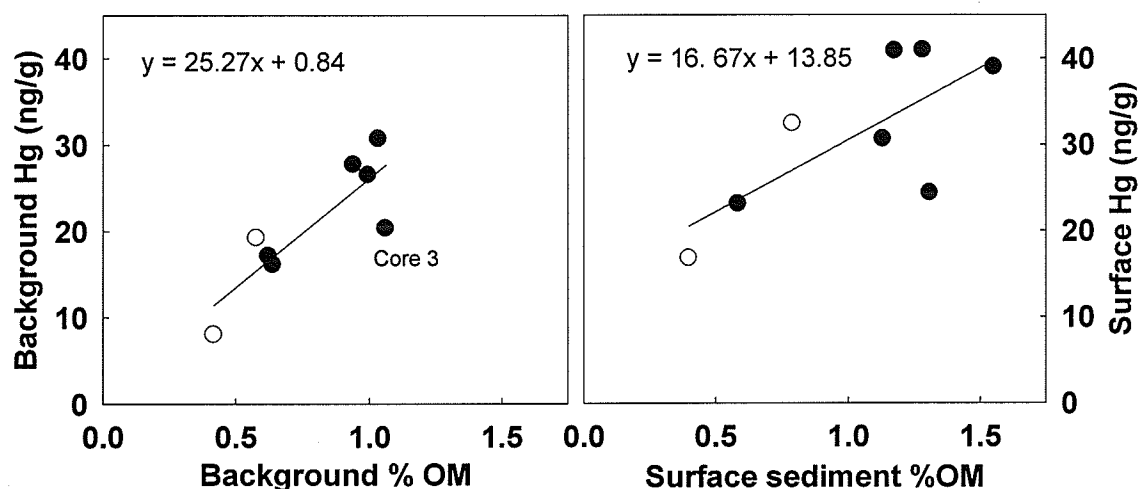


Figure 3-6. Relationships between Hg and OM content in background (left) and surface (right) sediments. Open circles represent cores located near river outlets, filled circles represent all remaining cores with steady background Hg concentrations.

Since all fluxes in Table 3-4 reflect the focusing of particles through their transport, resuspension, and deposition into quiescent areas, an estimate of the Bay-wide mean surface sediment Hg flux can be obtained from the total sediment burial flux of Hg in HB from Hare et al. (2008) (4.5 tonnes/yr). This estimate represents the burial flux of Hg for the system because it represents only that Hg captured by areas of the seafloor considered permanently depositional (10 % to 15% of the total area, (Hare et al. 2008, Kuzyk et al. 2009). Taking the surficial area of HB to be 8.41×10^5 km² (Jakobsson et al. 2003), the total mass flux (4.5 tonnes/yr) implies a mean flux of 0.4 to 0.6 ng/cm²/yr across the entire surface of the Bay and is representative of a

bulk focus-corrected flux for HB. This value is comparable to the focus-corrected Hg fluxes for two marine HB cores reported by Lockhart et al. (1998) (0.6 to 1.6 ng cm⁻² yr⁻¹), and is somewhat below focus-corrected freshwater Arctic and sub-Arctic Hg fluxes reported by Muir et al. (2009) (1.1 to 2.7 ng cm⁻²yr⁻¹) and Hermanson (1998) (1.8 ng cm⁻²yr⁻¹). The difference perhaps implies that there is a net flux of recently deposited Hg across the sediment-water interface due to mixing, even in areas which are considered not permanently depositional.

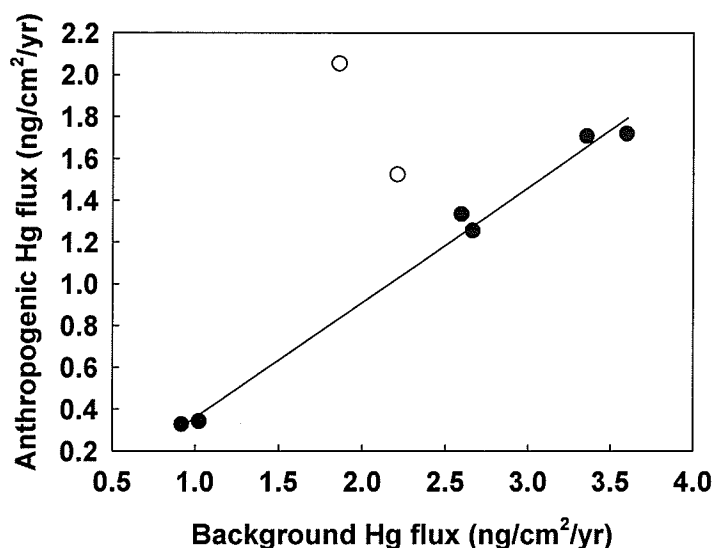


Figure 3-7. The relationship between Anthropogenic and Background Hg fluxes. Open circles represent cores located near river outlets, filled circles represent all remaining cores with steady background Hg concentrations.

Surface enrichment factors (SEFs), calculated as the ratio between the surface and background sediment flux, range from 1.3 to 2.1 and are comparable to those observed by Lockhart et al. (1998) (1.4) in eastern HB and by Muir et al. (2009) (1.1 to 5.1) in 14 sub-Arctic lakes. The consistency of SEFs in most cores (1.3 to 1.5) (Table 3-4) indicates that anthropogenic Hg loadings are generally proportional to background Hg concentrations. This implies the SEFs are mainly controlled by

similar rates of Hg scavenging by incident particles rather than by, for example, regional differences in modern Hg sources, which would de-couple the connection to background Hg concentrations. Consistent SEFs also support the assumptions of consistent particle size composition and sedimentation rates over time in HB, because unequal changes in these parameters would affect the Anthropogenic Hg loadings on incident particles disproportionately among the cores (Figure 3-5). However, higher SEFs are noticeable in cores 6 and 9, which were sited near major river outlets (Figure 3-1). These enrichments may reflect the transport of Hg on particles from the watershed into the coastal area; this process potentially augments vertical scavenging of atmospherically deposited Hg in these regions. In contrast to the spatial gradient of lake sediment SEFs in North America (Muir et al. 2009), SEFs in HB are only weakly negatively related to latitude ($r^2 = 0.29$). This relationship could reflect a longer water column residence time of Hg relative to the time period of water mass circulation, or that atmospheric Hg deposition is relatively equal across the latitudes represented by the core sites (55° N to 62° N).

Considering the role of vertical particle fluxes in sediment Hg distribution, sequestration by particles is an important mechanism in communicating changes in atmospheric Hg emissions to HB sediments. The involvement of OM is particularly implied by the relationship between Excess Hg Inventories and OM Inventories calculated to the same depth ($r^2 = 0.92$, $p < 0.02$, excluding cores 6 and 9) and the similar spatial distribution between excess Hg inventories and productive regions in HB. Core 6 and particularly, core 9 depart from this relationship because they contain the highest proportions of terrestrial carbon (Kuzyk et al. 2009) and exhibit different

Hg-OM relationships (Figure 3-5), possibly due to differences in the composition of marine and terrestrial OM. Excess sediment Hg inventories indicate increasing Hg capture throughout all HB (Figure 3-1) but generally mirror the pattern of higher productivity along the coast compared to offshore regions. The largest increases in Hg capture exist in the east (cores 3, 5, and 8), near rivers (cores 6 and 9), and along the west coast (cores 11 and 12), and the smallest in central HB (cores 10, 13 and 14) and in low depositional areas (cores 4 and 7). Excess Inventories range from 16 to 173 ng/cm² since the onset of increasing Hg concentrations. For comparison, excess (contaminant) Hg inventories in three Greenland lakes range from 21 to 57 ng/cm² for a 100 to 130 year period (Bindler et al., 2001). The higher excess inventories in HB sediments likely reflect higher sedimentation rates and increased proximity to anthropogenic Hg emissions relative to Greenland, which are both susceptible to contaminant transport from North American air masses (Davidson et al, 1993; Goto-Azuma and Koerner, 2001). The total amount of anthropogenic Hg stored in HB sediments can be estimated by scaling the excess inventories to the total area of the HB seafloor considered depositional. Excluding excess inventories from cores 10 and 13 due to evidence of large underlying natural enrichments, roughly 52 to 80 tonnes of anthropogenic Hg are stored in HB sediments. This is equivalent to just 29% to 45% of the Hg emission estimated for North America in 2006 alone (Streets et al., 2009).

3.6 Impact of Anthropogenic Hg on marine sediment Hg distribution

The impact of anthropogenic Hg on HB sediments can be widely observed in the simple Hg flux histories that largely mirror the known timeline of industrial Hg emissions over the last century and a half, and in the SEFs determined from modern and preindustrial Hg fluxes. The Hg flux histories also indicate that anthropogenic Hg has contributed to a nearly ubiquitous increase in Hg concentrations in sediments, compared to those present during the most recent post-glacial preindustrial period. Nevertheless, the concentrations resulting from the elevated industrial-era atmospheric Hg concentrations only marginally exceed the pre-industrial range in sedimentary Hg concentrations measured in this system. This is particularly evident in those cores that distinctly demonstrate anthropogenic Hg contributions (e.g. 3, 6, 7, 9, and 12) but display surface Hg concentrations similar or less than background Hg concentration observed elsewhere in HB (e.g., cores 4, 8 and 14) (Figure 3-2). Moreover, the large increases in Hg concentrations in sections of cores 10 and 13 representing deposition before the industrial period (2.4 to 3 fold, Figure 3-1) are greater than the enrichments that occurred during the industrial period in the same cores. A similar observation was made by Lindeberg et al. (2006) who demonstrated that Hg variations in preindustrial-era Greenland lake sediments as large as those observed during the industrial era can be attributed to natural processes, particularly in relatively pristine environments with low levels of contamination. Given the links between increased industrial-era exposure to environmental Hg and elevated Hg levels in contemporary biological tissues (Dietz et al., 2006; EEA, 2005; Eide et al., 1993; Outridge et al., 2002; Sun et al., 2006; Thompson et al., 1992), these

observations emphasize the biological impact of relatively small anthropogenic additions of Hg to natural environmental Hg concentrations.

3.7 References

- Asmund, G. and Nielsen, S., 2000. Mercury in dated Greenland marine sediments. *Science of The Total Environment*, 245: 61-72.
- Bindler, R., Olofsson, C., Renberg, I. and Frech, W., 2001a. Temporal Trends in Mercury Accumulation in Lake Sediments in Sweden. *Water, Air, & Soil Pollution: Focus*, 1(3): 343-355.
- Bindler, R., Renberg, I., Appleby, P.G., Anderson, N.J. and Rose, N.L., 2001b. Mercury Accumulation Rates and Spatial Patterns in Lake Sediments from West Greenland: A Coast to Ice Margin Transect. *Environmental Science & Technology*, 35(9): 1736.
- Davidson, C.I., Jaffrezo, J.-L., Small, M.J., Summers, P.W., Olson, M.P. and Borys, R.D., 1993. Trajectory analysis of source regions influencing the south Greenland Ice Sheet during the Dye 3 Gas and Aerosol Sampling Program. *Atmospheric Environment. Part A. General Topics*, 27(17-18): 2739-2749.
- Delongchamp, T.M., Lean, D.R.S., Ridal, J.J. and Blais, J.M., 2009. Sediment mercury dynamics and historical trends of mercury deposition in the St. Lawrence River area of concern near Cornwall, Ontario, Canada. *Science of The Total Environment*, 407(13): 4095-4104.
- Dietz, R., Riget, F., Born, E.W., Sonne, C., Grandjean, P., Kirkegaard, M., Olsen, M.T., Asmund, G., Renzoni, A., Baagoe, H. and Andreassen, C., 2006. Trends in Mercury in Hair of Greenlandic Polar Bears (*Ursus maritimus*) during 1892 - 2001. *Environmental Science & Technology*, 40(4): 1120-1125.
- EEA, 2005. Environment and Health, European Commission, Copenhagen.
- Eide, R., Wesenberg, G.R. and Fosse, G., 1993. Mercury in primary teeth in preindustrial Norway. *European Journal of Oral Sciences*, 101(1): 1-4.
- Fitzgerald, W.F., Engstrom, D.R., Lamborg, C.H., Tseng, C.M., Balcom, P.H. and Hammerschmidt, C.R., 2005. Modern and Historic Atmospheric Mercury Fluxes in Northern Alaska: Global Sources and Arctic Depletion. *Environ. Sci. Technol.*, 39(2): 557-568.

- Gagnon, C., Pelletier, E. and Mucci, A., 1997. Behaviour of anthropogenic mercury in coastal marine sediments. *Marine Chemistry*, 59: 159-176.
- Gobeil, C. and Cossa, D., 1993. Mercury in Sediments and Sediment Pore Water in the Laurentian Trough. *Can. J. Fish. Aquat. Sci.*, 50: 1794-1800.
- Gobeil, C., Macdonald, R.W. and Smith, J.N., 1999. Mercury Profiles in Sediments of the Arctic Ocean Basins. *Environ. Sci. Technol.*, 33(23): 4194-4198.
- Goto-Azuma, K. and Koerner, R.M., 2001. Ice core studies of anthropogenic sulfate and nitrate trends in the Arctic. *Journal of Geophysical Research D: Atmospheres*, 106(D5): 4959-4969.
- Hare, A., Stern, G.A., Macdonald, R.W., Kuzyk, Z.Z. and Wang, F., 2008. Contemporary and preindustrial mass budgets of mercury in the Hudson Bay Marine System: The role of sediment recycling. *Science of The Total Environment*, 406(1-2): 190.
- Hermanson, M.H., 1998. Anthropogenic Mercury Deposition to Arctic Lake Sediments. *Water, Air, and Soil Pollution*, 101: 309-321.
- Jakobsson, M., 2002. Hypsometry and volume of the Arctic Ocean and its constituent seas. *Geochemistry Geophysics Geosystems*, 3(5).
- Johannessen, S., Macdonald, R.W. and Eek, K.M., 2005. Historical Trends in Mercury Sedimentation and Mixing in the Strait of Georgia, Canada. *Environ. Sci. Technol.*, 39: 4361-4368.
- Josenhans, H., Balzer, S., Henserson, P., Nielson, E., Thorliefson, H. and Zevenhuizen, J., 1988. Preliminary seismostratigraphic and geomorphic interpretations of the Quaternary sediments of Hudson Bay, Geological Survey of Canada.
- Kirk, J.L. and St. Louis, V.L., 2009. Multiyear Total and Methyl Mercury Exports from Two Major Sub-Arctic Rivers Draining into Hudson Bay, Canada. *Environmental Science & Technology*, 43(7): 2254.
- Kuzyk, Z.A., Goñi, M.A., Stern, G.A. and Macdonald, R.W., 2008. Sources, pathways and sinks of particulate organic matter in Hudson Bay: Evidence from lignin distributions. *Marine Chemistry*, 112(3-4): 215.

- Kuzyk, Z.A., Macdonald, R.W., Johannessen, S.C., Gobeil, C. and Stern, G.A., 2009. Towards a Sediment and Organic Carbon Budget for Hudson Bay. *Marine Geology*, 264: 190-208.
- Lamborg, C.H., Fitzgerald, W.F., O'Donnell, J. and Torgersen, T., 2002. A non-steady-state compartmental model of global-scale mercury biogeochemistry with interhemispheric atmospheric gradients. *Geochimica et Cosmochimica Acta*, 66(7): 1105.
- Leitch, D.R., Carrie, J., Lean, D., Macdonald, R.W., Stern, G.A. and Wang, F., 2007. The delivery of mercury to the Beaufort Sea of the Arctic Ocean by the Mackenzie River. *Science of The Total Environment*, 373(1): 178.
- Lindeberg, C., Bindler, R., Bigler, C., Rosen, P. and Renberg, I., 2007. Mercury Pollution Trends in Subarctic Lakes in the Northern Swedish Mountains. *AMBIO: A Journal of the Human Environment*, 36(5): 401-405.
- Lindeberg, C., Bindler, R., Renberg, I., Emteryd, O., Karlsson, E. and Anderson, N.J., 2005. Natural Fluctuations of Mercury and Lead in Greenland Lake Sediments. *Environmental Science & Technology*, 40(1): 90.
- Lockhart, W.L., Wilkinson, P., Billeck, B.N., Danell, R.A., Hunt, R.V., Brunskill, G.J., Delaronde, J. and St. Louis, V., 1998. Fluxes of mercury to lake sediments in central and northern Canada inferred from dated sediment cores. *Biochemistry*, 40: 163 - 173.
- Lorey, P. and Driscoll, C.T., 1999. Historical Trends of Mercury Deposition in Adirondack Lakes. *Environmental Science and Technology*, 33: 718-722.
- Lucotte, M., Mucci, A., Hillaire-Marcel, C., Pichet, P. and Grondin, A., 1995. Anthropogenic mercury enrichment in remote lakes of northern Québec (Canada). *Water, Air, & Soil Pollution*, 80(1): 467-476.
- Macdonald, R.W. and Thomas, D.J., 1991. Chemical interactions and sediments: The western Canadian Arctic Shelf. *Continental Shelf Research*, 11: 843-864.
- Mason, R.P., Fitzgerald, W.F. and Morel, F.M.M., 1994. The biogeochemical cycling of elemental mercury: Anthropogenic influences. *Geochimica et Cosmochimica Acta*, 58: 3191-3198.

- Mason, R.P. and Sheu, G.P., 2002. Role of the ocean in the global mercury cycle
Global Biogeochem. Cycles, 16(4): 1093.
- Muir, D.C.G., Wang, X., Yang, F., Nguyen, N., Jackson, T.A., Evans, M.S., Douglas,
M., Kock, G., Lamoureux, S., Pienitz, R., Smol, J.P., Vincent, F. and Dastoor,
A., 2009. Spatial Trends and Historical Deposition of Mercury in Eastern and
Northern Canada Inferred from Lake Sediment Cores. Environ. Sci. Technol.,
43: 4802-4809.
- Outridge, P.M., Hobson, K.A., McNeely, R. and Dyke, A., 2002. A comparison of
modern and preindustrial levels of mercury in the teeth of Beluga in the
Mackenzie delta, Northwest Territories, and Walrus at Igloodok, Nunavut,
Canada. Arctic, 55(2): 123-132.
- Outridge, P.M., Sanei, H., Stern, G.A., Hamilton, P.B. and Goodarzi, F., 2007.
Evidence for Control of Mercury Accumulation Rates in Canadian High
Arctic Lake Sediments by Variations of Aquatic Primary Productivity.
Environ. Sci. Technol., 41(15): 5259-5265.
- Perry, E., Norton, S.A., Kamman, N.C., Lorey, P.M. and Driscoll, C.T., 2005.
Deconstruction of Historic Mercury Accumulation in Lake Sediments,
Northeastern United States. Ecotoxicology, 14(1): 85-99.
- Smith, J.N. and Schafer, C.T., 1999. Sedimentation, bioturbation, and Hg uptake in
the sediments of the estuary and Gulf of St. Lawrence. Limnol. Oceanogr.,
44(1): 207-219.
- Streets, D.G., Zhang, Q. and Wu, Y., 2009. Projections of Global Mercury Emissions
in 2050. Environmental Science and Technology, 43: 2983-2988.
- Sun, L., Yin, X., Liu, X., Zhu, R., Xie, Z. and Wang, Y., 2006. A 2000-year record of
mercury and ancient civilizations in seal hairs from King George Island, West
Antarctica. Science of The Total Environment, 368(1): 236.
- Swain, E.B., Engstrom, D.R., Brigham, M.E., Henning, T.A. and Brezonik, P.L.,
1992. Increasing rates of atmospheric mercury deposition in midcontinental
North America. (lakes of Minnesota & Wisconsin). Science,
v257(n5071): p784(4).

Thompson, D.R., Furness, R.W. and Walsh, P.M., 1992. Historical changes in mercury concentrations in the marine ecosystem of the north and north-east Atlantic ocean as indicated by seabird feathers, *Journal of Applied Ecology*. Blackwell Publishing Limited, pp. 79-84.

CHAPTER 4

Biogeochemistry of Organic Matter and Mercury in Recent Marine Sediments from Hudson Bay, Canada

Abstract

A combination of Rock Eval and elemental analyses are used to characterize the sources and organization of sedimentary organic matter in modern marine sediments of Hudson Bay, Canada. The pattern of labile and residual carbon indicates a greater influence of terrestrial organic matter along the southern coast and marine organic matter offshore and towards the north. These patterns reflect locations of higher primary productivity, watershed runoff, and the distribution of vegetation of the surrounding watershed. The characteristics of residual organic matter are consistent with a strong presence of sediment recycling, particularly of organic matter originating from marine sources. Fresh and reworked material can be distinguished in recent sediments and related to nearby sources or internal processing. Identification of classes of carbon compounds via their temperature of peak hydrocarbon yield (T_{max}) are consistent with the marine and terrestrial OM distribution interpreted from labile and residual carbon patterns. Separation of the total organic carbon into carbon fractions permits distinguishing the role of particular forms of organic carbon as carriers in the vertical particle flux of a common particle-reactive metal, mercury. The unique sedimentary dynamics functioning in Hudson Bay can be observed through a distinct relationship between a mercury and oxygenated and reworked marine carbon.

4.0 Introduction

Marine sediments often provide a valuable record of past and present organic matter (OM) capture that reveals the depositional environment and how major biogeochemical processes function in a marine system. The characterization of marine sediments by Rock-Eval (RE) analyses provides an assessment of the OM record by separating sedimentary OM into fractions based on their lability under pyrolytic (oxygen-free combustion) and oxidizing conditions. RE is a conventional petroleum geoscience method used to assess the hydrocarbon potential of sedimentary rocks but has also been used to investigate the organic composition of soils and recent freshwater sediments (di-Giovanni et al., 1998; Disnar et al., 2003; Sanei et al., 2000; Sanei et al., 2005; Sebag et al., 2006). Such an evaluation can help distinguish the relative contribution of aquatic versus terrestrial OM, the degree of post-depositional diagenetic decay, and identify the classes of carbon compounds composing the OM, complementary to other geochemical assessments such as isotopic and elemental ratios (Schulz and Zabel, 2000). RE analyses have been also used to investigate modern marine sediments because of their utility in identifying OM source and composition (e.g. (Liebezeit and Wiesner, 1990; Marchand et al., 2003; Marchand et al., 2008). Recent work in modern freshwater sediments has also shown that RE analyses can help address the issue of explaining temporal variation in Hg, a particle-reactive heavy metal of concern in many aquatic systems (Outridge et al., 2007; Sanei and Goodarzi, 2006; Stern et al., 2009; Carrie et al. 2009). In particular, the “S2” component of hydrocarbon yield has the capacity to track temporal changes in Hg capture in some lakes through its role in scavenging Hg and transporting it via

particle flux to the sediments. This relationship may partly explain Hg enrichments in surface sediments in some freshwater systems and provides an additional piece of evidence of the role that OM plays in distributing Hg within aquatic systems.

This study provides insight into the source, distribution, processing and classes of OM in HB sediments accumulated since the last deglaciation (~10 ky.a). Recent geochemical studies in HB provide substantial supporting information that characterizes OM sources and degradation processes with a variety of elemental and biomarker measurements (Kuzyk et al., 2008; Kuzyk et al., 2009a; Kuzyk et al., 2009b). These studies provide an opportunity to investigate how RE parameters describe a complicated coastal marine system with multiple sources of old and modern OM. They further provide an opportunity to investigate the relationship between carbon fractions defined by RE analyses and Hg in a marine setting. The organization of sedimentary OM described by RE analyses demonstrates a spatial distribution of terrestrial and marine OM in sediments across the Bay that corresponds to known patterns of productivity and watershed contributions. The distribution of labile and residual carbon is also consistent with a strong role of lateral sedimentary redistribution and extensive reworking of marine OM. These processes are reflected in a distinctive relationship between Hg and reworked marine OM.

4.1 Experimental Methods

4.1.1 Study Area

Hudson Bay (HB) is one of the largest shelf seas in the world and is separated from the global oceans by Baffin Island. It contains mainly Arctic Ocean surface

water and supports Arctic marine species at latitudes as far south as 55 °N (Stewart and Lockhart, 2005). HB surface waters cycle annually from > 9/10^{ths} ice-covered to completely ice-free, and the annual process of ice-melt, augmented by extensive river discharge, vertically stratifies the water column throughout most of the open water season (Prinsenbergh, 1988; Saucier et al., 2004). Nutrient replenishment above the pycnocline is largely restricted by this stratification, thereby limiting most primary production to the northeast and eastern coasts and the extreme west where coastal currents, rivers, or upwellings near islands and polynyas supplement the surface nutrient pool (Kuzyk et al., 2009b). HB is considered an oligotrophic system with mean annual primary production ranging between 24 g C/m²/year (Jones and Anderson, 1994) to as high as 70 g C/m²/yr (Sakshaug, 2004). HB sediments, which also receive terrestrial particulates from the large drainage basins surrounding the Bay, reflect a latitudinal gradient of temperate to Arctic vegetation in the sedimentary OM (Kuzyk et al., 2008).

All of HB was extensively covered by the Laurentide Ice Sheet during the last glaciation (8 to 10 k.y.a.) and the basin was depressed several hundred metres relative to current levels. Since the disappearance of the Ice Sheet, HB has experienced rapid isostatic rebound at a rate of up to >1 m per century at many southern and southwestern coastal sites, but a far lower rate of rebound occurs in northern regions (Hillaire-Marcel and Fairbridge, 1978). New coastal flats are emerging in the south and west at rates up to 15 m per year, exposing large sections of seabed to erosion by waves and currents and by ice scouring, which occurs at depths up to 20 m (Héquette et al., 1999).

Vast shallows extend far offshore from the southern and western coasts of HB with the deepest basins attaining only around 250 m, although depths greater than 500 m are found in Hudson Strait to the north (Ingram and Prinsenberg, 1998). Much of the basin is underlain by sedimentary rocks dominated by carbonates. However, crystalline Canadian Shield rock composes large portions of the coastal margin along the east and northwest coasts and near the Belcher Islands (Stewart and Lockhart, 2005). Unconsolidated materials such as gravels, sand, silt and clay overlay much of the bedrock along the southern coast but diminish towards the north where exposed rock is more prevalent.

4.1.2 Sample Collection

Sediments were collected as previously described in Hare et al. (2008). Briefly, 13 box cores from HB and HS were collected in 2005 during the ArcticNet expedition onboard the *CCGS Amundsen* (Figure 4-1). Cores were sub sectioned at 1 cm intervals for the upper 10 cm, and at 2 cm and 5 cm intervals for depths from 10 to 20 cm and 20 to 45 cm, respectively. All layers were individually homogenized and immediately further sub-sampled for separate analyses. Heterogeneous pockets of coarse-grained materials were visually apparent in deep layers of cores 10 and 13. Samples were stored frozen at -20 °C during transport and storage at the Freshwater Institute in Winnipeg, Canada. Sediments were subsequently freeze dried and stored in the dark at room temperature until analyses.

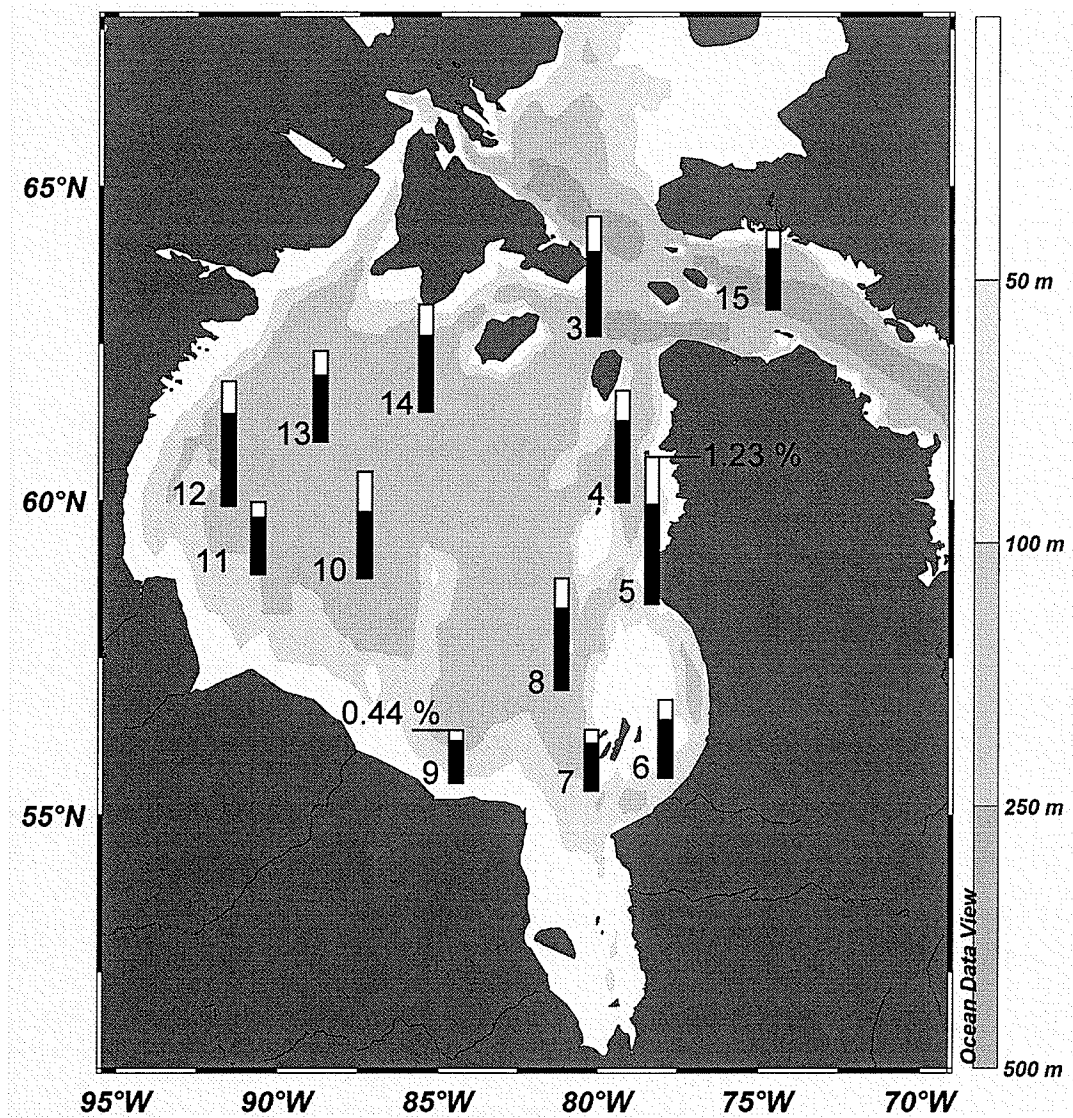


Figure 4-1. Box core locations and relative proportions of PC and RC fractions in marine sediments from Hudson Bay. White bars = PC, (PC = S1 + S2 + S3), black bars = RC. Highest and lowest surface values of TOC are indicated. Numbers refer to core designations in the text.

4.1.3 Grain size analysis

Grain size measurements were determined for one surficial layer in each core (core 3: 2-3 cm, all other cores: 1-2 cm) by organic matter removal with extended peroxidation and a Beckman Coulter LS200 laser diffraction grain size analyzer at Queen's University (Kingston, ON).

4.1.4 Organic Matter measurements

Organic matter (OM) was measured and classified by Rock Eval-6 (Vinci Technologies) performed at the Geological Survey of Canada in Calgary, AB, according to standard protocols (Behar et al., 2001). This procedure releases carbon compounds sequentially from sediments by heating up to 800 °C in an oxygen-free atmosphere (pyrolysis) and detects the released hydrocarbons by a flame ionization detector. The remaining material is then combusted in an oxidation oven at 850 °C. During both steps the CO and CO₂ are simultaneously monitored to measure pyrolizable oxygen-containing organic matter, inert OM (residual carbon; RC), as well as mineral carbon, which generally begins to decompose above 400 °C. Pyrolizable Carbon (PC) includes free hydrocarbons (S1), hydrocarbons released by the pyrolytic cracking of kerogen (S2), and CO/CO₂ released by oxygen-containing organic matter (S3) during pyrolysis stage. The Total Organic Carbon (TOC) is composed PC and additional CO and CO₂ groups released during oxidation of the refractory organic carbon (Residual Carbon (RC)). Hydrogen and Oxygen indices (HI and OI, respectively) are determined as the ratio of S2/TOC for HI and S3/TOC for OI. The distinction between CO and CO₂ yields permits the calculation of OICO,

which represents only the CO fraction of TOC and is determined from the ratio $S3CO/TOC$. All units of carbon measurements are calculated using the dry weight of the sediments. Analysis of the standard reference materials 160000 ($n = 3$) from the Institut Français du Pétrol and 9107 Shale Standard ($n = 45$) from the Geological Survey of Canada showed relative standard deviations from 1 to 9 % for all major parameters. Acid digestion and re-analysis of a subset of samples demonstrated little evidence of inorganic carbon contributions to the measured carbon yields except in OICO measurements in 3 of 4 layers in core 10. This may represent a limited contribution of Siderite, which can produce both CO and CO₂ after pyrolysis (Marchand et al., 2008). However, OI values were only slightly reduced with no relationship to mineral carbon content and all RE measurements presented here are original data. OM inventories were calculated for each core by integrating the total mass yield of hydrocarbons in sediment layers representing the most recent 130 years (1875 to 2005) of accumulation based on the core-specific linear sedimentation rate.

4.1.5 Elemental and Isotopic Analyses

C:N ratios were determined by analysis on a Carlo-Erba NA-1500 Elemental Analyzer at the University of British Columbia, and $\delta^{13}C$ was measured similarly but from acid-decarbonated samples and with an inline isotope ratio mass spectrometer. The relative precision for these analytes was $\pm 0.3\%$ and $\pm 1.6\%$, respectively. RE6 and elemental analysis by other techniques demonstrate nearly identical results for the determination of organic and mineral carbon (Behar et al. 2001).

4.2 Results and Discussion

4.2.1 Contributions of terrestrial and marine OM

Differences in the proportions of carbon fractions between terrestrial and marine OM provide information about the relative contributions of these OM sources to the sediments. While all carbon fractions are present in both marine and terrestrial OM, marine OM generally contains higher proportions of S1 and S2 carbon than terrestrial plant OM, which generally contains higher proportions of S3 or RC fractions (Lüniger and Schwark, 2002; Marchand et al., 2008; Sanei et al., 2005). These differences arise from the largely algal origin of marine OM, which lack the celluloses and lignins found in terrestrial OM and compose the highly oxygenated or recalcitrant compounds that compose the S3 and RC fractions. The distribution of hydrocarbon, oxygenated carbon and recalcitrant compounds is broadly reflected in the pattern of labile and residual carbon, which show higher proportions of PC offshore and in the northeast, and higher proportions of RC along the southern and southwest coasts (Figure 4-1). Nevertheless, the proportions of the carbon fractions can also be altered by weathering and biological degradation, which can reduce the labile carbon content and increase the oxygen index (Lüniger and Schwark, 2002; Vandenbroucke and Largeau, 2007), thereby enriching the S3 and RC fractions in sediments.

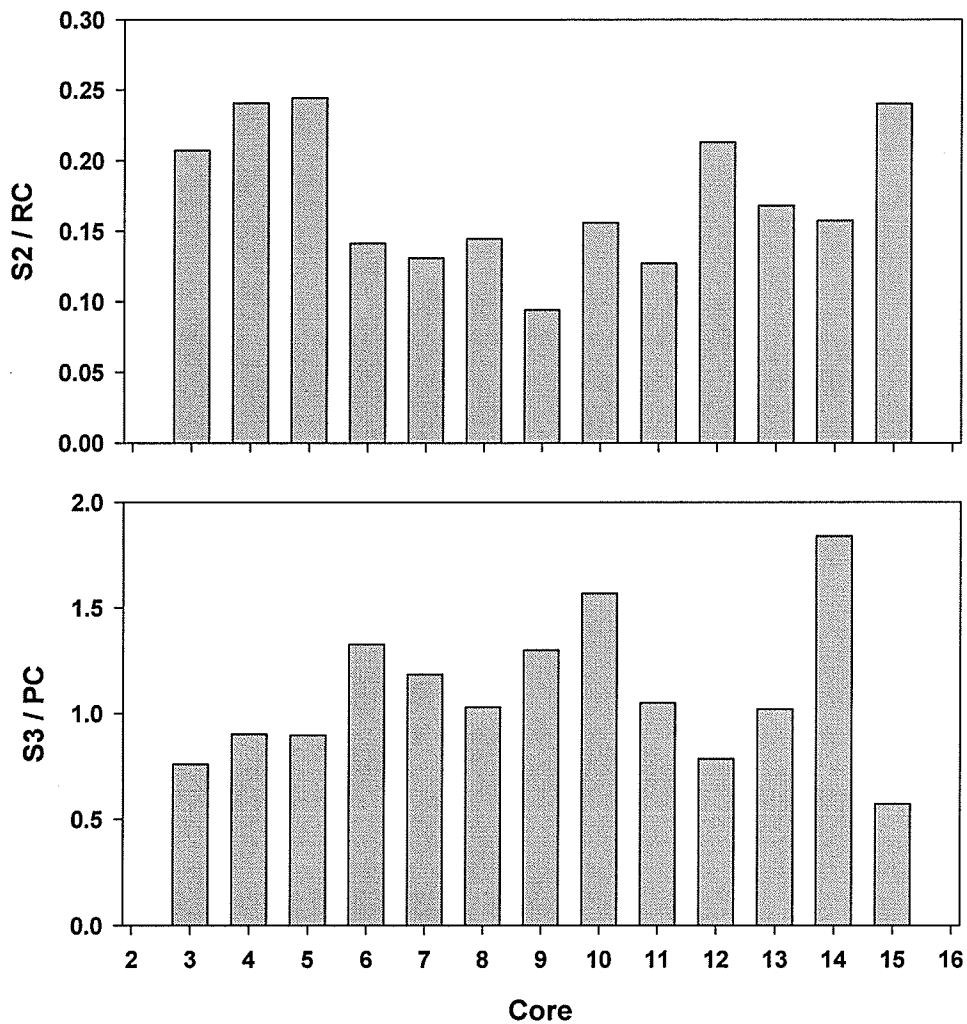


Figure 4-2. Inventories of labile carbon in HB. Left panel, S2 Carbon Inventories normalized to RC Inventories. Right panel, S3 Carbon Inventories normalized to PC Inventories. Inventories were calculated for a 130 year period prior to sample collection.

The variation in marine and terrigenous OM sources in HB is also reflected in the spatial pattern of the relative composition of S2 carbon to RC carbon (Figure 4-2). Total S2 carbon inventories normalized to RC inventories are much larger in the north east (cores 3, 4, 5, and 15) and the extreme west (core 12) than in cores from the south and south western coasts (6, 7, 9 and 11) (Figure 4-2). This distribution does not arise from variable rates of production and preservation because both the southern

coastal margin and north east regions of HB display higher productivity than offshore, and OM oxidation does not appear to explain this spatial pattern based on the pattern of OM burndown displayed in vertical S2/RC profiles (Figure 4-3).

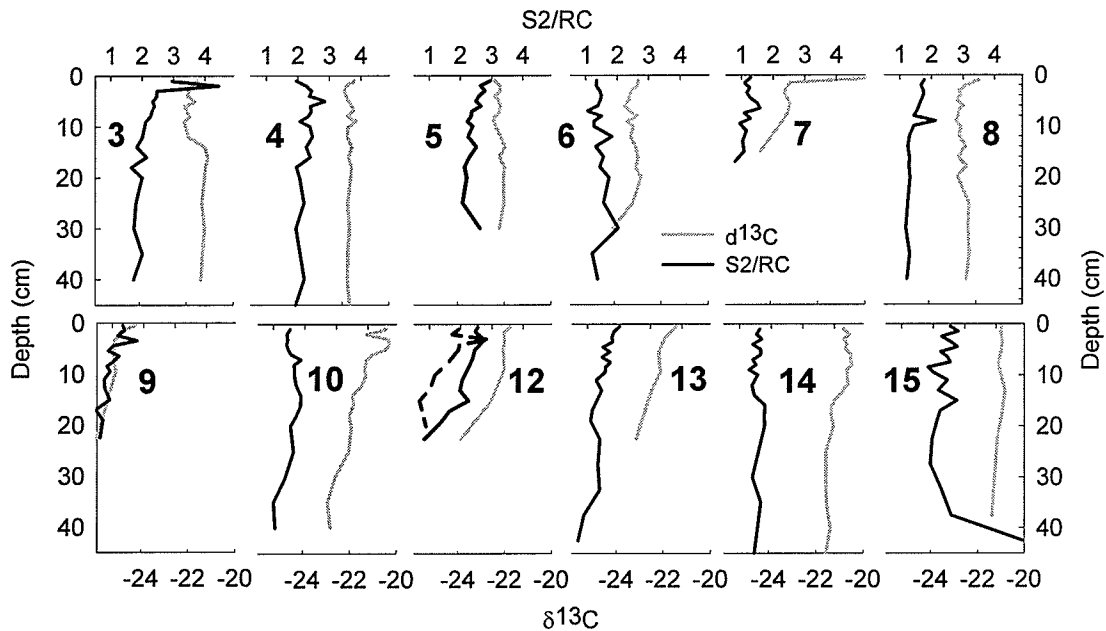


Figure 4-3. S2/RC and $\delta^{13}\text{C}$ (‰) content in HB marine sediments.

Furthermore, in situ OM oxidation rates in HB are generally low with little evidence of diagenetic decay in most areas (Kuzyk et al., 2009a). Rather, the distribution of S2 carbon inventories suggests that the north eastern and extreme western regions of HB receive a greater proportion of labile OM than the southern coast, which receives larger proportions of residual OM. The locations of higher proportions of S2 carbon are consistent with regions of recurring polynyas and higher water column nutrients in the north east and extreme west (Irwin et al., 1988; Saucier et al., 2004). Such areas support higher levels of productivity in the water column than elsewhere in HB (Harvey et al., 1997) and could be expected to transfer this signal to the sediments beneath. This distribution is also consistent with the mean Hydrogen Index (HI)

values (determined by S2-TOC regression to avoid a matrix effect from the mineral portion of the sediments (Dahl et al., 2004; Langford and Blanc-Valleron, 1990) which separate the cores into two groups by mean HI values of 161 and 119 (Figure 4-4). These HI values are similar to those commonly observed in sediments from other Arctic Ocean shelf seas, where they reflect greater preserved marine OM and greater preserved terrigenous OM in sediments, respectively (Stein and Macdonald, 2004).

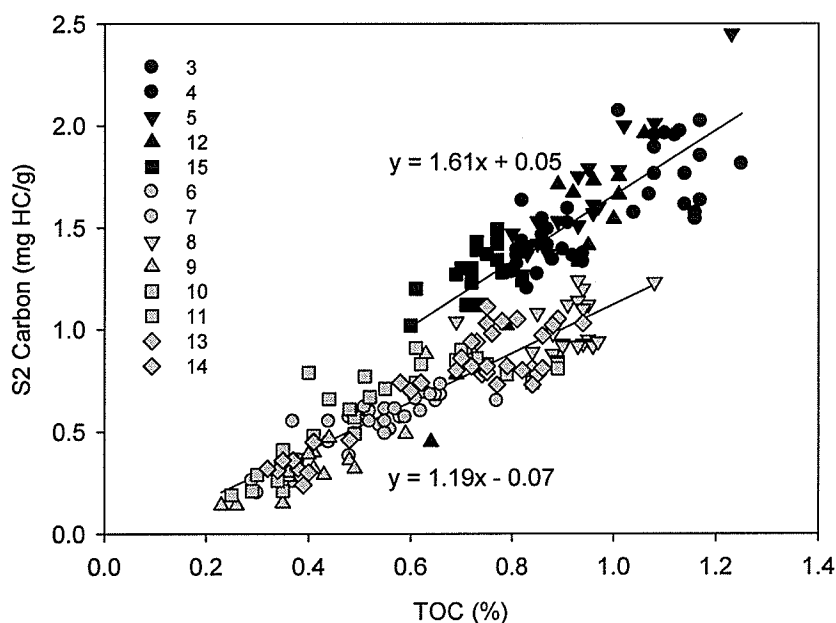


Figure 4-4. Determination of the mean HI in two groups of sediments of HB.

In contrast, terrestrial OM from the watershed is largely delivered to HB along the south and south western coasts in river runoff, as indicated by lignin and CDOM surveys (Granskog et al., 2007; Kuzyk et al., 2008). Terrestrial OM contributions are reflected in the S3/PC ratio, which, excluding cores 10 and 14, demonstrates a spatial distribution roughly opposite to that of S2 carbon (Figure 4-2). Given the distance of cores 10 and 14 from terrestrial OM sources (> 200 km) and low lignin content in

these sediments (Kuzyk et al. 2008), the high S3 carbon proportions of PC may rather reflect re-worked, oxidized marine OM.

4.2.2 Contributions of fresh and degraded OM

The broad pattern of RC in HB suggests that most OM originates from marine rather than terrestrial OM. RC composes the majority of TOC in all cores (63 to 85%, Figure 4-1) and RC inventories display a similar spatial distribution as TOC inventories ($r^2 = 0.99$). These relationships imply that RC is a degradation product of TOC rather than a terrigenous component delivered in the detritus from the watershed. Moreover, the highest concentrations of RC are located in cores with the highest proportion of labile carbon, further implicating a marine source. The presence of largely degraded marine OM is also consistent with the distribution of HB sediments displayed in a Van Krevelen diagram. Overall, OM in HB sediments displays characteristics typical of Type III kerogen (Figure 4-5). Comparison of T_{max} temperatures and HI offers an alternative method of assessing kerogen characteristics of sedimentary OM independent of CO or CO₂ yields, and is also consistent with predominantly Type III kerogen characteristics of sedimentary OM in HB (Figure 4-5).

The low HI in HB sediments, ranging from 70 to 200 except for a few isolated values (Figure 4-5), indicates that fresh OM contributes minimally to the OM content because both algal and higher plant materials generally have higher HI when fresh (typically > 300) (Luniger and Schwark, 2002, Marchand et al. 2008). Such dehydrogenated OM reflects biological processing as hydrogen is consumed during

metabolism of organic carbon. Oxygen Index (OI) values generally cluster between 140 and 300 in the majority of sediments but are up to 450 in cores 6 and 13, and reach nearly 800 exclusively in cores 10 and 14 (Figure 4-5). OI values in fresh algal materials tend to be lower than in higher plant materials due to the absence of celluloses and lignins which contain more oxygen-based functional groups. Some aquatic systems prone to selective capture of leaves and non-woody terrigenous tissues by low-velocity streams can also display low sedimentary OI from terrigenous OM (Lüniger and Schwark, 2002; Marchand et al., 2008), but such characteristics contrast with those of the HB watershed. Thus, the low OI sediments in these sediments likely reflect degraded marine OM rather than terrigenous OM. Similarly, although elevated oxygen content is commonly attributed to terrestrial OM, it can also arise from the dehydrogenation and oxygenation of OM through biological processing. Thus while high OI values are commonly found in terrestrial OM they also predominate in reworked marine OM after oxidation has lowered the hydrogen content (Schulz and Zabel, 2000). Since the highest OI values (cores 10, 13 and 14) come from sediments of the offshore region, far from terrestrial sources of OM and low in lignin content (Kuzyk et al., 2009a), they more likely represent highly weathered marine OM. However, the elevated OI values in core 6 more likely reflect terrestrial OM because it is located next to a major river and displays lower S₂/RC and a higher proportion of RC (Figures 1 and 2).

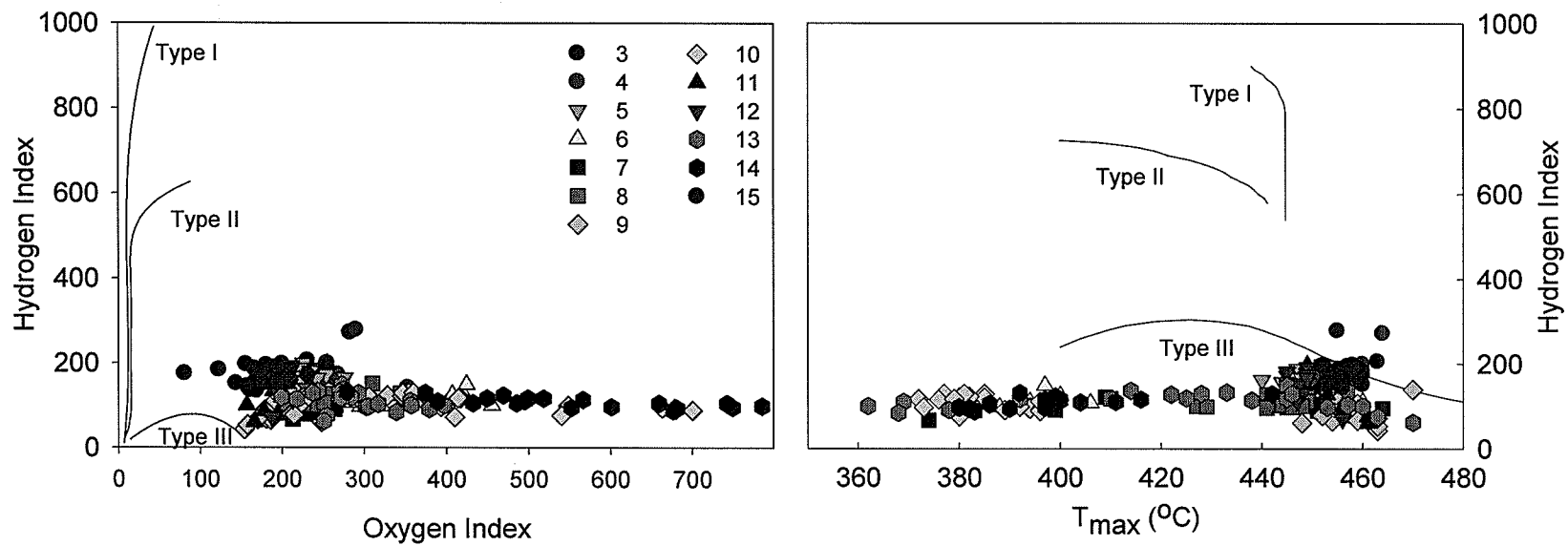


Figure 4-5. Van Krevelen-type diagrams of HB sediments. Solid black lines refer to classical kerogen maturation pathways.

4.2.3 Comparison of RE and Elemental analyses

Elemental analyses show the majority of these sediments are characteristic of marine OM rather than terrestrial OM because most (~85%) are associated with C:N ratios below 10, and terrestrial OM exhibits higher C:N ratios of ~10 to 24 in river particulates delivered to HB (Kuzyk et al., 2009a). Consequently, across all sediments the RC content has a weak, but significant, negative correlation with C:N ratio ($r^2 = 0.28$, $p < 0.001$) (Figure 4-6). This association is likely even stronger than implied by Figure 4-6, given that the sediment OM has undergone biological degradation which favours nitrogen and therefore would increase C:N above the marine (Redfield) ratio of 6.6. C:N and $\delta^{13}\text{C}$ ratios further indicate that the freshest OM is marine, whereas

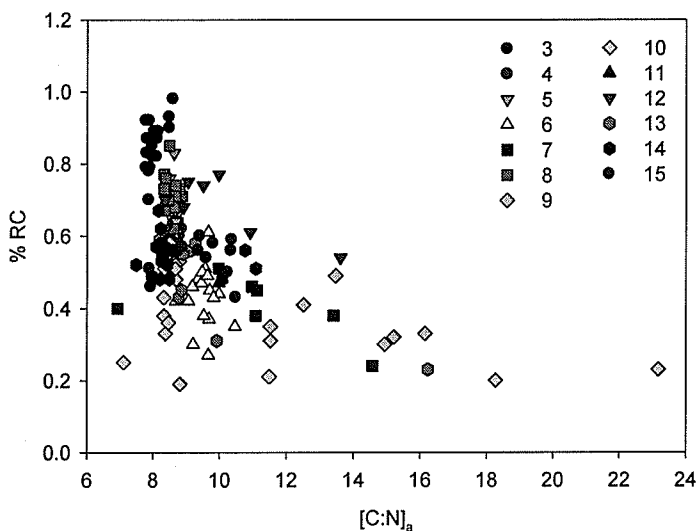


Figure 4-5. C:N ratios and RC content of HB sediments. Each point represents a single section from an individual core.

nearly all of the terrestrial OM appears reworked. This is demonstrated by the comparatively small range of C:N (7.8 to 10.9) and $\delta^{13}\text{C}$ content (-22.8 to -20.8 ‰), typical of marine OM in HB (Kuzyk et al., 2009), that is associated with HI values >

150 (Figure 4-7). The freshest marine OM appears in cores 3 and 15, where the enriched $\delta^{13}\text{C}$ content coincides with the highest HI values and the lowest OI values (Figure 4-7). A much wider range in ratios (C:N = 7 to 23.2 and $\delta^{13}\text{C}$ = -25.9 to 19.3 ‰), and values more typical of terrigenous OM, accompany HI values <150.

Sediments with the highest OI values (> 550, cores 10 and 14) have $\delta^{13}\text{C}$ signatures heavier than -21.2 ‰ while sediments with the lowest OI values (<200) span a range of $\delta^{13}\text{C}$ content from nearly -26 ‰ to nearly -21 ‰ (Figure 4-7). Inorganic carbonate such as Siderite cannot be the source of enriched $\delta^{13}\text{C}$ as observed elsewhere (Chow et al., 1996; Jacob et al., 2004) because carbonates were removed from the sediments before $\delta^{13}\text{C}$ measurements were performed. Rather, the high $\delta^{13}\text{C}$ values and low C:N ratios in cores 10 and 14 strongly implicate marine OM which, according to the OI, has been highly weathered. Although a shallow water column (200 to 250 m) argues against extensive degradation of labile OM during vertical transport and, consequently, little enrichment of OI (with corresponding elevation of S3 carbon), the limited local productivity in the water column contributes little OM to the sediments beneath. In contrast, lateral transport of sediment from the vast shallow 'pseudo-shelves' of HB appears to provide a major portion of the OM to the offshore sedimentary sink (Kuzyk et al., 2009a) and during transport this OM could become extensively reworked. According to this scheme, the interior basin sediments mostly reflect degraded material that has lost its labile carbon fractions (S1 and perhaps S2) during lateral transport and potentially oxygenated the remaining carbon compounds. This relationship reflects the sediment dynamics of the HB system. In contrast to Arctic Ocean basin sediments, where terrigenous OM is

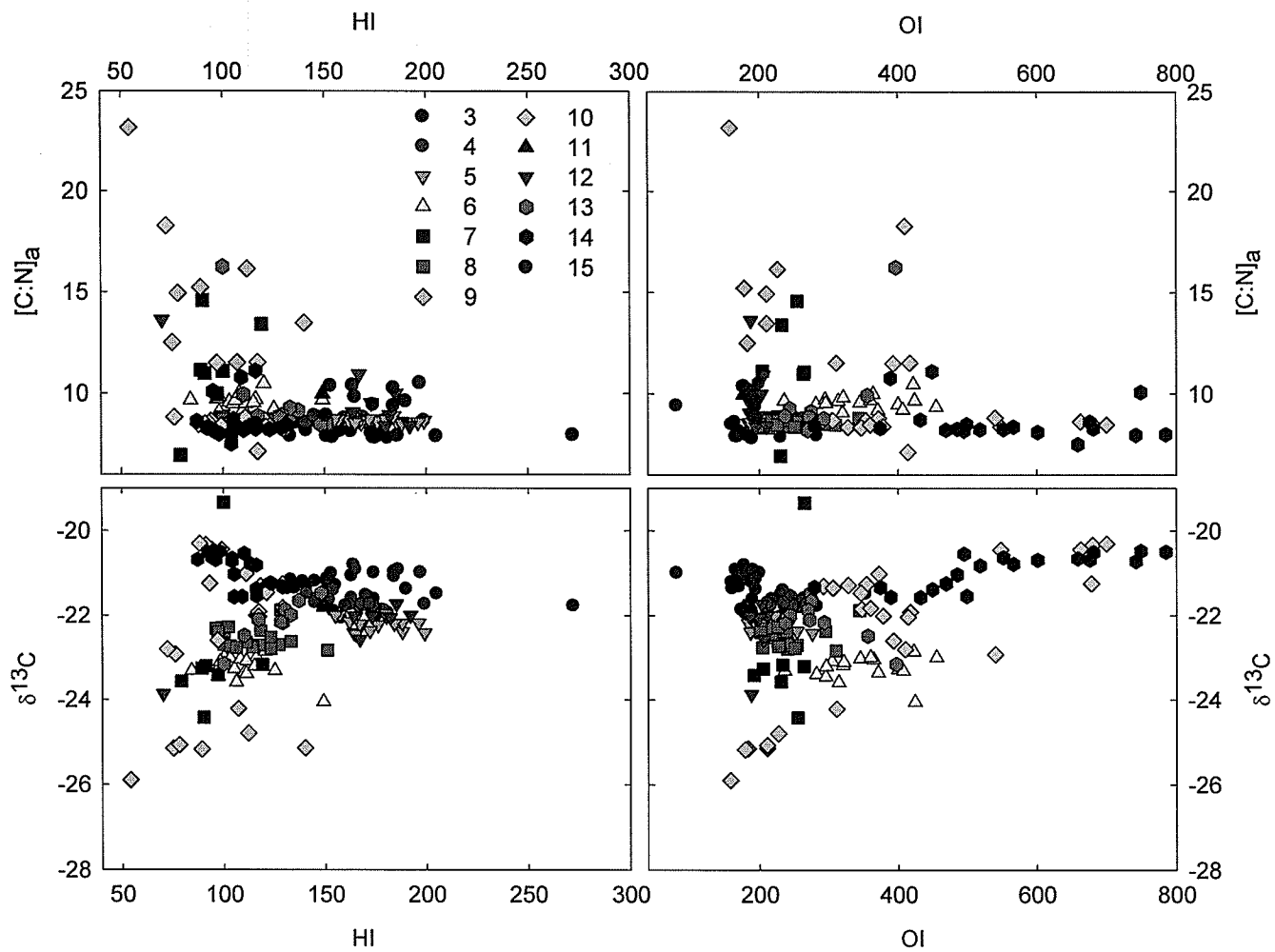


Figure 4-7. Comparison of HI and OI with elemental measurements of marine OM.

a large component (Stein and Macdonald, 2004), most RC in HB originates from marine OM, which can be inferred to have had higher proportions of labile carbon initially. However, the in-situ oxidation of OM appears to only play a minor role in determining the spatial variability of labile carbon (Kuzyk et al., 2009a). Rather, labile carbon oxidation mostly occurs during repeated cycles of resuspension along the vast shallow southern and western coasts (Kuzyk et al., 2009a). Recycling of OM in this way has the potential to enrich the RC fraction through degradation of labile OM and thereby increase the oxygen content of the OM. In an analogous manner, degradation of Type I kerogen can often be observed as a shift towards Type III kerogen with consequent elevation of the OI (Disnar et al., 2003; Jacob et al., 2004; Lüniger and Schwark, 2002; Vandembroucke and Largeau, 2007). This resuspension process provides a simple and plausible explanation for the marine origin of the S3 carbon observed in HB sediments.

Despite little evidence of fresh terrigenous OM, a distinction in the degree of degradation of terrestrial OM can be obtained from $\delta^{13}\text{C}$ in combination with OI, and OICO values, which represent the release of CO groups during pyrolysis. Similarly to OI, OICO values tend to increase in OM as it degrades. Reworked terrestrial OM is likely present in core 6 where OI values reach > 400 in sediments with $\delta^{13}\text{C}$ as low as -24‰ (Figure 7). In contrast, relatively fresher terrestrial OM appears in core 9 where sediments with $\text{OI} < 200$ and $\delta^{13}\text{C}$ below -25‰ are present (Figure 4-7, Table 4-1). Therefore, to offset the higher terrigenous content in core 9 and present higher OI in core 6, the OM in core 6 must be more degraded. This inference is supported by lignin data showing that sediments from core 9 contained fresher plant material than those in core 6 (Kuzyk et al., 2008). Similarly, sediments in cores 6 and 7 display higher OICO values

(mean = 64) than those in core 9 (mean = 23), despite containing greater proportions of marine carbon content based on $\delta^{13}\text{C}$ (Table 4-1). Yet, lignin ratios implied that terrestrial OM in sediments from core 9 originated from woody tissue while those in core 6 originated from predominantly non-woody tissue (e.g. leaves, needles, bark, pollen and stems) (Kuzyk et al., 2008), which should contribute to lower OICO in core 6 (Marchand et al., 2008). This discrepancy indicates that the extent of degradation of OM has greater influence on OICO than does the type of higher plant tissue.

Table 4-1. OICO, OI and $\delta^{13}\text{C}$ measurements in cores 6 and 9.

Depth (cm)	Core 6			Core 9		
	OICO	OI	$\delta^{13}\text{C}$	OICO	OI	$\delta^{13}\text{C}$
1	38	455	-23.0	11	311	-24.2
2	35	345	-23.0	7	227	-24.8
3	68	400	-23.3	12	220	
4	75	371	-23.4	22	211	-25.1
5	55	282	-23.4	61	190	
6	58	314	-23.6	25	183	-25.2
7	86	236	-23.3	52	185	
8	97	364	-23.0	0	179	-25.2
9	86	295	-23.5	124	181	
10	28	320	-23.2	36	211	-25.1
12	105	407	-23.3	2	186	
14	86	321	-23.1	0	170	
16	48	360	-23.0	0	215	
18	42	304	-23.1	3	154	
20	94	422	-22.9	13	248	
25	96	296	-23.2	0	158	-25.9
30	14	424	-24.1			
35	61	261				
40	47	286				
Mean	64	340	-23.3	23	202	-25.1

4.2.4 Labile and humic classes of compounds

In recent sediments the temperature of peak S2 carbon yield, called T_{\max} in standard applications of RE6 pyrolysis, represents the thermal stability of organic compounds remaining from the original OM deposited and provides insight into their identity. The T_{\max} pattern in HB sediments suggests two main organic groups: OM with T_{\max} temperatures from 360 to 400 °C and OM with T_{\max} temperatures from 440 to 470 °C (Figure 5). The low- T_{\max} group includes cores 10, 14 and intermittent layers of cores 6 and 7, and the high T_{\max} group includes most of the other samples with the exception of a few layers from cores 8 and 13, which span the two groups (Figure 5). The low end of the T_{\max} range usually indicates fresher OM such as ‘bio-macromolecules’ and biopolymers such as cellulose and lignins, while the upper end usually represents humic substances and more recalcitrant materials (Disnar et al., 2003; Hetényi et al., 2006; Liebezeit and Wiesner, 1990). Given the strong terrestrial carbon influence indicated by $\delta^{13}\text{C}$ in cores 6 and 7 (Figure 4-7), the low T_{\max} temperatures are partly a product of cellulose and lignins (Figure 4-5). On the other hand, the low T_{\max} values in cores 10, 14 and parts of core 13 must be a product of marine OM because these samples contain little terrestrial carbon (Figure 4-5). Low temperatures of thermal stability may be attributed to short-chain hydrocarbons common in algal OM (Meyers and Ishiwatari, 1993) that have become oxygenated through re-working, or to high levels of deoxy sugar content linked to elevated microbial degradation, as previously observed in fine particulate OM (Marchand et al., 2005). In contrast, the high T_{\max} temperatures observed in the majority of sediments (Figure 4-5) reflect large amounts of humic OM that correspond to the generally high proportion of RC in HB sediments (Figure 4-1). This sort of OM could

comprise marine humic acids, common in Arctic marine algae and known to contribute a large part of the DOC flux in several other Arctic shelf seas (Perminova and Petrosyan, 1993). Noticeably, the high T_{\max} values observed in core 9 are anomalous considering the evidence of somewhat fresher terrestrial OM compared to cores 6 and 7 (Figures 4-5 and 4-7). In this core higher thermal stability may reflect abundant epicuticular waxes that are composed of highly hydrogenated long-chain carbohydrates that have higher decomposition temperatures than short chain hydrocarbons more commonly found in algae (Lüniger and Schwark, 2002). These waxes are produced in large quantities by conifers such as the Black Spruce that dominate the southern HB watershed (Cape and Percy, 1993; Gordon et al., 1998), and this type of OM probably contributes abundantly to terrigenous OM loads in river discharge. Another possibility is that sediments in core 9, located near a major river, contain an admixture of char from forest fires, a common phenomenon in the southern HB watershed that would contribute highly degraded, thermally stable carbon to river loads of OM.

4.2.5 Impact of reworked OM on the transport and fate of Hg in HB

The speciation and distribution of OM in aquatic systems are recognized as key components in the mobility and fate of Hg (Lindberg and Harris, 1974), largely due to the high affinity of Hg for thiol (reduced-sulphur containing) groups commonly found in organic tissues (Haitzer et al; 2002, Ravichandran, 2004). The relationship between Hg and OM is a main feature in the distribution and down core trends of Hg in HB sediments, as well (Table 4-2). Fractionation of OM according to lability through pyrolysis provides the opportunity to investigate which components of the OM play an

active role in Hg transport and sequestration in HB sediments. The data suggest that labile components of OM are more effective at distributing Hg than recalcitrant compounds, with for example, the PC fraction showing a stronger relationship with surface sediment Hg concentrations than the RC fraction (Table 4-2). Examining the composite fractions of PC reveals that this relationship is largely due to the S3 carbon fraction, which alone explains nearly 90% of the spatial variance in surface Hg concentrations (Table 4-2). A similar relationship exists in sediments from the core bottoms, suggesting consistency in this connection for the last several centuries, which represents the time span of sediment deposition recorded in most cores, based on their linear sedimentation rates (Kuzyk et al., 2009). Furthermore, inventories of OM fractions and Hg in the sediment cores, which integrate the amount of these materials permanently captured over time, demonstrate a progressively stronger relationship between OM fractions and Hg in the order of TOC < PC < S3 (Table 4-2). The poorer spatial Hg-S2 relationships, both for surface sediment concentrations and core inventories, suggests that inter-core variability of the vertical flux of recent detritus from primary production in HB does not contribute strongly to the spatial variability of Hg capture in underlying sediments. The absence of a strong spatial relationship between Hg and fresh algal OM, represented by S2 carbon, is notable because previous studies have demonstrated a strong link between changes in S2 carbon capture by sediments and sediment Hg content in freshwater lakes (Outridge et al; 2007). However, in those lakes autochthonous OM production essentially represented the sole OM source to sediments, with negligible contributions from S3. The situation in HB, where S3 dominates the trends with Hg, may

reflect the considerably higher proportion of alternative OM sources such as recycled and terrestrial materials relative to the autochthonous production of algal OM in this system.

Table 4-2. Correlation Coefficients and Prevalence of Significant Relationships between Carbon Fractions, Hg distribution, and Grain Size.

Parameter	Carbon Fraction					
	S1	S2	S3	PC	RC	TOC
Hg in all cores, all depths	0.32	0.14	0.58	0.53	0.29	0.36
Surface Sediment Hg Concentration	0.10	0.02	0.88	0.49	0.21	0.32
Background Sediment Hg Concentration ¹	0.53	0.40	0.87	0.72	0.23	0.33
Total Hg Inventory	-	0.57	0.81	0.69	0.78	0.79
Surface grain size (% < 63 μM)	0.14	0.06	0.61	0.42	0.29	0.36

¹ Determined as the mean Hg concentration within each core with stable deep Hg concentrations, across all depths > 130 years prior to sample collection, based on linear sedimentation rates.

The strength of the relationship observed between Hg and S3 carbon reflects the unique sedimentary regime of HB in which old coastal deposits, undergoing resuspension due to isostatic rebound (falling relative sea level), provide the major source of fine-grained sediments and associated OM to offshore areas (Kuzyk et al. 2009). S3 carbon is uniquely associated with the fine grained fraction of surface sediments (% < 63 μM) (Table 4-2), identifying it as the mineral-bound fraction of OM. This association provides resistance to microbial degradation (Mayer, 1994; Bergamaschi et al. 1997) and could provide greater preservation of the S3 carbon fraction compared to the S1 and S2 carbon fractions. Such a discrepancy provides a mechanism for enriching the oxygen content of sedimentary OM during transport to locations of burial by loss of the comparatively more labile, hydrocarbon compounds in the S1 and S2 fractions during repeated cycles of resuspension. The resuspended sediments, which are of glaciomarine origin, also may have been enriched in S3 originally. Mineral association is also consistent with a larger

proportion of S3 carbon transported laterally from recycled shallow coastal sediments than S1 and S2 carbon because such materials likely originate to a greater extent from recent autochthonous production. Since the resuspension of coastal sediments has also been demonstrated to provide a large portion of the total burial flux of Hg in HB to offshore regions (Hare et al. 2008), this scheme provides a simple explanation for the simultaneous transport and coincident capture of Hg and S3 carbon.

The large relative impact of the resuspension process in HB consequently indicates that the S3 carbon fraction provides probable ligands for the reliable, long-term capture, transport and sequestration of Hg in HB. The potential of the S3 carbon fraction to provide a platform for Hg transport is enhanced by its greater preservation in the water column and increased duration of exposure to Hg in the water column, during repeated cycles of deposition and resuspension prior to ultimate burial. Association with fine grain sizes also provides S3 carbon with the greatest surface area for binding Hg compared to the other labile carbon fractions which appear associated with particles of various sizes (Table 4-2). Given that S3 carbon inventories generally represent less organic carbon than S2 carbon inventories in HB, S3 carbon must function with similar binding efficiency as the hydrocarbon compounds in the S2 carbon fraction. Thus, the more degraded nature of S3, relative to S2, does not appear to impact its efficacy at binding Hg, perhaps because the thiol groups on which the interaction relies are also abundant, commonly at higher concentrations even in oxic surface waters than natural Hg concentrations (Benoit et al. 1999). Hg binding to oxygenated functional groups such as carboxylic acids, which would be abundant in S3, is also possible but generally occurs only at high DOM concentrations, well above those found in HB bottom water (Haitzer et

al. 2002). The presence of thiol groups may be abundant in the S3 carbon originally, considering the glaciomarine origin and low C:N ratio of these sediments (Figure 4-6), which indicates higher protein content. Collectively, these associations indicate that the unique sedimentary processes operating in HB create a distinctive relationship between sediment Hg concentrations and recycled marine carbon that produce a role for S3 carbon in the mobility and fate of Hg. In systems where marine OM is not redistributed and reworked as extensively as in HB, fresher and less oxygenated OM may play a more obvious role in the capture and transport of Hg because of its higher rate of preservation and more direct vertical association between the water column and sediments. Indeed, in HB, there are generally synchronous variations between Hg concentrations and all the labile carbon fractions, including S1 and S2, down core. The strength (average $r^2 = 0.75$ to 0.81), variability (standard deviation of $r^2 = 0.08$ to 0.17) and number of cores showing significant relationships with Hg ($n = 9$ to 11) are relatively equal for the S1, S2 and S3 carbon fractions. This suggests that at a particular site, Hg capture may be influenced by variations in the flux of any of the various types of labile OM. Some of the parallel trends between labile OM and Hg within cores may not reflect association of the materials prior to deposition but rather, could arise coincidentally from the widespread increases in contaminant Hg deposited to aquatic systems in recent decades (e.g., Perry et al., 2005; Swain et al., 1992) and naturally higher rates of OM content in recently deposited sediments compared to deeper layers where some OM remineralization has occurred. Examination of the S2/RC ratio reveals declining values with increasing depth in cores 3, 5, 8 and 9, which represent loss of captured OM over time, likely through oxidation. Yet several cores in western HB (11, 12 and 13) also display declining S2/RC with depth that

appears due to changing OM source rather than diagenesis (Figure 4-3). Such relationships warrant further investigation to assess whether the labile carbon fractions play a greater role in temporal variations in Hg capture than in the spatial patterns.

4.3 References

- Behar, F., Beaumont, B. and Penteadó, H.d.B., 2001. Rock-Eval 6 Technology: Performances and Developments. *Oil & Gas Science and Technology - Rev. IFP*, 56(2): 111-134.
- Bergamaschi, B.A., Tsamakis, E., Keil, R.G., Eglinton, T.I., Montlucon, D.B. and Hedges, J.I., 1997. The effect of grain size and surface area on organic matter, lignin and carbohydrate concentration, and molecular compositions in Peru Margin sediments. *Geochimica et Cosmochimica Acta*, 61(6): 1247-1260.
- Cape, J.N. and Percy, K.E., 1993. Environmental Influences on the Development of Spruce Needle Cuticles. *New Phytologist*, 125(4): 787.
- Chow, N., Morad, S. and Al-Aasm, I.S., 1996. Origin of authigenic carbonates in Eocene to Quaternary sediments from the Arctic Ocean and Norwegian-Greenland Sea. Texas A & M University, Ocean Drilling Program, College Station, TX, United States P. 415-434 ISSN: 0884-5891, ODP Ocean Drilling Program.
- Dahl, B., Bojesen-Koefoed, J., Holm, A., Justwan, H., Rasmussen, E. and Thomsen, E., 2004. A new approach to interpreting Rock-Eval S2 and TOC data for kerogen quality assessment. *Organic Geochemistry*, 35(11-12): 1461.
- di-Giovanni, C., Disnar, J.R., Bichet, V., Campy, M. and Guillet, B., 1998. Geochemical characterization of soil organic matter and variability of a postglacial detrital organic supply (chaillexon lake, france). *Earth Surface Processes and Landforms*, 23(12): 1057-1069.
- Disnar, J.R., Guillet, B., Keravis, D., Di-Giovanni, C. and Sebag, D., 2003. Soil organic matter (SOM) characterization by Rock-Eval pyrolysis: scope and limitations. *Organic Geochemistry*, 34(3): 327.

- Gordon, D.C., Percy, K.E. and Riding, R.T., 1998. Effects of u.v.-B radiation on epicuticular wax production and chemical composition of four *Picea* species. *The New Phytologist*, 138(3): 441-449.
- Granskog, M.A., Macdonald, R.W., Mundy, C.J. and Barber, D.G., 2007. Distribution, characteristics and potential impacts of chromophoric dissolved organic matter (CDOM) in Hudson Strait and Hudson Bay, Canada. *Continental Shelf Research*, 27: 2032-2050.
- Hare, A., Stern, G.A., Macdonald, R.W., Kuzyk, Z.Z. and Wang, F., 2008. Contemporary and preindustrial mass budgets of mercury in the Hudson Bay Marine System: The role of sediment recycling. *Science of The Total Environment*, 406(1-2): 190.
- Harvey, M., Therriault, J. and Simard, N., 1997. Late-summer distribution of phytoplankton in relation to water mass characteristics in Hudson Bay and Hudson Strait (Canada). *Can. J. Fish. Aquat. Sci.*, 54: 1937 - 1952.
- Héquette, A., Tremblay, P. and Hill, P.R., 1999. Nearshore erosion by combined ice scouring and near-bottom currents in eastern Hudson Bay, Canada. *Marine Geology*, 158(1-4): 253.
- Hetényi, M., Nyilas, T., Sajgó, C. and Brukner-Wein, A., 2006. Heterogeneous organic matter from the surface horizon of a temperate zone marsh. *Organic Geochemistry*, 37(12): 1931-1942.
- Hillaire-Marcel, C. and Fairbridge, R.W., 1978. Isostasy and eustasy of Hudson Bay. *Geology*, 6: 117-122.
- Ingram, R. and Prinsenberg, S.J., 1998. Coastal Oceanography of Hudson Bay and Surrounding Eastern Canadian Arctic Waters *The Sea*, 11: 835-861.
- Irwin, B., Dickie, P., Hodgson, M. and Platt, T., 1988. Primary Production and Nutrients on the Labrador Shelf, in Hudson Strait and Hudson Bay in August and September 1982. *Canadian Data Report of Fisheries and Aquatic Sciences*, 692.
- Jacob, J., Disnar, J.-R., Boussafir, M., Sifeddine, A., Turcq, B. and Spadano Albuquerque, A.L., 2004. Major environmental changes recorded by lacustrine sedimentary organic matter since the last glacial maximum near the equator (Lagoa do Caçó, NE Brazil). *Palaeogeography, Palaeoclimatology, Palaeoecology*, 205(3-4): 183.

- Jones, E. and Anderson, L., 1994. Northern Hudson Bay and Foxe Basin: Water Masses, Circulation and Productivity. *Atmosphere-Ocean*, 32(2): 361-374.
- Kuzyk, Z.A., Gofñi, M.A., Stern, G.A. and Macdonald, R.W., 2008. Sources, pathways and sinks of particulate organic matter in Hudson Bay: Evidence from lignin distributions. *Marine Chemistry*, 112(3-4): 215.
- Kuzyk, Z.A., Macdonald, R.W., Johannessen, S.C., Gobeil, C. and Stern, G.A., 2009a. Towards a Sediment and Organic Carbon Budget for Hudson Bay. *Marine Geology*, 264: 190-208.
- Kuzyk, Z.A., Macdonald, R.W., Tremblay, J. and Stern, G., 2009b. Elemental and stable isotopic constraints on river influence and patterns of nitrogen cycling and biological productivity in Hudson Bay. *Continental Shelf Research*, Submitted.
- Langford, F. and Blanc-Valleron, M., 1990. Interpreting Rock-Eval Pyrolysis Data Using Graphs of Pyrolizable Hydrocarbons vs. Total Organic Carbon. *The American Association of Petroleum Geologists Bulletin*, 74(6): 799 - 804.
- Liebezeit, G. and Wiesner, M.G., 1990. Pyrolysis of recent marine sediments - I. Biopolymers. *Advances in Organic Geochemistry*, 16(4 - 6): 1179 - 1185.
- Lindberg, S.E. and Harris, R.C., 1974. Mercury-organic matter associations in estuarine sediments and interstitial water. *Environmental Science and Technology*, 8: 459 - 462.
- Lüniger, G. and Schwark, L., 2002. Characterisation of sedimentary organic matter by bulk and molecular geochemical proxies: an example from Oligocene maar-type Lake Enspel, Germany. *Sedimentary Geology*, 148(1-2): 275.
- Marchand, C., Disnar, J.R., Lallier-Vergès, E. and Lottier, N., 2005. Early diagenesis of carbohydrates and lignin in mangrove sediments subject to variable redox conditions (French Guiana). *Geochimica et Cosmochimica Acta*, 69(1): 131-142.
- Marchand, C., Lallier-Vergès, E. and Baltzer, F., 2003. The composition of sedimentary organic matter in relation to the dynamic features of a mangrove-fringed coast in French Guiana. *Estuarine, Coastal and Shelf Science*, 56: 119-130.
- Marchand, C., Lallier-Vergès, E., Disnar, J.R. and Kéravis, D., 2008. Organic carbon sources and transformations in mangrove sediments: A Rock-Eval pyrolysis approach. *Organic Geochemistry*, 39(4): 408.

- Mayer, L.M., 1994. Surface area control of organic carbon accumulation in continental shelf sediments. *Geochimica et Cosmochimica Acta*, 58(4): 1271-1284.
- Meyers, P.A. and Ishiwatari, R., 1993. Lacustrine organic geochemistry. An overview of indicators of organic matter sources and diagenesis in lake sediments. *Organic Geochemistry*, 20(7): 867-900.
- Outridge, P.M., Sanei, H., Stern, G.A., Hamilton, P.B. and Goodarzi, F., 2007. Evidence for Control of Mercury Accumulation Rates in Canadian High Arctic Lake Sediments by Variations of Aquatic Primary Productivity. *Environ. Sci. Technol.*, 41(15): 5259-5265.
- Perminova, I.V. and Petrosyan, V.S., 1993. Marine humic acids as an important constituent of the dissolved organic carbon flux in the Bering and Chukchi Sea ecosystems. Proceedings of the Conference on Carbon Cycling in the Boreal Forests and Subarctic Ecosystems. OSU, Corvallis, September 9 - 13, 1991, EPA/MR-126546.: 43-49.
- Perry, E., Norton, S.A., Kamman, N.C., Lorey, P.M. and Driscoll, C.T., 2005. Deconstruction of Historic Mercury Accumulation in Lake Sediments, Northeastern United States. *Ecotoxicology*, 14(1): 85-99.
- Prinsenber, S.J., 1988. Ice-Cover and Ice-Ridge Contributions to the Freshwater Contents of Hudson Bay and Foxe Basin. *Arctic*, 41(1): 6-11.
- Sakshaug, E., 2004. Primary and secondary production in the Arctic seas. *The Organic Carbon Cycle in the Arctic Ocean*. Springer, Berlin.
- Sanei, H. and Goodarzi, F., 2006. Relationship between organic matter and mercury in recent lake sediment: The physical-geochemical aspects. *Applied Geochemistry*, 21: 1900-1912.
- Sanei, H., Goodarzi, F., Snowdon, L.R., Stasiuk, L.D. and Flier-Keller, E.V.D., 2000. Characterizing the Recent Sediments from Pigeon Lake, Alberta as Related to Anthropogenic and Natural Fluxes. *Environmental Geosciences*, 7(4): 177-189.
- Sanei, H., Stasiuk, L.D. and Goodarzi, F., 2005. Petrological changes occurring in organic matter from Recent lacustrine sediments during thermal alteration by Rock-Eval pyrolysis. *Organic Geochemistry*, 36(8): 1190.

- Saucier, F., Senneville, S., Prinsenberg, S., Roy, F., Smith, G., Gachon, P., Caya, D. and Laprise, R., 2004. Modelling the sea ice-ocean seasonal cycle in Hudson Bay, Foxe Basin and Hudson Strait, Canada. *Climate Dynamics*, 23: 303-326.
- Schulz, H.D. and Zabel, M., 2000. *Marine Geochemistry*. Springer-Verlag, xx + 455 pp.
- Sebag, D., Disnar, J.R., Guillet, B., DI GIOVANNI, C., VERRECCHIA, E.P. and DURAND, C.A., 2006. Monitoring organicmatter dynamics in soil profiles by 'Rock-Eval pyrolysis': bulk characterization and quantification of degradation. *European Journal of Soil Science*, 57(June): 344-355.
- Stein, R. and Macdonald, R., 2004. *The Organic Carbon Cycle in the Arctic Ocean*. Springer-Verlag Berlin Heidelberg, 363 + xix pp.
- Stern, G., Sanei, H., Roach, P., Delaronde, J. and Outridge, P., 2009. Historical interrelated variations of mercury and aquatic organic matter in lake sediment cores from a sub-arctic lake in Yukon, Canada; further evidence toward the algal-mercury scavenging hypothesis. *Environmental Science and Technology*, in press.
- Stewart, D.L. and Lockhart, W.L., 2005. An overview of the Hudson Bay marine ecosystem. *Can. Tech. Rep. Fish. Aquat. Sci.* , 2586: vi + 487 p.
- Swain, E.B., Engstrom, D.R., Brigham, M.E., Henning, T.A. and Brezonik, P.L., 1992. Increasing rates of atmospheric mercury deposition in midcontinental North America. (lakes of Minnesota & Wisconsin). *Science*, v257(n5071): p784(4).
- Vandenbroucke, M. and Largeau, C., 2007. Kerogen origin, evolution and structure. *Organic Geochemistry*, 38: 719-833.

CHAPTER 5

Synthesis of Results

5.0 Overview of Research

The objectives of this thesis were to determine the modern and preindustrial Hg cycles in Hudson Bay, to investigate the impact of natural and anthropogenic influences on the capture of Hg in marine sediments, and to explore the nature of the particulate flux transporting Hg to the sediments. In order to achieve these objectives, this thesis has provided a mass balance model of Hg for the Hudson Bay system that identifies two important features that are subsequently investigated. First, this study identifies an uncommon mechanism of Hg supply to offshore marine sediments that must be considered when interpreting the impact of environmental fluxes of Hg to an aquatic system. The process of resuspension and lateral transport of sedimentary Hg is demonstrated to occur coherently with reworking and lateral transport of largely marine OM, which is consistent with the known sediment and OM dynamics of Hudson Bay (Kuzyk et al., 2008a; Kuzyk et al., 2009a) and the significant role of OM as a carrier for Hg in aquatic systems (Lindberg and Harris, 1974). Secondly, the contribution of anthropogenic Hg to the marine Hudson Bay system is identified through changes in the mass budgets of Hg over the industrial era. The ultimate locations of these contributions are then identified by examining the depositional histories of Hg in the sediments. These depositional histories provide perspective on the magnitude of anthropogenic Hg contributions to HB, which appears similar to that conferred by natural processes and

spatial variation. The nature of the particulate Hg flux is then explored by examining the distribution of the fractions of organic carbon in the sediments. The unique relationship observed between reworked organic matter and Hg corroborates the large relative role of sediment recycling indicated by the modern and preindustrial Hudson Bay Hg cycles.

5.1 The Role of Sediment Recycling and Lateral Transport of Hg in HB

The compilation of mass budgets of Hg in Hudson Bay demonstrate that natural internal processes of sediment transport play a large relative importance in distributing and burying Hg in marine sediments. Under steady state conditions, sedimentation of Hg via particle flux is the largest net flux of Hg to, from and within HB. Although recent models of the global and Arctic oceans have indicated that water Hg concentrations are not at steady state with global atmospheric Hg concentrations (Lamborg et al., 2002; Outridge et al., 2008; Sunderland and Mason, 2007), their annual rates of increase are small relative to their reservoirs, and the mixing time of surface and deep water masses in Hudson Bay are on the order of one to two magnitudes shorter than those of the global ocean and its constituent seas. Moreover, the imbalance produced by excluding lateral transport of Hg is unreasonable considering the plausible error ranges of the other Hg fluxes. These facts suggest that the preindustrial and contemporary mass balance models of Hg in Hudson Bay are a useful representation of the current quantitative and qualitative scheme of Hg transport to and from HB.

The strong role of lateral sediment transport in Hg distribution can be observed in the relationship between Hg and reworked marine OM. Lateral sediment transport increases the apparent residence time of particulate matter in the water column, and

subsequently promotes its degradation through exposure to oxidative biological metabolism. The extensive impact of this process is demonstrated through the pattern of labile and residual carbon in HB, indicated by its level of hydrogenation, oxygen content and thermal lability. The major distinguishing characteristics of sedimentary OM in Hudson Bay based on RE analyses are low HI and high OI values. These characteristics strongly suggest reworked and/or terrestrial OM largely compose the OM pool in Hudson Bay sediments. This is further supported by the extensive RC component of sedimentary TOC. However, the spatial distribution and elemental analyses of OM carbon fractions support a marine origin for the majority of RC and high-OI sediments in HB. This interpretation is consistent with the expected OM composition if resuspension, reworking and lateral transport of OM from the extensive shallow 'pseudo-shelves' are major processes in HB. Since Hg is a particle-reactive component of the particle flux in HB, it follows that such predominant processes should be reflected in the sedimentary distribution of Hg. The association of Hg with S3 carbon clearly indicates this relationship, because S3 carbon is composed of highly oxygenated compounds that, in HB, appear to originate largely from reworked marine OM.

The implication of these results on the Hudson Bay Hg cycle is complicated to predict given that Hudson Bay is currently undergoing widespread climatic and ecological change that could plausibly strongly alter the existing Hg and OM regimes. Certainly the sea ice is one of the greatest physical forces in HB, affecting its physical, chemical and biological organization (Jones and Anderson, 1994; Kuzyk et al., 2008b; Prinsenber, 1988; Saucier et al., 2004). Loss of sea ice will no doubt permit increased wave and current scouring of the shallow coastal sediments, partly offsetting a reduction

in ice scouring. Conceivably, even stronger resuspension and reworking of OM may persist, particularly considering that the relative sea level drop in Hudson Bay will continue into the foreseeable future. Nonetheless, such increased reworking of OM will likely be accompanied by increased inputs of fresh autochthonous OM because of reduced ice cover and longer growing seasons. Although the sea ice provides an important platform for ice algae, their net contribution to primary production is likely small relative to that of pelagic species (Roff and Legendre, 1986). Furthermore, sea ice perhaps more strongly constrains primary production through its contribution to the surface mixed layer of the ocean, which restricts nutrient replenishment into the surface waters. Reduced sea ice inputs may reduce the depth, and perhaps permanence of this zone, permitting phytoplankton increased access to the nutrient pool in deeper waters. Sub-thermocline algal blooms in Hudson Bay have been observed, and under shallow surface mixed layer conditions, such phenomena may occur more frequently. The result of such changes on Hg cycling in the water column would likely be a shift in the association of some portion of the available Hg, from reworked marine OM to fresh marine OM because the latter is more likely to contain reduced functional groups such as thiols, which are strong Hg ligands.

Further change to the Hg cycle in Hudson Bay will come from its watershed. The southern Hudson Bay watershed contains one of the largest regions of wetlands globally, which commonly present ideal conditions for Hg methylation. Warming temperatures will provide longer periods of unfrozen water and sediments that may well permit greater Hg methylation in these ecosystems. Although there are few anadromous species inhabiting Hudson Bay to connect increased MeHg from coastal wetlands to marine food

chains, high chromophoric dissolved organic carbon in the rivers and resuspended sediments along the southern coast provide ideal conditions for MeHg transport by attenuating light penetration into the water column and subsequent photo-degradation of MeHg. In fact, MeHg production in Arctic wetlands and the release of Hg bound in permafrost have been identified as two significant potential impacts of climate change to contaminant cycling in the Arctic. Considering the more direct impact of MeHg on biotic Hg concentrations than inorganic Hg, and the extent of the wetland ecosystem and their Hg reservoir, the release of previously soil-bound inorganic Hg and its subsequent methylation could conceivably eclipse the impact of anthropogenic Hg to the Hudson Bay system. Nevertheless, this situation may yet be muted by various ecological processes because the existing bioavailable Hg pools in the oceans appear already in excess of those in their biological constituents (Outridge et al., 2008; Rolfhus and Fitzgerald, 1995). Thus, while MeHg contributions to the Hg cycle appear poised to increase in the future, the threat to biota is unclear due to the uncertainty in how trophic relationships will change.

5.2 The Impact of Anthropogenic Hg to HB

The exercise in comparing preindustrial and contemporary Hg fluxes also identifies increased atmospheric Hg deposition, both direct and through watershed contributions, as the source of Hg that has increased the most over the industrial era. This is partly due to geological and physical parameters, such as lower erosion rates than in other coastal Arctic systems, and little water mass exchange with the global oceans. Nevertheless, the actual magnitude of increased atmospheric deposition is small relative

to the reservoir size of Hg in the water column, and presumably that of the sediments as well. This result provides important perspective to the net influence of changes in atmospheric Hg fluxes to marine Hg concentrations by demonstrating that only gradual changes are possible given the current balance. This implies that a long recovery time is required to return Hudson Bay to preindustrial conditions, should legislative regulations or improved technologies reduce anthropogenic Hg emissions to the system.

Nonetheless, evidence of atmospheric contribution of anthropogenic Hg to Hudson Bay via the mass budgets of Hg provides the impetus to investigate industrial era impacts to marine systems. Since evidence of atmospheric anthropogenic Hg impacts to marine sediments has been largely lacking, this study fills an important gap intuitively known but largely overlooked in the global Hg cycle. Sediments in most areas of Hudson Bay reflect the known history of anthropogenic emissions of Hg to the atmosphere in North America. Those regions that appear unresponsive are identified as locations with little vertical particle flux. This result highlights the importance of the internal particle flux of aquatic systems in communicating changes in atmospheric concentrations to sediments. This is a particularly relevant point in light of recent studies that suggest changes in the quantitative particle flux of organic ligands may account for a portion of the surface sediment enrichments commonly seen in aquatic sediments, irrespective of atmospheric Hg concentrations (Outridge et al., 2007; Stern et al., 2009).

The demonstration of atmospheric anthropogenic Hg impacts to marine sediments in Hudson Bay also provides insight into their magnitude relative to natural variation in Hg distribution, temporally and spatially. While time lines of Hg deposition correspond well with known time lines of anthropogenic Hg emissions to the atmosphere, the

observed enrichments of Hg are within the range of natural Hg variation recorded in Hudson Bay sediments. None of the surface enrichments in Hg concentration have yet exceeded those observed during the industrial era in the offshore western region of HB, and most cores demonstrate surface Hg concentrations below the uppermost background Hg concentrations in northern HB.

Although this result may be interpreted as evidence against a large impact of anthropogenic activities on aquatic Hg cycles, it does not suggest that anthropogenic contributions to the amount of Hg circulating in the Earth's surface ecosystems are insignificant. Marine sediments record Hg that has been removed from the water column, which in turn reflects a combination of Hg delivered from terrestrial environments and exchanged with the atmosphere. Communications between the sediments and the water column, and the water column and the atmosphere and land, may take place over long periods of time depending on a wide range of parameters such as the particle residence time in the atmosphere and in the water column, precipitation and geomorphology, and redox reactions that change the particle-reactivity and volatility of Hg. This means that the amount of Hg in sediment reflects a past situation of Hg in the water column, not the present situation. Moreover, the amount of Hg in sediments also does not linearly reflect the amount of Hg in other environmental reservoirs because of spatial heterogeneity in sediment Hg distribution. For example, although anthropogenic Hg influences on Hg concentrations in Hudson Bay sediments appears of similar magnitude to natural variation, the anthropogenic Hg contribution to the atmosphere above Hudson Bay (and globally) appears nearly 3 times that of natural sources.

A reduction in the apparent relative contribution of anthropogenic Hg to natural systems implies that such additions are of greater concern than previously considered. Industrial-era increases in body burdens of Hg in a wide variety of biota, including humans, compared to the preindustrial era are indisputable considering the available evidence. These increases appear largely driven by increased inorganic Hg content in surface ecosystems even though its connection to bioaccumulated and biomagnified Hg is not direct. Therefore, the large scale implication of reduced relative anthropogenic Hg emissions is that smaller contributions of Hg cause the observed changes in biological Hg burdens. This scheme is analogous to the adjustment of the paradigm of Hg biomagnification in marine biota during the 1980's when improved analytical techniques demonstrated that water Hg concentrations were actually a magnitude lower than previously reported, but measurements of Hg concentrations in fish tissues were accurate. Thus, lower abiotic Hg concentrations were actually responsible for the high biotic concentrations and biomagnification was an order of magnitude higher.

5.3 Perspectives for Future Studies

The major data gaps pertaining to Hg in the Hudson Bay System involve the spatial and temporal variability of inorganic Hg, and nearly all aspects of organic Hg. The distinct range in background Hg concentrations demonstrated by the vertical sediment Hg profiles in Chapter 3 indicate unique spatial patterns of Hg capture despite generally low geological contributions across the Bay. The true extent of this range is uncertain considering evidence of Hg-enriched rocks in a Zn-bearing 'green belt' in the Kivalliq region of northwestern Hudson Bay (McMartin et al., 2000), where no sediment cores

were collected. Yet, evidence of very low historical Hg levels in at least two sediment cores indicate that some areas of Hudson Bay naturally contain Hg concentrations well below the average for the Earth's crust. Increasing our knowledge of the natural spatial variability of sedimentary Hg across Hudson Bay would permit a better understanding of how anthropogenic inputs actually influence the system-wide storage of Hg. If anthropogenic additions of Hg to marine sediments are small relative to natural concentrations then either marine systems are more sensitive to Hg additions than currently demonstrated, or the human impact to marine biological Hg burdens arises through non-sedimentary processes. The possibility of the latter situation appears more likely considering two recent studies demonstrating MeHg production in the marine water column (Cossa et al., 2009; Sunderland et al., 2009), which bypasses the requirement for sediment Hg methylation as observed in freshwater systems. Since Hudson Bay has a very large surface area to receive direct atmospheric Hg inputs and relatively accessible shallow marine sediments without known point sources of Hg, it provides an excellent system to contrast anthropogenic impacts with natural variation.

The MeHg distribution in Hudson Bay is also largely unknown. MeHg concentrations have been reported for a few locations in the marine water column, and in two rivers entering the Bay (Kirk and St. Louis, 2009; Kirk et al., 2008). MeHg concentrations in the sediments and in other rivers are unknown. Given the large relative contributions of rivers to Hudson Bay relative to other shelf seas, MeHg concentrations could conceivably be higher than in other marine systems, particularly along the southern coast where river waters are concentrated along a coastal current. Anomalously high MeHg concentrations have also been observed in other Arctic waters (St. Louis et al.,

2007), suggesting that cryospheric processes may contribute to the production or preservation of MeHg in these types of systems. Previous research has also demonstrated that the process of sediment resuspension contributes to higher MeHg burdens in biota (Kim et al., 2006; Sunderland et al., 2004). Considering the extensive sediment resuspension process in HB, MeHg studies may find greater fluxes from the sediments or higher bioaccumulation rates in phytoplankton and benthic biota.

Lastly, data on the composition of Hg-bearing particles in the water column is lacking in HB, as it is in other oceans. Rather, the composition of the vertical Hg flux is commonly inferred from relationships observed in the sediments. However, identifying the relationships in sediment does not always translate into the identity of the particles scavenging Hg from the water column because of post-depositional dynamics. As a result, interpretation of sedimentary Hg distribution depends at least in part on the type of analyses performed and the number of water column and sediment processes considered. Direct analysis of the particulate Hg in the water column would provide superior insight into the mechanism by which Hg is removed from the water column. This would permit development of an improved model of how the nearly ubiquitous surface sediment Hg enrichments observed in aquatic systems around the globe are produced.

References

- Cossa, D., Averty, B. and Pirrone, N., 2009. The origin of methylmercury in open Mediterranean waters. *Limnol. Oceanogr.*, 54(3): 837-844.
- Jones, E. and Anderson, L., 1994. Northern Hudson Bay and Foxe Basin: Water Masses, Circulation and Productivity. *Atmosphere-Ocean*, 32(2): 361-374.

- Kim, E.-H., Mason, R.P., Porter, E.T. and Soulen, H.L., 2006. The impact of resuspension on sediment mercury dynamics, and methylmercury production and fate: A mesocosm study. *Marine Chemistry*, 102(3-4): 300-315.
- Kirk, J.L. and St. Louis, V.L., 2009. Multiyear Total and Methyl Mercury Exports from Two Major Sub-Arctic Rivers Draining into Hudson Bay, Canada. *Environmental Science & Technology*, 43(7): 2254.
- Kirk, J.L., St. Louis, V.L., Hintelmann, H., Lehnher, I., Else, B. and Poissant, L., 2008. Methylated Mercury Species in Marine Waters of the Canadian High and Sub Arctic. *Environmental Science & Technology*, 42(22): 8367.
- Kuzyk, Z.A., Gofii, M.A., Stern, G.A. and Macdonald, R.W., 2008a. Sources, pathways and sinks of particulate organic matter in Hudson Bay: Evidence from lignin distributions. *Marine Chemistry*, 112(3-4): 215.
- Kuzyk, Z.A., Macdonald, R.W., Granskog, M.A., Scharien, R.K., Galley, R.J., Michel, C., Barber, D. and Stern, G., 2008b. Sea ice, hydrological, and biological processes in the Churchill River estuary region, Hudson Bay. *Estuarine, Coastal and Shelf Science*, 77(3): 369-384.
- Kuzyk, Z.A., Macdonald, R.W., Johannessen, S.C., Gobeil, C. and Stern, G.A., 2009. Towards a Sediment and Organic Carbon Budget for Hudson Bay. *Marine Geology*, 264: 190-208.
- Lamborg, C.H., Fitzgerald, W.F., O'Donnell, J. and Torgersen, T., 2002. A non-steady-state compartmental model of global-scale mercury biogeochemistry with interhemispheric atmospheric gradients. *Geochimica et Cosmochimica Acta*, 66(7): 1105.
- Lindberg, S.E. and Harris, R.C., 1974. Mercury-organic matter associations in estuarine sediments and interstitial water. *Environmental Science and Technology*, 8: 459 - 462.
- McMartin, I., Hall, G., Kerswill, J., Sangster, A., Douma, S. and Vaive, J., 2000. Mercury Cycling in Perennially Frozen Soils of Arctic Canada, Kaminak Lake Area, Nunavut. In: G.S.o. Canada (Editor), *International Conference on Heavy Metals in the Environment*, Ann Arbor, MI.

- Outridge, P., Macdonald, R.W., Wang, F., Stern, G. and Dasoor, A.P., 2008. A mass balance inventory of mercury in the Arctic Ocean. *Environmental Chemistry*, 5: 89-111.
- Outridge, P.M., Sanei, H., Stern, G.A., Hamilton, P.B. and Goodarzi, F., 2007. Evidence for Control of Mercury Accumulation Rates in Canadian High Arctic Lake Sediments by Variations of Aquatic Primary Productivity. *Environ. Sci. Technol.*, 41(15): 5259-5265.
- Prinsenberg, S.J., 1988. Ice-Cover and Ice-Ridge Contributions to the Freshwater Contents of Hudson Bay and Foxe Basin. *Arctic*, 41(1): 6-11.
- Roff, J.C. and Legendre, L., 1986. Physico-chemical and biological oceanography of Hudson Bay. In: I.P. Martini (Editor), *Canadian Inland Seas*. Elsevier, New York, pp. 265-291.
- Rolfhus, K.R. and Fitzgerald, W.F., 1995. Linkages between atmospheric mercury deposition and the methylmercury content of marine fish. *Water, Air, & Soil Pollution*, 80(1): 291-297.
- Saucier, F., Senneville, S., Prinsenberg, S., Roy, F., Smith, G., Gachon, P., Caya, D. and Laprise, R., 2004. Modelling the sea ice-ocean seasonal cycle in Hudson Bay, Foxe Basin and Hudson Strait, Canada. *Climate Dynamics*, 23: 303-326.
- St. Louis, V., Hintelmann, H., Graydon, J.A., Kirk, J.L., Barker, J., Dimock, B., Sharp, M.J. and Lehnerr, I., 2007. Methylated Mercury Species in Canadian High Arctic Marine Surface Waters and Snowpacks. *Environmental Science & Technology*, 41(18): 6433-6441.
- Stern, G., Sanei, H., Roach, P., Delaronde, J. and Outridge, P., 2009. Historical interrelated variations of mercury and aquatic organic matter in lake sediment cores from a sub-arctic lake in Yukon, Canada; further evidence toward the algal-mercury scavenging hypothesis. *Environmental Science and Technology*, in press.
- Sunderland, E., Gobas, F.A.P.C., Heyes, A., Branfireun, B., Bayer, A., Cranston, R. and Parsons, M., 2004. Speciation and bioavailability of mercury in well-mixed estuarine sediments. *Marine Chemistry*, 90(1-4): 91-105.

- Sunderland, E.M., Krabbenhoft, D.P., Moreau, J.W., Strode, S.A. and Landing, W.M., 2009. Mercury sources, distribution, and bioavailability in the North Pacific Ocean: Insights from data and models. *Global Biogeochem. Cycles*, 23.
- Sunderland, E.M. and Mason, R.P., 2007. Human impacts on open ocean mercury concentrations. *Global Biogeochem. Cycles*, 21.

APPENDIX

Additional mercury data for the Hudson Bay system.

The following tables and figure provide additional data pertaining to the Hudson Bay system that was not used in the previous manuscripts.

Water Hg Concentrations

Samples were collected along vertical or horizontal transects across the freshwater/seawater interface. Sample collection and analyses were performed as described in Chapter 2.

Table A-1. Vertical Distribution of Hg in Dissolved and Particulate Phases in the Churchill River Estuary

Date	Depth (m)	Salinity (‰)	Hg in fraction (ng/L)		
			Total	Dissolved	Particulate
28-Apr-05	2	2.5	3.81	1.19	2.62
	5	12.21	3.44	0.42	3.02
	10	32.2	0.93	0.44	0.49
29-May-05	2	3.4	3.19	2.46	0.73
	5	13.5	2.62	1.96	0.66
	10	25.6	0.96	0.8	0.16

Table A-2. Horizontal and Vertical Distribution of Hg in Dissolved and Particulate Phases in the Nelson and Hayes River Estuaries, July 2005

River	Latitude	Longitude	Depth (m)	Salinity (‰)	Total ^a	Hg in fraction (ng/L)			Particulate ^c
						Range +/- ng/g	Dissolved ^b	Range +/- ng/g	
Nelson	57.0773	-92.4973	0.5	0.11	2.23	0.05	1.9	0.03	0.33
	57.1454	-92.3861	0.5	5.17	2.19	0.37	0.93		1.26
	57.1454	-92.3861	6.5	15.6	2.82	0.09	0.81	0.02	2.01
	57.2134	-92.2754	0.5	23.3	0.87	0.03	0.67	0.02	0.2
	57.2134	-92.2754	6.5	24.03	0.94	0.09	0.64	0.05	0.3
	57.3149	-92.1087	0.5	21.34	0.81	0.19	0.7	0.06	0.11
	57.3149	-92.1087	12.5	27.79	0.91	0.12	0.56	0.06	0.35
Hayes	56.9530	92.5960	0.5	0	2.83	0.92	1.78	0.1	1.05
	57.0303	-92.2613	0.5	0.07	2.81	0.15	2.05		0.76
	57.0859	-92.1310	0.5	4.7	1.9	0.2	1.21		0.69
	57.0859	-92.1310	5	7.36	2.56		1.62	0.41	0.94
	57.1534	-92.0201	0.5	16.1	1.28	0.12	1.38		-0.1
	57.1534	-92.0201	7.5	21.4	2.96		0.93	0.32	2.03

^a values represent mean of two field replicates

^b sample collected through a 0.45 µm pore-size filter

^c calculated by difference between Total and Dissolved Hg fractions

Table A-3. Horizontal Hg Distribution in Dissolved and Particulate Phases in Estuary Surface Waters of the Hudson Bay System

Date	River Estuary	Latitude	Longitude	Salinity (%)	Total ^a Hg (ng/L)	stdev /range	n	Dissolved ^b Hg (ng/L)	Stdev /range	n	Particulate ^c Hg (ng/L)
Sep 28/05	Povungnituaq	60.0398	-77.2175	0	1.36	0.37	2	0.54	0.08	2	0.82
		60.0017	-77.3383	5.2	0.96	0.36	2	0.77	0.26	2	0.19
		60.0116	-77.3306	24.9	0.56	0.02	2	0.6		1	-0.04
Sep 29/05	Inuksuak	58.4582	-78.0974	0.16	0.81		1				
		58.4528	-78.0983	0.34	1.32		1				
		58.4482	-78.1022	13.2	1.05		1				
		58.6082	-78.1123	18.4	0.85		1				
Sep 30/05	Grande Baleine	55.2666	-77.7799	0	2.62	0.03	2				
		55.2736	-77.8173	20.4	1.18	0.01	2				
		55.2868	-77.8729	26.6	0.69	0.06	2				
Oct 10/05	Hayes	57.0303	-92.2613	0.07	2.09	0.11	3	1.87			0.22
				0.17	2.15	0.18	2	1.84		0.31	
				0.22	2.1	0.04	2	1.88		0.22	
		57.0859	-92.1310	9.35	2.13	0.13	2	1.41			0.72
		57.1534	-92.0201	13.3	1.84	0.11	2	1.35			0.49
Oct 9/05	Nelson	57.0398	-92.5955	0.11	2.43	0.3	2	1.64			0.79

57.0430	-92.5521	0.28	2.49	0.13	4	1.77	0.72
57.1114	-92.4416	2.38	3.05	0.09	2	1.57	1.48
57.1454	-92.3861	6.8	2.51	0.05	4	1.62	0.89
57.1791	-92.3312	17	1.66	0.15	4	1.7	-0.04
57.1977	-92.3000	18.17	1.56	0.24	4	1.43	0.13
57.2134	-92.2754	18.25	1.61	0.07	3		
57.2470	-92.2199	26.1	1.63	0.18	3	1.06	0.57
57.2810	-92.1640	25.8	1.24	0.05	2	1.18	0.06
57.3149	-92.1087	25.15	1.09	0.03	2		

Table 3 Continued:

^a Mean of field replicates

^b filtered through a 0.45 μm pore-size filter

^c Determined as the difference between Total and Dissolved Hg

Sediment Hg concentrations

Sediments were collected and analyzed for Hg as described in Chapter 3.

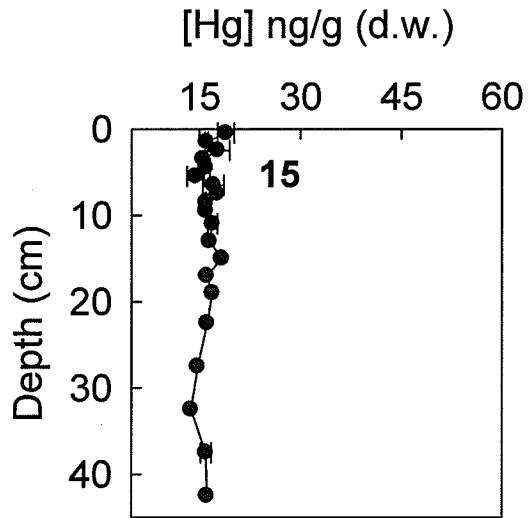


Figure A-1. Vertical profile of Hg in sediments of Core 15.